



---

All Theses and Dissertations

---

2013-07-05

# Developmental Signaling Requires Inwardly Rectifying K<sup>+</sup> Channels in *Drosophila melanogaster*

Giri Raj Dahal

*Brigham Young University - Provo*

Follow this and additional works at: <https://scholarsarchive.byu.edu/etd>

 Part of the [Biochemistry Commons](#), and the [Chemistry Commons](#)

---

## BYU ScholarsArchive Citation

Dahal, Giri Raj, "Developmental Signaling Requires Inwardly Rectifying K<sup>+</sup> Channels in *Drosophila melanogaster*" (2013). *All Theses and Dissertations*. 4168.

<https://scholarsarchive.byu.edu/etd/4168>

This Dissertation is brought to you for free and open access by BYU ScholarsArchive. It has been accepted for inclusion in All Theses and Dissertations by an authorized administrator of BYU ScholarsArchive. For more information, please contact [scholarsarchive@byu.edu](mailto:scholarsarchive@byu.edu), [ellen\\_amatangelo@byu.edu](mailto:ellen_amatangelo@byu.edu).

Developmental Signaling Requires Inwardly Rectifying K<sup>+</sup> Channels  
in *Drosophila melanogaster*

Giri Raj Dahal

A dissertation submitted to the faculty of  
Brigham Young University  
in partial fulfillment of the requirements for the degree of  
Doctor of Philosophy

Emily A. Bates, Chair  
Barry M. Willardson  
Allen R. Buskirk  
David Busath  
Jeffery R. Barrow

Department of Chemistry and Biochemistry  
Brigham Young University

July 2013

Copyright © 2013 Giri Raj Dahal

All Rights Reserved

## ABSTRACT

### Developmental Signaling Requires Inwardly Rectifying K<sup>+</sup> Channels in *Drosophila melanogaster*

Giri Raj Dahal

Department of Chemistry and Biochemistry, BYU

Doctor of Philosophy

Inwardly rectifying potassium (IRK/Kir) channels regulate intracellular K<sup>+</sup> concentrations and membrane potential. Disruption of Kir2.1 causes dominantly inherited Andersen Tawil Syndrome (ATS). ATS patients suffer from cardiac arrhythmias, periodic paralysis, and cognitive impairment. These symptoms are consistent with current understanding of the role of ion channels in muscle cells and neurons. However, ATS symptoms also include craniofacial and digital deformities such as cleft palate, dental defects, wide set eyes, low set ears, and crooked or fused digits. These developmental defects were not consistent with current understanding of developmental signaling or previously described roles for ion channels. We found that phenotypes exhibited by the Kir2.1 knockout mouse recapitulate ATS symptoms. The Kir2.1 knockout mouse phenotypes are strikingly similar to those that occur when Transforming Growth Factor  $\beta$ /Bone Morphogenetic Protein (TGF $\beta$ /BMP) signaling is disrupted. Based on this observation, we hypothesized that Kir2.1 may play a role in TGF $\beta$ /BMP signaling. We tested this hypothesis using *Drosophila melanogaster*. We reduced a Kir2.1 homologue Irk2 by siRNA, eliminated the Irk2 channel with a deficiency, and abolished heteromeric Irk channel function with a dominant negative Irk2. Reduction of Irk2 function caused wing patterning defects and size reduction that are similar to BMP/Decapentaplegic (DPP) mutant phenotypes. Ubiquitous expression of *Irk2DN* is lethal. Wing specific *Irk2DN* expression caused severe defects compared to *irk2Df* demonstrating that Irk channels are heteromeric. We found that two downstream targets of Dpp were reduced in *irk2Df* and *siRNA* expressing wing discs showing that Dpp requires Irk2 activity. We found that wing specific expression of *Irk2DN* completely prevents Mad phosphorylation and induces apoptosis. Suppression of apoptosis does not rescue MAD phosphorylation showing that apoptosis is caused by lack of an external signal. We systemically tested the components of the Dpp signaling cascade to find at what point in Dpp signaling Irk2 is required. We found that Irk2 is not directly required for the intracellular propagation of the Dpp signal. Irk2DN could not eliminate the phosphorylation of Mad by a constitutively activated Tkv. We showed that Irk2 affects Dpp spread across the disc. We speculate that Irk2 affects the endocytic pathway that transports Dpp from medial cells to lateral cells. We tested the impact of *irk2DN* on the development of the *Drosophila* eye where Irk2 is expressed and Dpp is required for normal patterning. We found that abolition of Irk channels causes eye defects that are similar to those that occur with the loss of Dpp signaling. Trachea development also depends on Dpp. Blocking Irk2 in the developing trachea results in severe defects. We conclude that Irk2 plays a global role in Dpp signaling. Kir/Irk channels could be therapeutic targets to treat diseases that are impacted by TGF $\beta$ /BMP signaling, such as cancer. Furthermore, the demonstration that Irk2 is a node for BMP-like signaling could be used to control cell fate decisions for regenerative medicine or stem cell therapeutics.

Key words: Irk, Kir, ATS, DPP

## ACKNOWLEDGEMENTS

I would like to express wholehearted gratitude to my supervisor Dr Emily Bates for her guidance and continuous encouragement to carry out this work. I extend my sincere gratitude to my graduate committee members Drs Barry Willardson, Allen Buskirk, David Busath and Jeffery Barrow.

I reserve my deep note of appreciation to professors who help me to understand various aspects of science.

I want to acknowledge Dr Joel Rawson for his work at the start of this project. I would like to thank all my colleagues in my lab and my classes.

I would also like to acknowledge the Department of Chemistry and Biochemistry, the Graduate school, Cancer Research Center, and Graduate Student Society for their financial support.

Finally, I would like to mention the sustained inspiration provided by my wife Sabita, my son Gahan, my parents, and my brothers whose support led me to this career.

## TABLE OF CONTENTS

ABSTRACT.....	ii
ACKNOWLEDGEMENTS.....	iii
TABLE OF CONTENTS.....	iv
LIST OF FIGURES AND TABLES.....	vii
LIST OF ABBREVIATIONS.....	ix
CHAPTER 1: INTRODUCTION .....	1
CELL FATE DECISIONS.....	1
SIGNAL TRANSDUCTION PATHWAYS.....	1
<i>TGF-<math>\beta</math>/BMP signaling</i> .....	1
<i>Wnt signaling</i> .....	2
<i>Hedgehog signaling</i> .....	3
<i>Bioelectric signaling</i> .....	4
INWARDLY RECTIFYING K <sup>+</sup> CHANNEL 2 (Kir2.1/Irk2) .....	4
MUTATIONS THAT DISRUPT KIR2.1 CAUSE ANDERSEN-TAWIL SYNDROME.....	6
ANDERSEN- TAWIL SYNDROME SYMPTOMS.....	10
<i>Periodic paralysis</i> .....	10
<i>Heart arrhythmias</i> .....	10
<i>Dysmorphic features</i> .....	11
THESIS OVERVIEW.....	12
CHAPTER 2: AN INWARDLY RECTIFYING K <sup>+</sup> CHANNELS IS REQUIRED FOR PATTERNING.....	15
ABSTRACT.....	15
INTRODUCTION .....	16
RESULTS.....	17
<i>Kir2.1 mouse phenotypes</i> .....	17
<i>Irk2 deficiency disrupts wing patterning</i> .....	19
<i>Irk2 siRNA expression disrupts wing patterning</i> .....	23
<i>Expression of dominant-negative Irk2 causes severe wing defects</i> .....	25
<i>Reduced Dpp signaling enhances Irk2DN phenotypes</i> .....	30
<i>Dpp signaling is disrupted by aberrant Irk2 function</i> .....	32
DISCUSSION .....	37
MATERIALS AND METHODS.....	42
<i>Maintenance of Drosophila stocks</i> .....	42

<i>Generation of the UAS-Irk2DN and UAS-Irk2WT fly strains</i> .....	42
<i>Drosophila strains</i> .....	43
<i>Generation of Irk2Df strains</i> .....	43
<i>Quantitative RT-PCR</i> .....	44
<i>Immunohistochemistry and TUNEL staining</i> .....	45
<i>Imaging</i> .....	45
<i>Kir2.1 mouse</i> .....	46
<i>Statistical analysis</i> .....	46
ACKNOWLEDGEMENTS.....	46
CHAPTER3: THE MECHANISM OF THE <i>kir2.1</i> /IRK2 CONTRIBUTION TO DPP SIGNALING ...	47
INTRODUCTION .....	47
RESULTS .....	49
<i>Irk2 is not required for Hedgehog signaling</i> .....	49
<i>Expression of Dpp, Tkv and Dally remains normal in the Irk2DN expressing wing disc</i> .....	51
<i>Irk2 is not directly required for phosphorylation of Mad</i> .....	55
<i>Diffusion of the Dpp ligand is affected by Irk2</i> .....	56
<i>The requirement for Irk2 is non-cell autonomous</i> .....	58
DISCUSSION.....	60
MATERIALS AND METHODS.....	63
<i>Drosophila strains used</i> .....	63
<i>Clone generation</i> .....	63
<i>Immunohistochemistry</i> .....	63
<i>Imaging</i> .....	64
<i>Wing disc measurement</i> .....	64
CHAPTER 4: IRK2 PLAYS A GLOBAL ROLE IN DROSOPHILA DEVELOPMENT .....	65
INTRODUCTION .....	65
<i>Drosophila Eye Development</i> .....	65
<i>Morphogenetic Furrow and cellular signaling for cell fate decisions</i> .....	66
<i>Drosophila trachea development</i> .....	67
RESULTS .....	68
<i>Irk2 is expressed in the eye disc</i> .....	68
<i>Loss of Irk channels causes visible eye phenotypes</i> .....	68
<i>Eye phenotypes due to loss of Irk2 are similar to Wg overexpression phenotypes</i> .....	71

<i>Irk2DN does not cause apoptosis in the eye disc</i> .....	71
<i>Irk2 is expressed in the trachea</i> .....	73
<i>Irk2 is required for trachea development</i> .....	74
DISCUSSION .....	74
MATERIALS AND METHODS.....	76
<i>Drosophila strains used</i> .....	76
<i>Scoring eye phenotype</i> .....	77
<i>Drosophila eye light microscopy imaging</i> .....	77
<i>Drosophila eye preparation for Scanning Electron Microscopy</i> .....	77
<i>Immunohistochemistry</i> .....	77
<i>TUNEL staining</i> .....	77
ACKNOWLEDGEMENTS.....	78
REFERENCES .....	79

## LIST OF FIGURES AND TABLES

Figure 1-1. Molecular architecture of Kir channels.	6
Table 1-1. Current and Proposed expansion of phenotype for ATS diagnosis.	8
Figure 1-2. Topology of Kir2.1 channel with known mutation and deletions.	9
Figure 2-1. Knockout of mouse Kir2.1 causes cleft of the secondary palate and patterning defects of the skeletal digits.	18
Figure 2-2. <i>irk2</i> expression.	19
Figure 2-3. Map of genomic region including <i>irk2</i> showing the start and end points of each deficiency.	20
Figure 2-4. Reduced <i>Irk2</i> function wing phenotypes.	24
Table 2-1. Wing venation defects	20
Figure 2-5. Reducing function of <i>irk2</i> causes hinge defects similar to the Dpp ‘wings held-out’ phenotype.	23
Figure 2-6. Reducing function of <i>irk2</i> increases expression of other <i>irk</i> subunits.	24
Figure 2-7. Phenotypes of flies expressing <i>Irk2DN</i> .	26
Figure 2-8. <i>Irk1</i> and <i>Irk3</i> siRNA phenotypes.	27
Figure 2-9. Reduced Dpp or Thickveins function enhances <i>Irk2DN</i> phenotypes.	30
Figure 2-10. Reduced Mad phosphorylation in <i>Irk2DfA/Irk2DfB</i> and <i>Irk2 siRNA</i> wing discs.	32
Fig. 2-11. Immunohistochemistry demonstrates that Dpp signaling is reduced in <i>Irk2DN</i> and <i>Irk2DfA/Irk2DfB</i> .	33
Figure 2-12. <i>Irk2DN</i> expression causes apoptosis and eliminates p-Mad staining in the third instar larval imaginal wing disc.	34



Figure 2-13. Expression of <i>irk2DN</i> using wing-directed Gal4 drivers decreases anti-p-Mad staining.	35
Figure 2-14. Model for Irk channels in Dpp signaling.	39
Figure 3-1: Hedgehog signaling is not involved in Irk2 mediated wing patterning.	50
Figure 3-2: Irk channel function is not required for transcription of Dpp, Tkv or Dally.	53
Figure 3-3: Irk2 does not directly target Mad.	54
Figure 3-4: Spread of Dpp is impacted by Irk channels loss.	56
Figure 3-5: Irk2 channel is not required for reception of the Dpp signal.	58
Figure 3-6: Model for Irk channels in Dpp signaling.	59
Figure 4-1: Irk2 expresses in the eye disc.	68
Figure 4-2: Irk2DN expression causes eye defects.	69
Figure 4-3: Loss of Irk2 causes various eye phenotypes.	71
Figure 4-4: Irk2DN does not cause apoptosis in the eye disc.	72
Figure 4-5. <i>irk2</i> is expressed in trachea.	72
Figure 4-6: Irk2DN expression causes defects in trachea development.	73

## LIST OF ABBREVIATIONS

ATS	Andersen-Tawil Syndrome
BMP	Bone Morphogenetic Protein
Bnl	Branchless
Btl	Breathless
Dpp	Decapentaplegic-a ligand for BMP type signaling in <i>Drosophila</i>
Dad	Daughter of DPP
Dally	Development abnormally delayed- a proteoglycan that aids in the spread of Dpp across cells
En	Engrailed
GDF	Growth and Differentiation Factor
Hid	Head involution defective-caspase homolog
Kir/Irk	Inwardly Rectifying K <sup>+</sup> Channel
KO	knockout
MF	Morphogenetic Furrow
SEM	Scanning Electron Microscope
TGF- $\beta$	Transforming Growth Factor- $\beta$
Wnt	Wingless Int
Hh	Hedgehog

## CHAPTER 1: INTRODUCTION

### CELL FATE DECISIONS

How does a cell differentiate into a specific type? Cell fate can be acquired by lineage or by receiving an external signal. One mode of cell type specification involves signal transduction from neighboring cells. The ‘inducer cells’ send out inductive signals to promote changes in the neighboring cells called ‘responders’. Inductive signals can require cell to cell contact through surface proteins, such as Hippo and Notch<sup>1</sup>. Alternatively, inductive cells can release morphogens that diffuse to target responder cells. These morphogens diffuse long or short distances. The fate of responder cells depends on the amount of morphogen they receive. Examples of the signal transduction pathways that determine cell fate include; Hedgehog, Wingless, Transforming Growth Factor  $\beta$  (TGF $\beta$ ) /Bone Morphogenetic Protein (BMP), c-Jun N-terminal Kinase (JNK), Nuclear factor kappa-light-chain-enhancer of activated B cells (NF-kB), Janus Kinase (JAK)- Signal Transducer and Activator of Transcription (STAT), Epidermal Growth Factor (EGF), Fibroblast Growth Factor (FGF), and retinoic acid<sup>1</sup>.

Here, I focus on inductive cell fate determination comprising three major signaling pathways: TGF- $\beta$ /BMP, Wnt and Hh and pathways.

### SIGNAL TRANSDUCTION PATHWAYS

#### ***TGF- $\beta$ /BMP signaling***

Transforming Growth Factor Beta (TGF- $\beta$ ) is a family of conserved proteins that control the process of cell growth, differentiation, migration, adhesion, and death in a multitude of developmental contexts<sup>2-4</sup>. This superfamily consists of 5 families: TGF- $\beta$ , Bone Morphogenetic Protein (BMP), Growth and Differentiation Factor (GDF) Nodal and Activin<sup>5</sup>. Members of the

TGF- $\beta$  superfamily share a simple, but elegant mechanism. A dimeric ligand is released from the inducer cells. The dimer binds cell surface receptor proteins on the responding cell. The receptor proteins are transmembrane serine-threonine kinase receptors that consist of an intracellular kinase domain and a phosphorylation site. Ligand binding causes two receptors (type I and type II) to come together and start a chain of unidirectional phosphorylation events. First, the type II receptor is phosphorylated, then its kinase domain phosphorylates the type I receptor<sup>6-7</sup>. The type I receptor phosphorylates the R-SMADs that carry the extracellular signal to the nucleus. Phosphorylated R-SMADs recruit another set of SMADs called Co-SMADs to form a complex<sup>5</sup>. This complex enters into the nucleus to act as a transcription factor to express or inhibit target genes. Inhibitory SMADs (I-SMADs) block the signal by interfering with R-SMAD phosphorylation<sup>8</sup>. Since this signaling pathway is involved in so many cellular processes, mutations of different members disrupt the pathway and lead to similar phenotypes. This can cause several diseases such as hereditary chondrodysplasia, persistent mullerian duct syndrome,<sup>9</sup> and cancer<sup>10</sup>.

### ***Wnt signaling***

Wnt signaling consists of a family of conserved signaling molecules that regulate cell fate decisions from embryogenesis to organogenesis across species. Wnt family proteins pattern *Xenopus* neural systems<sup>11</sup>, vertebrates limbs<sup>12</sup> and *Drosophila* wings and eyes<sup>13-14</sup>. Typically, Wnt ligands are released from the inducer cells and diffuse into the territory of the responder cells. The ligand binds with the receptor complex composed of frizzled family proteins<sup>15-16</sup>. When Wnt binds its receptor, it suppresses the  $\beta$ -catenin destruction complex (Axin, adenomatous polyposis coli (APC) and Glycogen synthase kinase 3 (GSK-3)<sup>17</sup>. An increased level of hypo phosphorylated  $\beta$ -catenin in the cytoplasm makes its entry into the nucleus

possible. In the nucleus,  $\beta$ -catenin directs expression of target genes through cell-specific transcription factor/lymphoid enhancer-binding factor 1 (TCF/LEF) family of transcription factors<sup>18</sup>. In the absence of Wnt binding, the  $\beta$ -catenin destruction complex maintains the  $\beta$ -catenin level low in the cytoplasm by making it a target of proteasomal destruction. Because this pathway is well conserved and essential in many development processes, irregularity of the signaling causes various diseases. For example, loss of signaling components causes X-linked focal dermal hypoplasia<sup>19</sup>, early coronary disease, osteoporosis<sup>20</sup>, and obesity<sup>21</sup>. On the other hand, gain of function mutations have been associated with type II diabetes<sup>22-23</sup>, colon<sup>24</sup> and skin cancers<sup>25</sup>.

### ***Hedgehog signaling***

The hedgehog signaling pathway patterns organs such as the heart, lung, bone, cartilage, neurons, and teeth. Disruption of hedgehog signaling leads to a multitude of diseases<sup>26</sup>. Mammals have three types of Hedgehog: *Sonic hh*, *Indian hh*, and *Desert hh*, whereas *Drosophila* has only one. In *Drosophila*, Hh induces the expression of decapentaplegic (*dpp*)/*BMP* in the eye and wing disc to pattern those organs<sup>27</sup>. Hh binds to a 12 pass transmembrane receptor protein called Patched. Patched suppresses the expression and activity of a heptahelical transmembrane protein called smoothened<sup>28</sup>. Hh binding of patched releases smoothened from its suppresser and allows it to accumulate in the cytoplasm. Smoothened prevents the cleavage of transcription factor Gli by sequestering it to a microenvironment with the help of kinesin-like protein Costal-2<sup>29</sup>. In the absence of smoothened, several kinases such as Protein Kinase A, Glycogen synthase kinase 3  $\beta$ , and Casein kinase 1(CK1) phosphorylate Gli to make it a target of proteolytic cleavage. In the nucleus, uncleaved Gli activates the expression of *Hh* specific genes whereas cleaved Gli suppresses them. Vertebrates require a cilium for the

Hh signaling<sup>30</sup>. In the absence of hedgehog (Hh) binding, Patched inhibits the Smoothed from entering the cilia and converts the Gli and suppresser of fused (SUFU) complex to make the repressor Gli<sup>31</sup>. Binding of Hh relieves the suppression of Smoothed which accumulates in the cilium and signals downstream<sup>31</sup>. Misregulation of the Hh signaling pathway causes several developmental diseases such as Postaxial polydactyly type 3, Smith-Lemli-Opitz syndrome, Holoprosencephaly, Pallister-Hall syndrome, and cancers such as Sporadic medulloblastoma and Glioblastoma<sup>32</sup>.

### ***Bioelectric signaling***

Manipulating membrane potential to induce changes in cellular function is called bioelectric signaling. Bioelectric signaling plays an important role in signal transduction of excitable cells such as neurons and muscles, but its role in other tissues has been appreciated only recently. Modulation of ion channels, pumps, and gap junctions changes membrane potential or drives electric current across the cells<sup>33</sup>. This mode of signaling occurs in parallel or upstream of protein based signal transduction. Bioelectric signals can induce apoptosis or cell growth<sup>34</sup>. Changes in membrane potential can be a mechanism to achieve signaling<sup>34-35</sup>. A H<sup>+</sup>, K<sup>+</sup>-ATPase ion pump creates bioelectric signal, that shapes the head and organ size in planaria<sup>34</sup>. Artificial induction of membrane potential changes in non-eye tissue can induce ectopic eyes<sup>36</sup>. Voltage potential is involved in Xenopus tail regeneration<sup>37</sup>, planaria head regeneration<sup>38</sup> embryonic neural tube patterning<sup>39</sup>, cell migration<sup>40-42</sup>, and wound healing<sup>43</sup>.

### INWARDLY RECTIFYING K<sup>+</sup> CHANNEL 2 (KIR2.1/IRK2)

Inwardly rectifying K<sup>+</sup> channels are a group of channels that regulate the cellular resting membrane potential, control cell volume, maintain pH, and balance the ion concentrations. These channels allow K<sup>+</sup> into the cells liberally at negative resting potentials, but allow outward current

sparingly at positive membrane potentials so they are called inwardly rectifying. A crystal structure of a typical Kir channel shows that four Kir protein subunits assemble to form a functional channel. Each consists of a cytoplasmic amino and carboxyl terminal and a pore-forming domain (H5) surrounded by transmembrane domains (M1 and M2) (Figure 1-1). These channels can either be homo or heterotetrameric. The functions of inwardly rectifying  $K^+$  channels are diverse. Human Kir proteins are classified into four functional groups, namely: constitutively active classic Kir channels (Kir2.x), G protein gated Kir channels (Kir3.x), ATP-sensitive  $K^+$  channels (Kir6.x), and  $K^+$  transport channels (Kir1.x, 4.x, 5.x and 7.x)<sup>44</sup>.

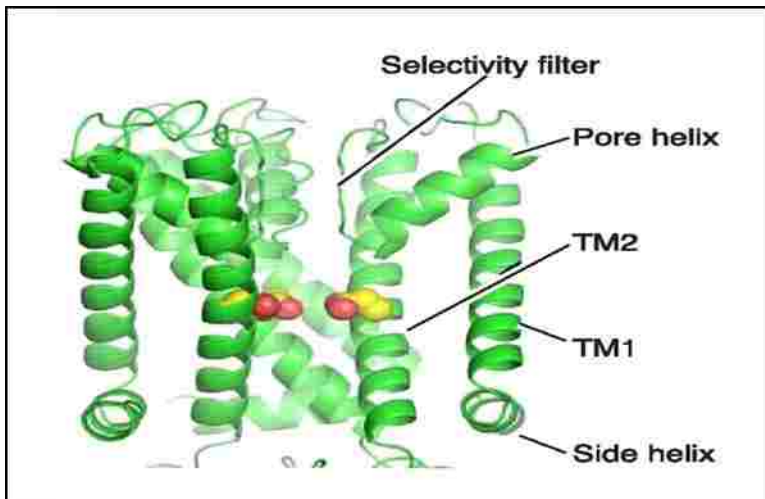


**Figure 1-1. Molecular architecture of Kir channels showing transmembrane domain.** It comprises three helices: TM1, Pore and TM2<sup>44-46</sup>

Irk channels are well-conserved from prokaryotes to eukaryotes. *Drosophila* Irk 1 and 2 are related to human Kir2, Kir3, and Kir6<sup>47</sup>. Kir2 subtypes (Kir2.1, Kir2.2, and Kir2.3) are constitutively active and maintain a strong inwardly rectified current. Kir 2.1 knockout animals have a complete cleft in their secondary palate that prevents them from feeding. In addition, these animals die within 12 hours after birth because of respiratory problems<sup>48</sup>. Kir2.1 knockout or dominant negative mice have a slower heart rate than wild type mice<sup>49</sup> because Kir channels are expressed in cardiac myocytes<sup>44, 50</sup>. Similarly,

Kir2.1 is also necessary for differentiation of myoblasts<sup>51</sup> and for the fusion of mononucleated myoblasts to form skeletal muscle fibers<sup>52</sup>. Abnormal Kir2.1 function is also associated with short Q-T syndrome, a distinct cardiac disease resulting in syncope, atrial fibrillation, and a high incidence of sudden cardiac death, among young patients<sup>53</sup>. Kir protein function is partially redundant. Loss of one Kir channel subunit can be restored by another subunit<sup>54</sup>; for example Kir 2.1 and 2.2 knockout mice exhibit no abnormal neuronal phenotype<sup>48</sup> which may be due to the compensation by other channels.

#### MUTATIONS THAT DISRUPT KIR2.1 CAUSE ANDERSEN-TAWIL SYNDROME

Mutations in the gene encoding Kir2.1 (KCNJ2) result in a rare dominantly inherited disorder called Andersen-Tawil Syndrome<sup>55</sup>. Andersen et al, described a peculiar case of an eight year old boy who had cardiac arrhythmia, periods of muscular weakness, and several developmental defects such as dwarfism, hypertelorism, low set ears, aplasia of teeth, curved fingers, bilateral ptosis, a broad nose and other abnormalities<sup>56</sup>. More than two decades later, Tawil et al, characterized the syndrome as “potassium sensitive, periodic paralysis, ventricular ectopy, and dysmorphic features”<sup>57</sup>. Furthermore, Tawil and others mapped the cause of Andersen’s syndrome to chromosome locus 17q23 with KCNJ2 gene that codes for inwardly rectifying potassium channel Kir2.1<sup>58</sup>. The syndrome was renamed as Andersen-Tawil syndrome (ATS) after the scientists A.D. Andersen and R. Tawil for their roles in the identification of this disease. Andersen-Tawil syndrome is an autosomal disorder characterized by the triad of periodic paralysis, heart arrhythmias and dysmorphic features. Since the description provided by Andersen and Tawil, research interest in this syndrome has increased dramatically, especially after the identification of the causative KCNJ2 mutations. As more subjects were analyzed, the



identification criteria have also been expanded and have been tabulated by Yoon and colleague in Table 1-1<sup>59</sup>.

Over 30 mutations in KCNJ2, which encodes Kir2.1, have been found to be associated with ATS (Fig 1-2). These mutations cause a dominant negative effect on the function of the Kir channel that leads to symptoms of ATS. The patients are heterozygous for the mutant KCNJ2 allele. The severity of the disease depends on the specific mutations. Some mutations cause all three phenotypes (periodic paralysis, heart arrhythmias and developmental defects) whereas others cause fewer phenotypes or no phenotypes and symptoms are usually more severe in males<sup>60-61</sup>.

**Table 1-1. Current and Proposed expansion of phenotype for ATS diagnosis<sup>59</sup>**

Current dysmorphic diagnostic criteria	Proposed expansion of diagnostic criteria
<p>Two or more of :</p> <p>Low set of ears</p> <p>Hypertelorism</p> <p>Small mandible</p> <p>Clinodactyly</p> <p>2-3 Syndactyly</p>	<p>Major features :</p> <p>Characteristic faces (broad forehead, short palpebral fissures, full nasal bridge with bulbous tip, malar, maxillary and mandibular hypoplasia, thin upper lip, triangular shape, mild asymmetry) palate (high arched or cleft)Dental abnormalities (persistent primary dentition, oligodontia, or abnormally long dental roots with open apices, narrow upper and lower dental arches, short jaw, notching of the lower mandible, dental crowding)</p> <p>Small hands and feet</p> <p>Variable brachydactyly</p> <p>Toe clinodactyly and 2-3 syndactyly</p> <p>Minor features: hypertelorism, 5th finger clinodactyly, small head circumference, short stature, prominent frontal sinuses, gracile ribs and long bones,</p> <p>Other features seen in ATS: scoliosis, scapular winging, copper beaten skull, delayed bone age</p>

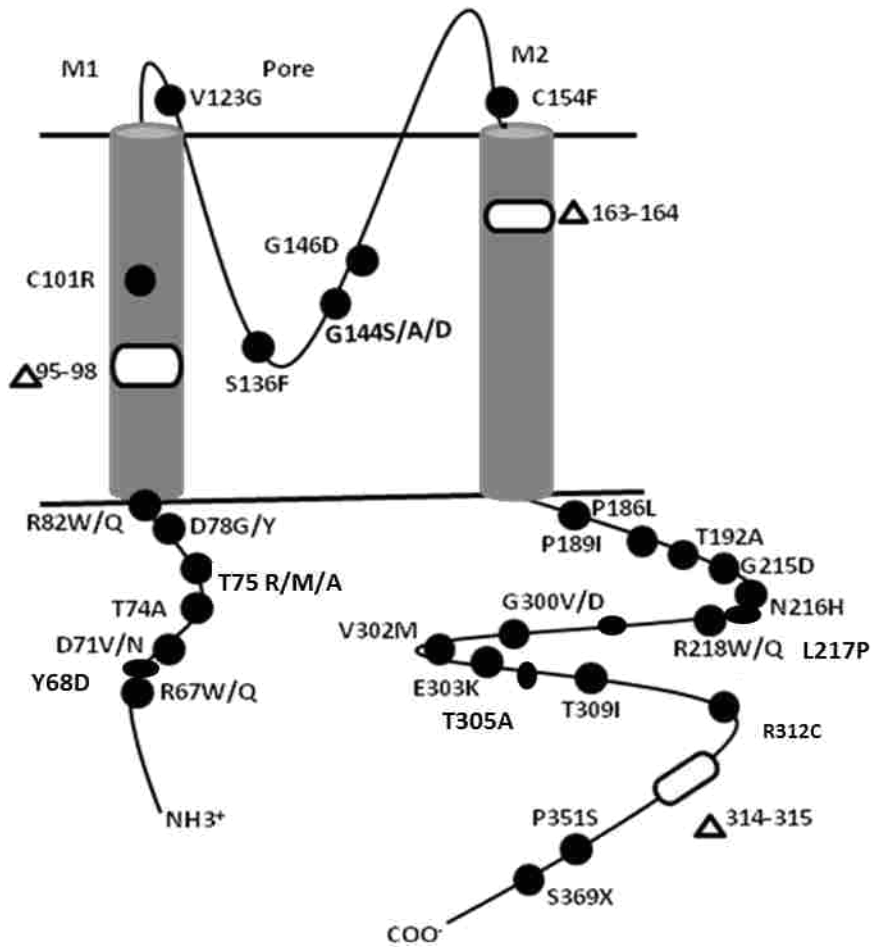


**Figure 1-2.** Topology of Kir2.1 channel with known mutation and deletions involved in ATS patients and carriers<sup>62-69</sup>.

ATS is caused by mutations that disrupt conserved regions of Kir2.1 (Figure1-2). Most of the mutations that occur in ATS cases are in the cytoplasmic side of the C-terminus (Figure1-2). For example V302 lies in the c-terminus on the cytoplasmic side of the channel. It is located in the G-loop that makes a flexible barrier for the  $K^+$  conductance. The V302M mutation alters the G-loop structure obstructing the proper channel function<sup>70</sup>. The C-terminus is important because it binds with  $Mg^{++}$  and polyamines so that  $K^+$  cannot pass through the channel towards the outside of the cell. Mutations that disrupt the conserved GYG pore domain disrupt the  $K^+$  channel. Mutations in this region compromise the selectivity of the channel. The N-terminus site

of the cytoplasmic region is important because it helps to anchor the protein to the cell membrane. Most mutations encode proteins that act in a dominant negative fashion.

## ANDERSEN- TAWIL SYNDROME SYMPTOMS

### ***Periodic paralysis***

Traits associated with ATS can vary in penetrance. One of the identifying characteristics of ATS is periodic paralysis. In one large kindred with ATS, Kir2.1 R67W causes an autosomal dominant trait of periodic paralysis only in males, but not in females<sup>60</sup>. Periodic paralysis can happen early in life-usually within the first 20 years of the life<sup>71</sup>. In a study of ten patients, nine showed episodic weakness with a mean age of 5 years and ranging from 8 months to 15 years<sup>72</sup>. The cause of periodic paralysis in ATS patients is Kir malfunction in the skeletal muscle. Kir is expressed ubiquitously in the skeletal muscle and shifts the resting potential ( $E_{res}$ ) towards hyperpolarization<sup>44</sup>. Mutations that disrupt Kir2.1 in ATS patients cause the resting potential to shift, reversing it towards depolarization. Depolarization leads to inactivation of  $Na^+$  channels.  $Na^+$  channels are needed to initiate and propagate action potential, so inactivation of the Kir channel ultimately leads to periodic paralysis. Kir channels are also important for differentiation of myoblasts<sup>51</sup> and to form multinucleated skeletal muscle fibers<sup>52</sup>. For both processes, Kir channels change the resting potential from -10mV to -70mV<sup>73</sup>. This change in membrane potential allows  $Ca^{++}$  channels to open for  $Ca^{++}$  entry.  $Ca^{++}$  is required for these processes. Kir2.1 null mice have mild muscle development defects because of impairment of channel properties<sup>74</sup>.

### ***Heart arrhythmias***

Kir2.1 is the major contributor to the inward  $I_{k1}$  current, which plays an important role in normal heart beat. Therefore, an  $I_{k1}$  anomaly causes heart arrhythmias.  $I_{k1}$  supplies current in the plateau phase of depolarization and controls the diastolic membrane potential. This is the reason

behind the heart arrhythmias and periodic paralysis in ATS patients. The penetrance of heart arrhythmias is variable in different individuals. Various mutations that affect Kir2.1 induce a different degree of cardiac arrhythmias. The most prevalent heart arrhythmia is prolongation of the QT interval causing rhythm abnormalities due to premature ventricular contractions (PVC-extra abnormal heartbeats), bidirectional couplets (PVC in a row), and polymorphic ventricular tachycardia (100 or more heart beats per minute)<sup>75</sup>. A boy with prominent ventricular arrhythmias and mild periodic paralysis had a S369X mutation in Kir2.1<sup>76</sup>. Reconstituted wild type Kir2.1 and S369X mutant Kir2.1 in a cultured cell line showed that this mutation causes defective transport from the ER to the plasma membrane. Increasing expression of the WT Kir2.1 subunit in comparison to the mutant partially restores the trafficking to the plasma membrane<sup>76</sup>. Some of the variability in ATS symptoms may have to do with the relative amounts of each channel subunit.

### ***Dysmorphic features***

Dysmorphic features are the early clues that patients have ATS because they appear in a high percentage of ATS patients and are apparent at birth. Like other ATS symptoms, dysmorphic features also have a high order of heterogeneity. Common dysmorphic features include syndactyly (fused fingers or toes), cleft palate, wide spaced eyes (hypertelorism), broad forehead, low-set ears, short stature, micrognathia (small jaw), broad nasal roots, curved fingers, scoliosis, and incomplete dentition<sup>58, 72</sup>. A 25 kindred study found that 78% of all Kir2.1 mutation carriers showed multiple dysmorphic features including low-set ears (39%) and hypertelorism (36%), small mandible (44%), clinodactyly (36%) syndactyly (11%), cleft palate (8%), and scoliosis (11%)<sup>58</sup>.

Dysmorphic features are more common in ATS patients with mutations in Kir2.1 than are other common symptoms like heart arrhythmia, and periodic paralysis. A study of 96 ATS patients with 24 different mutations found that 74% of the Kir2.1 mutant carriers showed dysmorphic features whereas only 52% had periodic paralysis and 41% had cardiac arrhythmias<sup>67</sup>.

The intracellular C terminal portion of Kir2.1 is essential for normal morphological development. The dysmorphic features are visible among 69% of N-terminus and M1 pore region mutation carriers, whereas those features are visible among 84% of C-terminus mutation carriers<sup>67</sup>. The Kir2.1 T192A mutant allele encodes a non-functional channel, but co-expression with the gene encoding wild type Kir2.1 makes it a functional channel in cell culture<sup>77</sup>.

## THESIS OVERVIEW

Mutations that disrupt the Kir2.1 channel cause periodic paralysis, heart arrhythmias and developmental defects. Kir2.1 has long been studied for its role in excitable cells such as cardiac muscle cells and skeletal muscle cells to explain the symptoms of periodic paralysis and heart arrhythmias respectively. However, there was no explanation for the dysmorphic features that result from mutations that disrupt Kir2.1. The developmental defects that are common in ATS patients are also associated with the disruption of developmental signaling pathways such as TGF- $\beta$ /BMP, Wnt, and Hh.

In chapter 2, I ask the question, does blocking or reducing Kir/Irk channel function in the mouse and the fruit fly *Drosophila melanogaster* recapitulate ATS phenotypes? Kir2.1 knockout mice have cleft palate and joined and curved digits. Similarly, deletion of a Kir2.1 fly homologue, Irk2, causes wing patterning defects. Thus disruption of Kir2.1 or Irk2 can be a

model for developmental defects recapitulating ATS phenotypes. The mouse craniofacial and limb patterning defects and fly wing patterning defects are reminiscent of defects that occur when BMP/DPP signaling goes awry. Is Kir2.1/Irk channel function important for Dpp/BMP signaling? By checking different components of the Dpp, Wg and Hh signaling pathways, I showed that Irk channels are specifically required for Dpp signaling while these channels are not necessary for Wg or Hh signaling. The results also showed that blocking Irk channels decreases Dpp signaling to cause apoptosis because loss of Dpp causes apoptosis.

In chapter 3, I characterize the mechanism by which Irk2 interacts with Dpp signal transduction. I determined if Irk2 is required for expression of components of the Dpp signal transduction pathway (the ligand *dpp*, the receptor *tkv* and *dally*, a Dpp stabilizing factor). Using immunohistochemistry in the wing precursor, I checked whether Irk2 is specifically required for the phosphorylation of a *Drosophila* homologue of R-SMAD (Mad). We found that Irk2 is not directly required for the type I Dpp receptor (Tkv) to phosphorylate Mad. In summary, I found that Irk2 impacts Dpp signaling downstream of Dpp and receptor translation and upstream of Mad phosphorylation. In other words, Irk2 is required for the release of Dpp from the inducing cell or for the spread of the ligand across the tissue to Dpp responding cells. Alternatively, it could be required for the processing of Dpp. Lastly, I tested whether the spread of the Dpp ligand is affected by blocking Irk2 in the wing discs. I found that Irk2DN expressing discs grow abnormally and the peak intensity of Dpp is different than normal.

In chapter 4, I ask whether Irk2 is required for Dpp signaling globally. I used the *Drosophila* eye and trachea because Dpp plays important roles to pattern these organs. The results showed that reducing function of Irk channels causes defects in both the eye and the

trachea. In conclusion, the answer to my question is that Irks plays a global role in patterning different organs as expected from its interaction with Dpp signaling.



## CHAPTER 2: AN INWARDLY RECTIFYING K<sup>+</sup> CHANNELS IS REQUIRED FOR PATTERNING

Adapted from: Dahal, G. R.; Rawson, J.; Gassaway, B.; Kwok, B.; Tong, Y.; Ptáček, L. J.; Bates, E., An inwardly rectifying K<sup>+</sup> channel is required for patterning. *Development* **2012**, *139* (19), 3653-3664.

### ABSTRACT

Mutations that disrupt function of the human inwardly rectifying potassium channel KIR2.1 are associated with the craniofacial and digital defects of Andersen-Tawil Syndrome, but the contribution of Kir channels to development is undefined. Deletion of mouse *Kir2.1* also causes cleft palate and digital defects. These defects are strikingly similar to phenotypes that result from disrupted TGF $\beta$ /BMP signaling. We use *Drosophila melanogaster* to show that a Kir2.1 homolog, *Irk2*, affects development by disrupting BMP signaling. Phenotypes of *irk2* deficient lines, a mutant *irk2* allele, *irk2* siRNA and expression of a dominant-negative *Irk2* subunit (*Irk2DN*) all demonstrate that *Irk2* function is necessary for development of the adult wing. Compromised *Irk2* function causes wing- patterning defects similar to those found when signaling through a *Drosophila* BMP homolog, Decapentaplegic (Dpp), is disrupted. To determine whether *Irk2* plays a role in the Dpp pathway, we generated flies in which both *Irk2* and Dpp functions are reduced. *Irk2DN* phenotypes are enhanced by decreased Dpp signaling. In wild-type flies, Dpp signaling can be detected in stripes along the anterior/posterior boundary of the larval imaginal wing disc. Reducing function of *Irk2* with siRNA, an *irk2* deletion, or expression of *Irk2DN* reduces the Dpp signal in the wing disc. As *Irk* channels contribute to Dpp

signaling in flies, a similar role for Kir2.1 in BMP signaling may explain the morphological defects of Andersen-Tawil Syndrome and the *Kir2.1* knockout mouse.

## INTRODUCTION

Mutations in inwardly rectifying K<sup>+</sup> channels are associated with patterning defects. For example, mutations that disrupt *Kir2.1* are associated with the morphological defects of Andersen-Tawil Syndrome (ATS): cleft palate, micrognathia, hypertelorism, dental abnormalities, clinodactyly, syndactyly and shortened phalanges<sup>56-57, 59, 71-72, 78</sup>. Furthermore, deletion of the mouse *Kir2.1* gene (*Kcnj2* – Mouse Genome Informatics) causes cleft palate and narrow maxilla<sup>48</sup>.

Inwardly rectifying K<sup>+</sup> channels comprise four subunits<sup>79-80</sup>. Mutations that disrupt *Kir2.1* cause periodic paralysis, heart arrhythmia and morphological defects in individuals with ATS. The most severe defects in such individuals are caused by dominant-negative Kir2.1 subunits that complex with other subunits and alter the selectivity filter, affecting K<sup>+</sup> conductivity of the entire heteromeric channels<sup>49, 80-81</sup>. The electrophysiological consequences of dysfunctional Kir2.1 are understandable, but the mechanism underlying the developmental abnormalities is unclear.

Despite the growing body of evidence for a role of K<sup>+</sup> channels in development, the mechanism by which they influence pattern formation is not understood. Similar cleft palate and digit defects can be caused by loss of transforming growth factor  $\beta$  (TGF $\beta$ )/bone morphogenetic protein (BMP), Wnt-Wingless (Wg) or Notch signaling<sup>82-95</sup>. We tested the hypothesis that inhibiting Kir2.1 channels interferes with TGF $\beta$ /BMP signaling.

The TGF $\beta$ /BMP superfamily has orthologous pathways in multicellular organisms<sup>96-100</sup>. In *Drosophila*, Dpp is a BMP homolog that is required for embryonic development, growth and patterning of adult structures, including the wing<sup>101-104</sup>. Dpp binds type 1 and type 2 kinase receptors<sup>103, 105-106</sup>. Upon Dpp binding, type 2 receptors phosphorylate type 1 receptors (thickveins), which phosphorylate Mothers against Dpp (Mad) to propagate the signal intracellularly<sup>107</sup>.

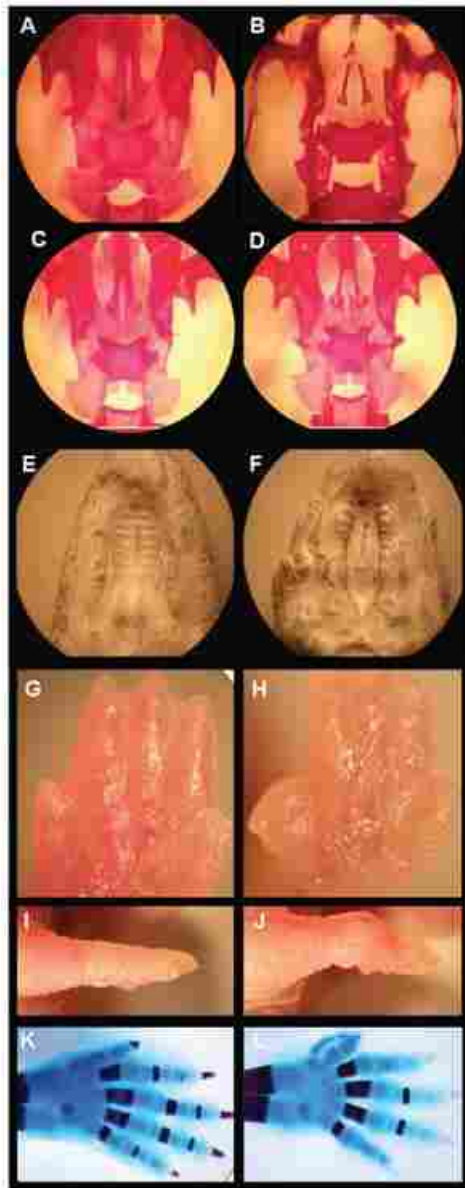
*Drosophila* is an excellent system for determining the mechanism underlying developmental defects, because conserved developmental signaling pathways are well-defined and non-redundant. Kir2.1 has three homologs in *Drosophila*. Irk2 is 50% identical and 69% similar to Kir2.1. Two other homologs, Irk1 and Irk3, may form heterotetrameric channels with Irk2 as with some Kir channels in mammals. Electrophysiological and expression studies demonstrate that these channels function similarly to mammalian Kir channels<sup>47</sup>. In this study, we test the hypothesis that Irk2 function is necessary for developmental signaling. We use an *Irk2* dominant-negative allele, *Irk2*-deficient alleles, an *Irk2* p-element allele and siRNA to show that Irk channels are necessary for patterning and growth of the *Drosophila* wing. We conclude that disruption of Irk channels leads to reduction in Dpp signaling and wing defects. These studies explain the mechanism by which K<sup>+</sup> channels regulate development and provide one possible explanation for the defects in individuals with ATS and in *Kir2.1* knockout mice.

## RESULTS

### ***Kir2.1* mouse phenotypes**

Deletion of the gene that encodes Kir2.1 in mice results in patterning defects that are similar to BMP knockout phenotypes. For example, Zaritsky et al. reported that homozygous

*Kir2.1* knockout mice have cleft palates<sup>48</sup>. We further characterized skeletal deformations in homozygous *Kir2.1* knockout animals (n=13) (Figure 2-1). The anterior and posterior palatine



of the right limb is shown. Anterior is upwards.

The developmental defects of *Kir2.1* knockout mice are similar to the cleft palate defects of *Tgfb2* and *Tgfb3* knockout animals<sup>108-109</sup>. Disruption of TGF $\beta$  co-factors, regulators and receptors also leads to cleft palate in mice<sup>84, 110-111</sup>. *Kir2.1* knockout digital defects are similar to

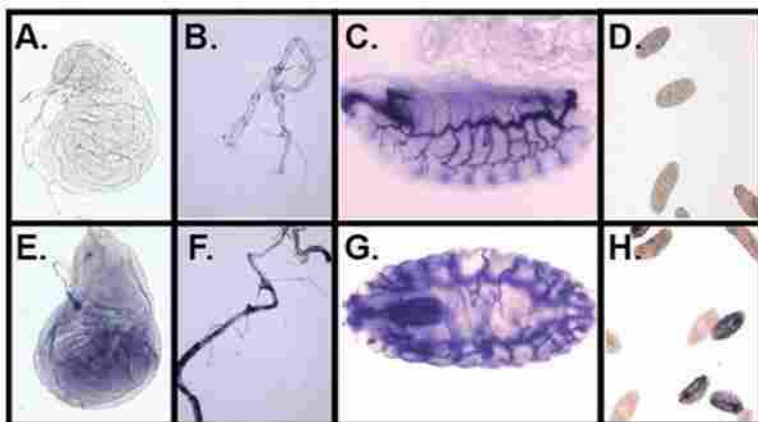
processes and vomer bones are reduced in size. In addition to the defects that were previously published, we found digit defects in all homozygous *Kir2.1* knockout animals (Figure 2-1). It has previously been reported that heterozygous *Kir2.1* animals appear normal. However, dissection of heterozygous *Kir2.1* mice revealed reduction in the size of anterior and posterior palatine processes and apparent decreased ossification in 98% of heterozygous pups (n=40) (Figure 2-1 C, D). By contrast, no palate or digit defects were found in wild-type siblings (n=41).

**Figure 2-1. Knockout of mouse *Kir2.1* causes cleft of the secondary palate and patterning defects of the skeletal digits.** (A-D) Ventral view of Alizarin Red (bone) staining of palates of newborn wild-type (A), *Kir2.1* knockout (B) and *Kir2.1* heterozygous knockout (C, D) pups. (E, F) Ventral view of wild-type palate (E) and *Kir2.1* knockout cleft of secondary palate (F). (G, H) Forelimb of wild-type (G) and *Kir2.1* knockout (H). (I, J) Ventral view of a wild-type (I) and *Kir2.1* knockout (J) forepaw. (K, L) Whole-mount forelimb skeletons from newborn animals stained with Alcian Blue and Alizarin Red: wild-type (K); preaxial digit duplication of the forelimb is shown in the *Kir2.1* knockout (L). The dorsal view

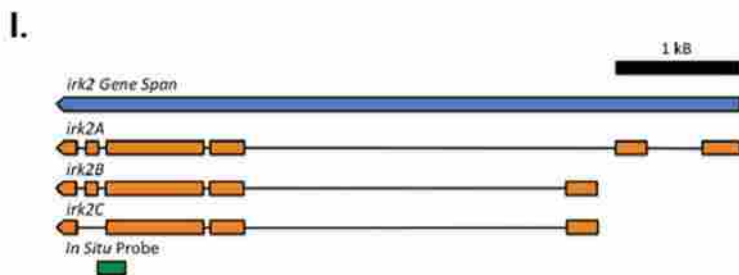
the BMP2/4 limb conditional knockout<sup>82</sup>. Other signaling pathways, such as Notch and Wnt, also contribute to these developmental processes<sup>83, 87, 92, 95</sup>. We tested the hypothesis that defective inwardly rectifying K<sup>+</sup> channels interfere with TGFβ/BMP signaling using the genetic tools of *Drosophila melanogaster*. The role of Dpp, a *Drosophila* BMP ligand, is well characterized in the wing<sup>101, 112</sup>, where *Drosophila* homologs of Kir2.1 are expressed (Figure 2-2)<sup>80</sup>. Thus, *Drosophila* provides an ideal system for investigating whether inwardly rectifying K<sup>+</sup> channel function is necessary for BMP signaling.

### ***Irk2* deficiency disrupts wing patterning**

To define the role of Irk2 in development, we examined the phenotypes of flies that lack *irk2* and the surrounding region from 19260K to 19350K of chromosome 3R (Figure 2-3). *Irk2*-deficient flies (*irk2DfA/irk2DfB*) were compared with wild-type flies. When *Irk2DfA/TM6* is mated to *irk2DfB/TM6*, more than the expected 33% of the progeny are *Irk2DfA/Irk2DfB*, indicating that Irk2 is not necessary for viability (n=380). The wings from *irk2*-deficient flies have wing venation defects: incomplete or branched posterior cross veins, incomplete L5 vein, bifurcations of L3 and L4 veins, and wing bristle transformations (Figure 2-4; Table 2-1).



**Figure 2-2. *irk2* expression.** (A-H) In situ with *irk2* sense (A,B,D) and *irk2* antisense (C, E-H) probes showing expression of *irk2* in the third instar larval imaginal wing disc (A,E), larval trachea (B,F), embryonic trachea and mouth hooks (C,D,G,H). We assayed for the presence of *irk2* mRNA transcripts in the embryo, the imaginal discs and other larval structures by in situ hybridization. An *irk2* antisense probe revealed that *irk2* is expressed in the *Drosophila* wing disc. *irk2* is also expressed in the embryonic larval trachea, mouth hooks and tracheal branches. (I) the location of the in situ probe is shown in a schematic.



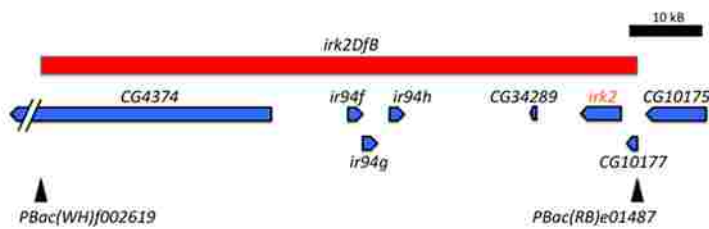


**Figure 2-3.** Map of genomic region including *irk2* showing the start and end points of each deficiency (*irk2DfA* and *irk2DfB*).

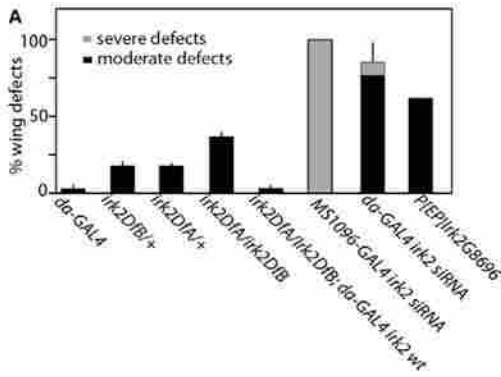
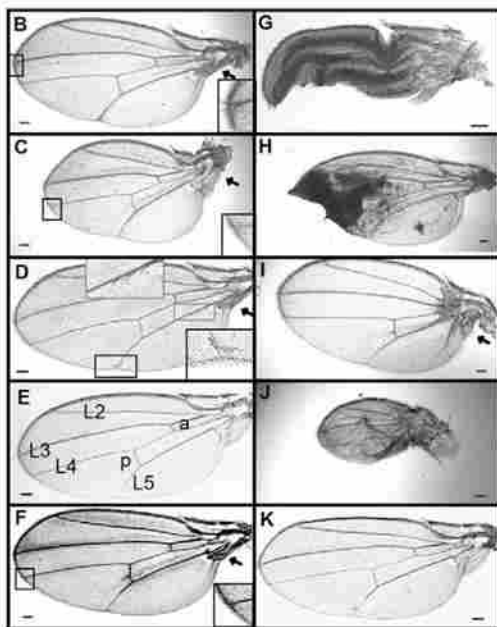


**Figure 2-4. Reduced *Irk2* function wing phenotypes.** (A) Quantification of wing defects when *irk2* function is decreased ( $n \geq 100$  flies). Error bars indicate s.e.m. (B) Bifurcation of L2 and L3 wing veins from *irk2DfA/irk2DfB* female. (C) Reduced wing size, angled hinge and bifurcation from L4 of *irk2DfA/irk2DfB* female. (D) Bristle transformations and incomplete L5 from male *irk2<sup>G8696</sup>*. (E) Wild-type male wing L2-5 longitudinal veins; anterior (a) and posterior (p) crossveins are labeled. (F) *irk2DfA/irk2DfB* male fly wing. (G) Wing expansion defects from *daughterless-GAL4; irk2 siRNA* female. (H) Ubiquitous expression of *irk2 siRNA* causes patches of wing tissue necrosis. (I) Small wing and hinge defects from *MS1096-GAL4; irk2 siRNA* female. (J) Small wing, hinge and venation defects from *MS1096-GAL4; Irk2 siRNA* male. (K) Rescued male *irk2DfA/irk2DfB; engrailed-GAL4; UAS-irk2<sup>WT</sup>* fly wing. Arrows indicate wing hinge defects. Scale bars: 100  $\mu$ m.



To verify that venation defects were the result of *irk2* deficiency, *irk2<sup>WT</sup>* was expressed ectopically in whole *Irk2*-deficient flies. Wing venation defects other than L5 defects are completely rescued by the ectopic expression of *Irk2<sup>WT</sup>*. Only 22% of wings of *irk2DfA/irk2DfB*;

*UAS-irk2<sup>WT</sup>* flies had L5 venation defects compared with 92% of *irk2*-deficient flies that had wing venation defects when raised under the same conditions (Table 2-1; Figure 2-4 F).

<b>Table 2-1. Wing venation defects</b>						
Genotype	L2	L3	L4	L5	Anterior crossvein	Posterior crossvein
<i>irk2DfB/irk2DfA</i> (n=192)	12%	21%	14%	92%	14%	9%
<i>irk2dfB/irk2DfA engrailed-Gal4 UAS-irk2WT</i> (n=50)	0%	0%	0%	37%	1%	0%
<i>engrailed-Gal4</i> (n=59)	1%	0%	0%	2.5%	0%	0%
<i>irk2dfB/irk2DfA actin-Gal4-irk2WT</i> (n=81)	0%	0%	0%	22%	0%	0%
<i>actin-Gal4</i> (n=59)	0%	0%	8%	0%	0%	0%
<i>irk2<sup>G8696</sup></i> (n=107)	2.8%	11%	36%	33%	0%	6.5%

Wing venation defects are quantified: in *irk2DfA/irk2DfB*, in the wing-specific rescue flies *engrailed-irk2WT*; *irk2dfA/irk2DfB*; in the ubiquitous rescue flies *actin-irk2WT*; *irk2df/irk2Df*; in *engrailed-GAL4* (control); and in *irk2<sup>G8696</sup>*. All flies represented are male.



To test for the tissue specificity of the requirement for *Irk2*, *irk2<sup>WT</sup>* was expressed using *engrailed-GAL4* in the posterior compartment of *irk2*-deficient wing discs. Wing L5 venation defects were decreased to 37% in flies that express exogenous *irk2<sup>WT</sup>* in an *irk2*-deficient background. All other *irk2<sup>Df/Df</sup>* wing defects were rescued by *engrailed-GAL4; UAS-Irk2<sup>WT</sup>* (Figure 2-4 F,K), indicating that loss of *irk2* function is responsible for wing venation phenotypes and the requirement is partially fulfilled if *irk2* is expressed in the posterior compartment of the wing. As a comparison, only 4% of the male flies harboring the *engrailed-GAL4* driver without the *irk2* transgene had wing venation defects (Table 2-1). We verified that endogenous *irk2* was deleted and that exogenous *Irk2* was provided in rescued flies by amplifying *irk2* DNA from single flies with primers specific to either genomic *Irk2* or the *UAS-irk2* transgene (Figure 2-4). These data show that *irk2* is required non-cell-autonomously in the wing disc to specify wing venation patterning and that the loss of *irk2* is responsible for venation phenotypes that are observed in *irk2*-deficient flies.

### ***Irk2 siRNA expression disrupts wing patterning***

To characterize the tissue-specific requirement for *Irk2*, we expressed small-interfering *irk2 RNA* (siRNA) under the control of either ubiquitous (*daughterless*) or wing-directed (MS1096) GAL4 drivers. When *irk2 siRNA* was expressed ubiquitously using *daughterless-GAL4*, we found defects in 84% of the wings: 73% of the wings had venation defects, 9% failed to expand correctly (Figure 2-4 G) and 4% of the wings had tissue necrosis (Figure 2-4 H). Wing-directed expression of *irk2 siRNA* causes reduction in wing size, wing venation defects and hinge defects that result in the held-out wings phenotype for all surviving flies (Figure 2-4; Figure 2-5). We designated venation defects and reduction in wing size as moderate defects; any additional defects are designated as severe. Male flies that express *Irk2 siRNA* have more severe

wing phenotypes than female flies of the same genotype. Ubiquitous expression of *irk2 siRNA* can lead to wing expansion defects, whereas wing-directed *irk2 siRNA* does not. The difference in phenotypes suggests that expansion of the wing requires Irk function outside the wing whereas patterning requires Irk channel function in the wing disc itself.

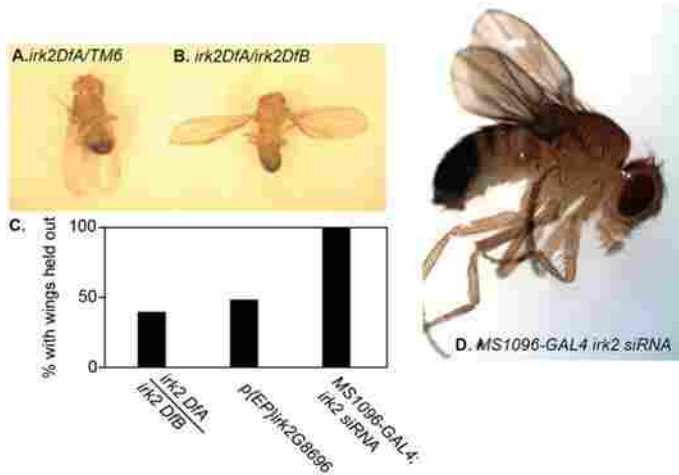


**Figure 2-5. Reducing function of *irk2* causes hinge defects similar to the Dpp ‘wings held-out’ phenotype.** (A) Heterozygous *irk2Df/+* with wild-type wing hinge. (B) The wings held out phenotype of *irk2DfA/irk2DfB* male fly. (C) Graph showing prevalence of the wings held out phenotype for the *irk2DfA/irk2DfB*, MS1096-GAL4; *irk2 siRNA*. (D) Side view of the hinge defect that results in the wings held-out phenotype of a MS1096-GAL4; *irk2 siRNA* male fly.

Phenotypes that result from

ubiquitous or wing-directed expression

of the *irk2 siRNA* are more severe and more penetrant than phenotypes associated with *irk2* deficiency. We reasoned that expression of *irk2 siRNA* could affect the transcription of other *irk* subunits (*irk1* and *irk3*). To determine whether *irk2 siRNA* changed the expression of *irk1* and *irk3*, we used quantitative RT-PCR to quantify *irk1*, *irk2* and *irk3* mRNA from flies that ubiquitously express *Irk2 siRNA* and compared mRNA levels with those from flies with the *daughterless-GAL4* driver without the *irk2 siRNA* transgene. *irk2 mRNA* is reduced 85.7% in flies that express *irk2 siRNA* demonstrating that the *irk2 siRNA* effectively reduces expression of *irk2*. Surprisingly, *irk1* was increased 14-fold and *irk3* mRNA levels are increased 4.6-fold in flies that express the *irk2 siRNA* (Figure 2-6).

To determine whether a similar increase in *irk1* and *irk3* expression occurred in *irk2*-deficient flies, we compared *irk1*, *irk2* and *irk3* mRNA levels in wild-type and *irk2*-deficient flies. As expected, no *Irk2* mRNA was detected in *irk2*-deficient flies. *irk3* mRNA levels

increased 3.4-fold, but *irk1* transcript levels were not significantly different in *irk2*-deficient flies compared with wild-type flies (Figure 2-6 B). Phenotypes of the *irk2*-deficient wings are less severe than those of *irk2 siRNA*. This leads to the conclusion that Irk subunits are not entirely functionally equivalent.

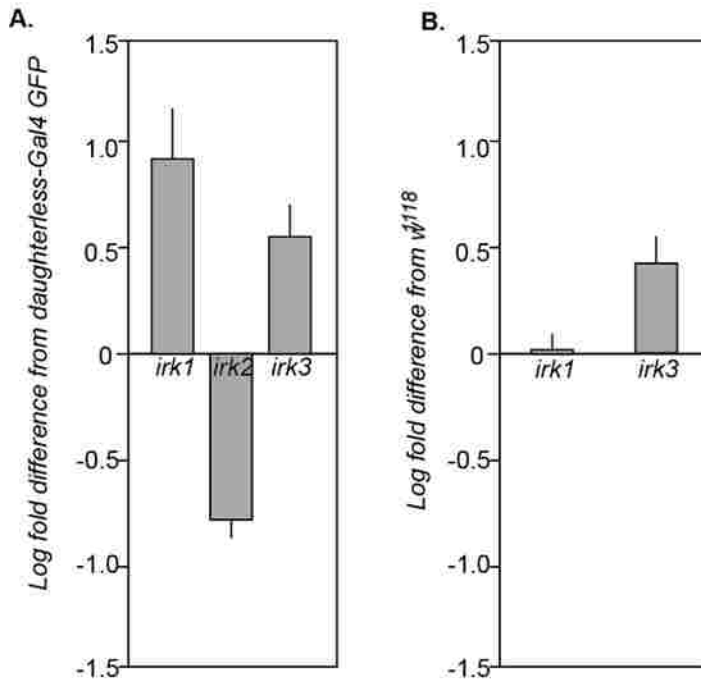


**Figure 2-6. Reducing function of *irk2* increases expression of other *irk* subunits.** Quantitative RT PCR of *irk1*, *irk2* and *irk3* transcripts isolated from *daughterless-GAL4; irk2 siRNA* compared with *daughterless-GAL4; GFP* (A) and *irk1*, and *irk3* transcripts from *irk2DfA/irk2DfB* compared with Berlin<sup>w118</sup>. Error bars represent s.e.m. Graph represents five independent experiments (B).

To block the function of the entire Irk channel, we generated a dominant-negative Irk2 subunit.

### Expression of dominant-negative Irk2 causes severe wing defects

Inwardly rectifying K<sup>+</sup> channel subunits can form heterotetrameric channels in mammals. Incorporation of a single subunit with a mutated selectivity filter (GYG to AAA) into the complex completely blocks ion flow through the channels in mammals<sup>81</sup>. We used the UAS/GAL4 system to express dominant-negative Irk transgenes to block the Irk channel in a tissue- and time-specific manner. A transgenic animal expressing this *Irk2* (*Irk2DN*) gene is expected to demonstrate the effects of the loss of the entire channel. By contrast, in an *irk2 null*, *irk1* and *irk3* could theoretically form a functional channel without *irk2*, thereby at least partially compensating for reduced *irk2* function. We generated three transgenic *Irk2DN* lines:

*Irk2DN5.1*, *Irk2DN5.2* and *Irk2DN13*. Ubiquitous expression of *Irk2DN* or *Irk2WT* was accomplished by mating transgenic *UAS-irk2WT*/balancer and *UAS-Irk2DN*/balancer flies with *actin-GAL4* or *daughterless-GAL4* transgenic flies. An approximately equal number of transgenic and balancer adult progeny result from the *UAS-irk2WT* cross. No *Irk2DN5.1*- or *Irk2DN5.2*-expressing flies survive from the *UAS-Irk2DN* cross whereas over 90 balancer sibling adults survive (Figure 2-7 A). *Irk2DN13*- expressing flies survive to adulthood when raised at 25°C, but only 20% of *Irk2DN13* survive when flies are raised at 18°C. Larvae that express *Irk2DN* are marked with *actin-GFP* and can be compared in survival to their balancer siblings after hatching. Only 17% of the larva expected to ubiquitously express *Irk2DN* hatch and none of these survive 48 hours after hatching (Figure 2-7 B). Endogenous *Irk2* functions in the developing wing, so we directed expression of *Irk2DN* to block *Irk* channels in the wing disc.

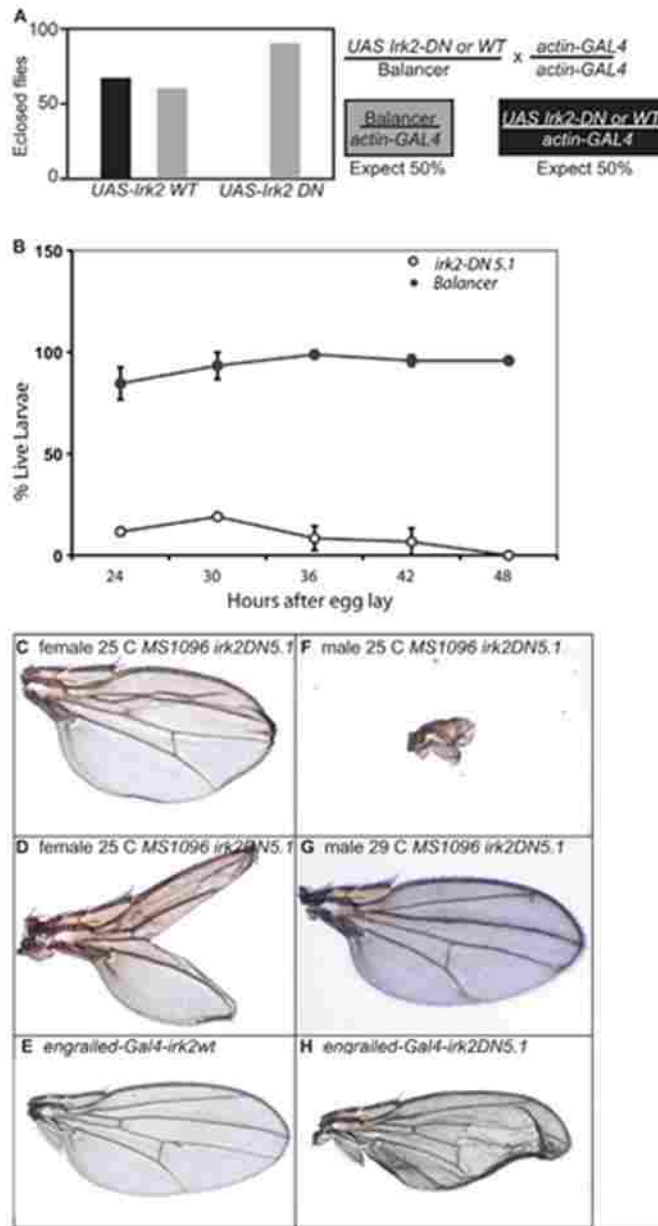


**Figure 2-7. Phenotypes of flies expressing *Irk2DN*.** (A, B) Graphs of adult (A) and larval (B) survival of *actin-GAL4; UAS-irk2WT*, *actin-GAL4; UAS-Irk2DN* and siblings without transgene. Error bars indicate s.e.m. (C) L2-3 fusion in wing from MS1096-GAL4; *Irk2DN5.1* female at 25°C. (D) Bifurcated wing from MS1096-GAL4; *Irk2DN5.1* at 25°C. (E) *engrailed-GAL4; UAS-irk2WT*. (F) Wing of MS1096-GAL4; *Irk2DN5.1* male at 25°C. (G) MS1096-GAL4; *UAS Irk2DN5.1* at 29°C. (H) *engrailed-GAL4; UAS Irk2DN5.1* at 25°C.

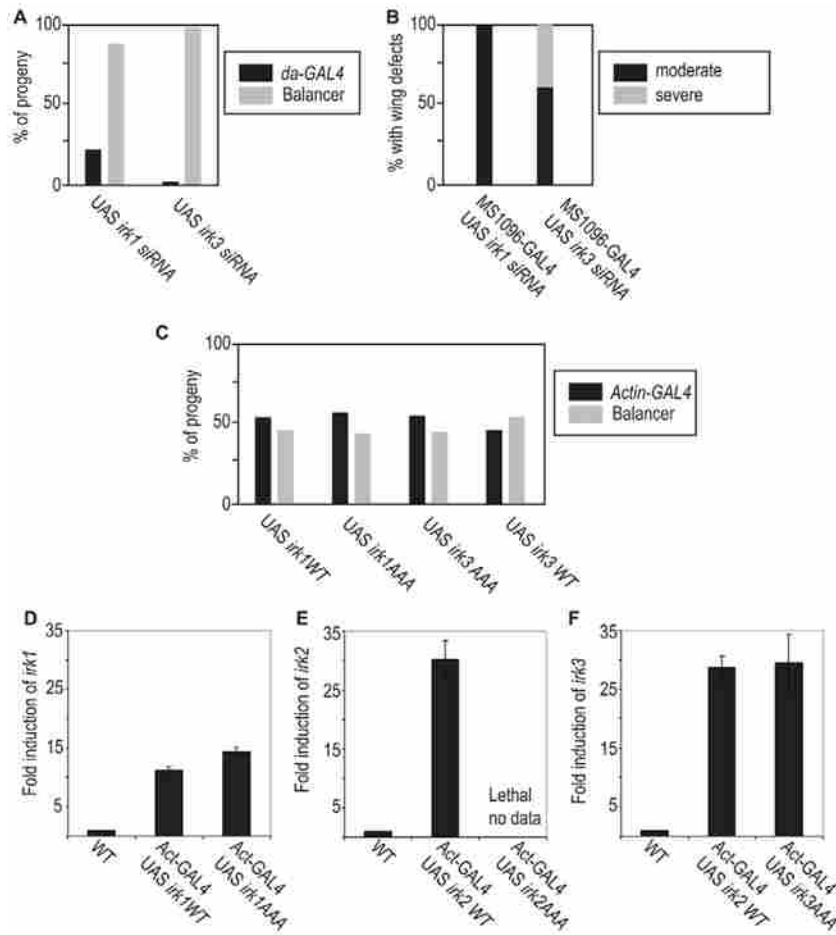


**Figure 2-8. Irk1 and Irk3 siRNA phenotypes.** (A) Ubiquitous expression of Irk1 and Irk3 siRNA causes lethality. (B) Wing-directed *irk1* and *irk3* siRNA causes wing venation defects and a reduction in wing size. (C) Irk1-AAA or Irk3-AAA ubiquitous expression does not decrease survival. (D) Quantification of Irk1 mRNA in wild-type, *actin-GAL4-UAS; irk1*WT and *actin-GAL4-UAS; Irk1AAA*. (E) Quantification of Irk2 mRNA in wild-type, *actin-GAL4-UAS; irk2*WT and *actin-GAL4-UAS; Irk2AAA*. (F) Quantification of Irk3 mRNA in wild-type, *actin-GAL4-UAS; Irk3*WT and *actin-GAL4-UAS; Irk3AAA*. Data are mean±s.e.m.

All of the flies that express *Irk2DN* in transgenic line 5.1 have wing defects with 6% of the wings classified with moderate defects and 94% with severe defects. Expression of *Irk2DN* in transgenic line 5.2 resulted in 42% moderate wing defects and 4% severe defects (Figure 2-9 G). Less than 25% of MS1096-GAL4; *UAS-irk2*WT flies have minor venation defects, similar to

MS1096-GAL4 without a UAS transgene. Expression of *Irk2DN5.2* using the *engrailed-GAL4* driver causes wing venation and blistering defects, whereas expression of *irk2WT* with the same driver does not cause defects (Figure 2-7 E, H). As *Irk2DN* expression causes defects that are more severe than loss of *Irk2*, we conclude that Irk2 forms a heteromeric channel that is necessary for patterning of the adult wing in *Drosophila*. We reasoned that heteromeric channels could be made up of a combination of Irk1, Irk2 and/or Irk3 subunits. Thus, Irk1 and Irk3 could form a partially functional channel when lacking the Irk2 subunit. If this was the case, we would expect that reduced *irk1* and *irk3* function should cause similar phenotypes to *irk2Df*, *siRNA* or *Irk2DN*. Ubiquitous expression of *irk1 siRNA* results in 88% lethality and ubiquitous expression of *irk3 siRNA* results in 98% lethality (n=145) (Figure 2-8 A). As *irk2*-deficient flies survive to adulthood, it is likely that Irk1 and Irk3 play a more substantial role in embryonic development than does Irk2. It is likely that ubiquitous expression of *Irk2DN* causes embryonic lethality by blocking the function of a heteromeric channel that includes Irk1 and/or Irk3.

To examine the contribution of Irk1 and Irk3 to the development of the wing, we expressed *irk1* and *irk3 siRNA* in the wing with MS1096-GAL4. Wing-directed expression of Irk1 and Irk3 siRNA in the wing results in venation defects in 100% of wings from animals of both genotypes (n=117 and n=92, respectively) (Figure 2-8 B). Expression of *Irk3 siRNA* caused a reduction in wing size and hinge defects in addition to venation defects in 40% of the wings. Wing defects that result from reduced *irk1* and *irk3* support the conclusion that Irk1, Irk2 and Irk3 form a heteromeric channel that is necessary for wing development.

To determine if the conserved GY (F) G of Irk1 and Irk3 play the same structural role as for Irk2, we generated mutant alleles of both, changing the conserved GY (F) G to AAA. Ubiquitous expression of *irk1-AAA*, *irk1WT*, *irk3-AAA* or *irk3WT* did not decrease survival or

cause wing defects (n=127 *Irk1-AAA*, 129 *Irk1WT*, 132 *Irk3-AAA* and 124 *Irk3WT*) nor did wing-directed expression of mutant *irk1-AAA* or *irk3-AAA* cause wing defects (n=107 and 113) (Figure 2-8). We ensured that the *Irk2DN* and *Irk2WT* constructs were expressed using QRT-PCR (n=3 trials) (Figure 2-8 D-F). We conclude that Irk1, Irk2 and Irk3 are important to channel function, but play different structural roles in the heteromeric Irk channel.

### ***Reduced Dpp signaling enhances Irk2DN phenotypes***

Disruption of *irk2* function with siRNA, *irk2* deficiency or expression of *Irk2DN* causes defects in the wing that are similar to defects caused by compromised Dpp signaling<sup>102-103, 113-116</sup>. A possible explanation for Irk2 developmental defects is that Irk channels are necessary for proper Dpp signaling. We undertook genetic interaction studies by disrupting the function of Dpp (BMP ligand) or Thickveins (Tkv, BMP type I receptor) in an *Irk2DN* background.

To determine how defective Dpp signaling affects the *Irk2DN* wing phenotype, either the *Irk2DN* or the *irk2WT* transgene was expressed in wings of *dpp<sup>hr92/+</sup>* or *tkv<sup>7/+</sup>* flies. Owing to differences in phenotype severity, we report defects from females only. Defective Dpp signaling enhances *Irk2DN* phenotypes (Figure 2-9).



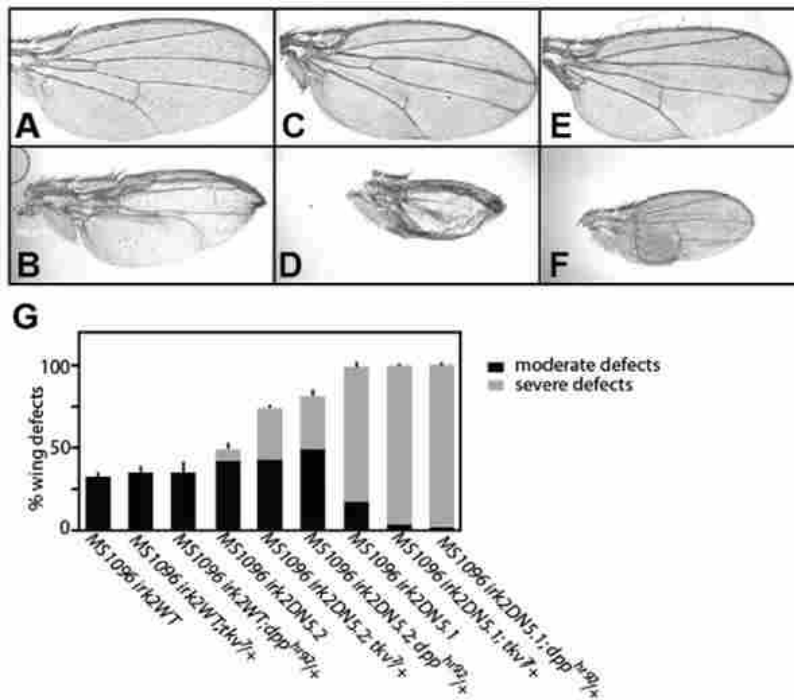


**Figure 2-9. Reduced Dpp or Thickveins function enhances *Irk2DN* phenotypes.** (A, B) *Irk2DN5.2* female incomplete L5. (C) Thickened, bifurcated veins of *dpp*<sup>hr92/+</sup> female wing. (D) *Irk2DN5.2/+*; *dpp*<sup>hr92/+</sup> female wing is small and missing veins. (E) Thickened, bifurcated L2, L3 and L4 veins, and incomplete anterior crossvein of *tkv*<sup>7/+</sup> female wing. (F) *Irk2DN5.2/+*; *tkv*<sup>7/+</sup> female wing is small and missing veins. (G) Quantification of wing defects of MS1096-GAL4; *UAS-irk2*WT, *UAS-Irk2DN5.1*; *UAS-Irk2DN5.2* and with *dpp*<sup>hr92/+</sup> or *tkv*<sup>7/+</sup>. n>100 for all genotypes. Data are mean±s.e.m.

When *Irk2DN5.2* is expressed in a *tkv*<sup>7/+</sup> mutant background, total wing defects increased from 46% to 72%. When *Irk2DN5.2* is expressed in a *dpp*<sup>hr92/+</sup> background, 84% of flies have wing defects and 29% are severely defective, whereas without compromised Dpp signaling, only 4% are classified as severe in the *Irk2DN5.2* line (Figure 2-9). In the more severe *Irk2DN5.1* transgenic line, 94% of flies have severe wing defects and when *Irk2DN5.1* is expressed in a *tkv*<sup>7/+</sup> background, 99% of the flies have severe wing defects. Similarly, 97% of flies have severe wing defects in *Irk2DN5.1*; *dpp*<sup>hr92/+</sup> flies. Expression of the wild-type *Irk2* transgene caused minor wing venation defects in 20% of the flies, but these defects did not increase in penetrance or severity when the transgene was expressed in the *dpp*<sup>hr92/+</sup> or *tkv*<sup>7/+</sup>

background (16% and 15%, respectively). Thus, *Irk2DN* phenotypes are enhanced by reducing function of Dpp or its type 1 receptor, Tkv.

### ***Dpp signaling is disrupted by aberrant Irk2 function***

Enhancement of *Irk2DN* phenotypes by reduced Dpp or Tkv function suggests that Dpp signaling is compromised in flies with defective Irk channel function. To explore this possibility, we looked at Dpp signaling in the larval wing imaginal disc, a precursor to the adult wing. Dpp-bound Tkv phosphorylates the C-terminal of Mothers against Dpp (Mad) in two stripes that form the border between the anterior and posterior compartments of the wing disc<sup>117</sup>.

To determine whether Dpp signaling is interrupted by disruption of *irk2* function, we used an antibody to measure phosphorylation of the C-terminal site of Mad (p-Mad). Two stripes of p-Mad are intact in *irk2 deficient* and *irk2 siRNA*-expressing wing discs, but the stripe intensity is lessened compared with wild type (Figure 2-10). TUNEL staining shows that reducing function of *irk2* does not cause apoptosis, and therefore is not the cause of decreased p-Mad (Figure 2-10). Spalt (Sal), a transcriptional target of Dpp, was reduced in *irk2DfA/irk2-DfB* wing discs and was not detectable in *Irk2DN*-expressing wing discs, supporting the conclusion that Dpp signaling is disrupted by blocking Irk channels (Figure 2-11). By contrast, patterns of two genes that are not regulated by Dpp, *wingless* and *achaete*, are intact in *irk2*-deficient wing discs (Figure 2-11).

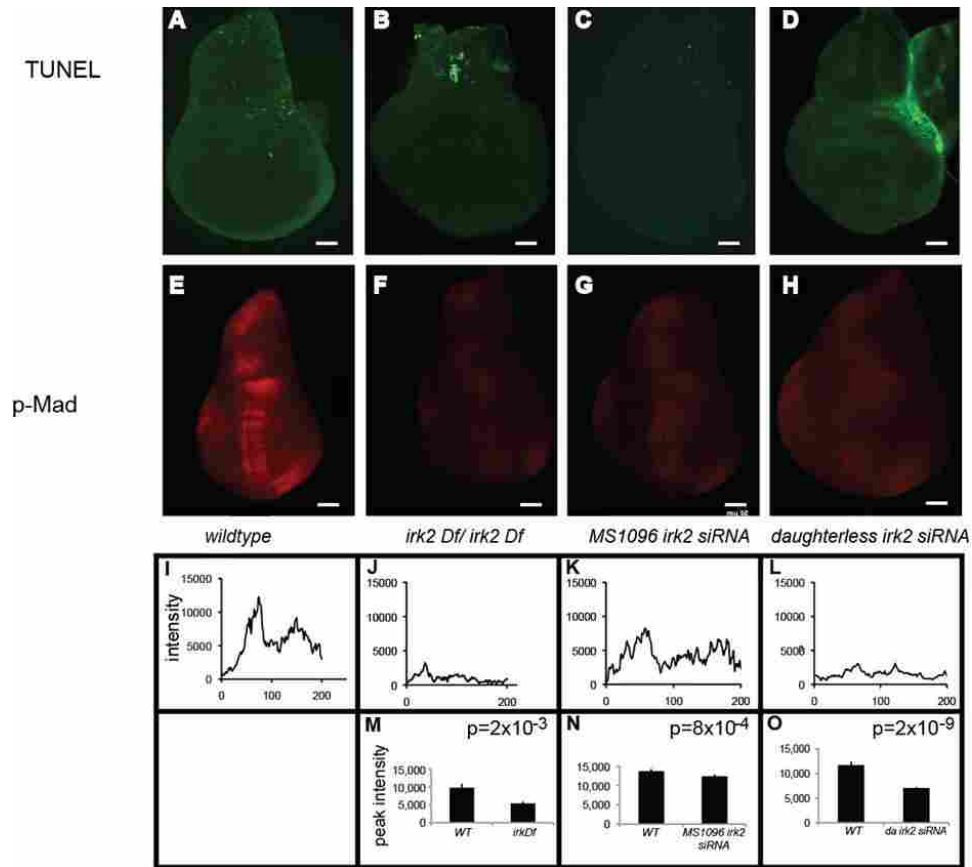


**Figure 2-10. Reduced Mad phosphorylation in *Irk2DfA/Irk2DfB* and *Irk2* siRNA wing discs.** (A-D) TUNEL-stained wing discs. Anterior is rightwards. (E-H) Anti-p-Mad stained wing discs. (I-L) Relative fluorescence intensity across a posterior to anterior cross-section of the anti-p-Mad-stained wing disc shown in E-H. (M-O) Graphs of average peak intensity of control and *irk2DfA/irk2DfB* (M), control and *MS1096-GAL4;UAS irk2 siRNA* (N), and control and *daughterless-GAL4;irk2 siRNA* (O). Control and experimental discs were stained and imaged in parallel. Graphs represent average peak intensities for  $n > 7$  anti-p-Mad-stained discs. Peak intensity is determined by subtracting minimum from maximum fluorescence intensity in a posterior to anterior cross-section of the anti-p-Mad stained wing disc. Data are mean  $\pm$  s.e.m. Scale bars: 50  $\mu$ m.

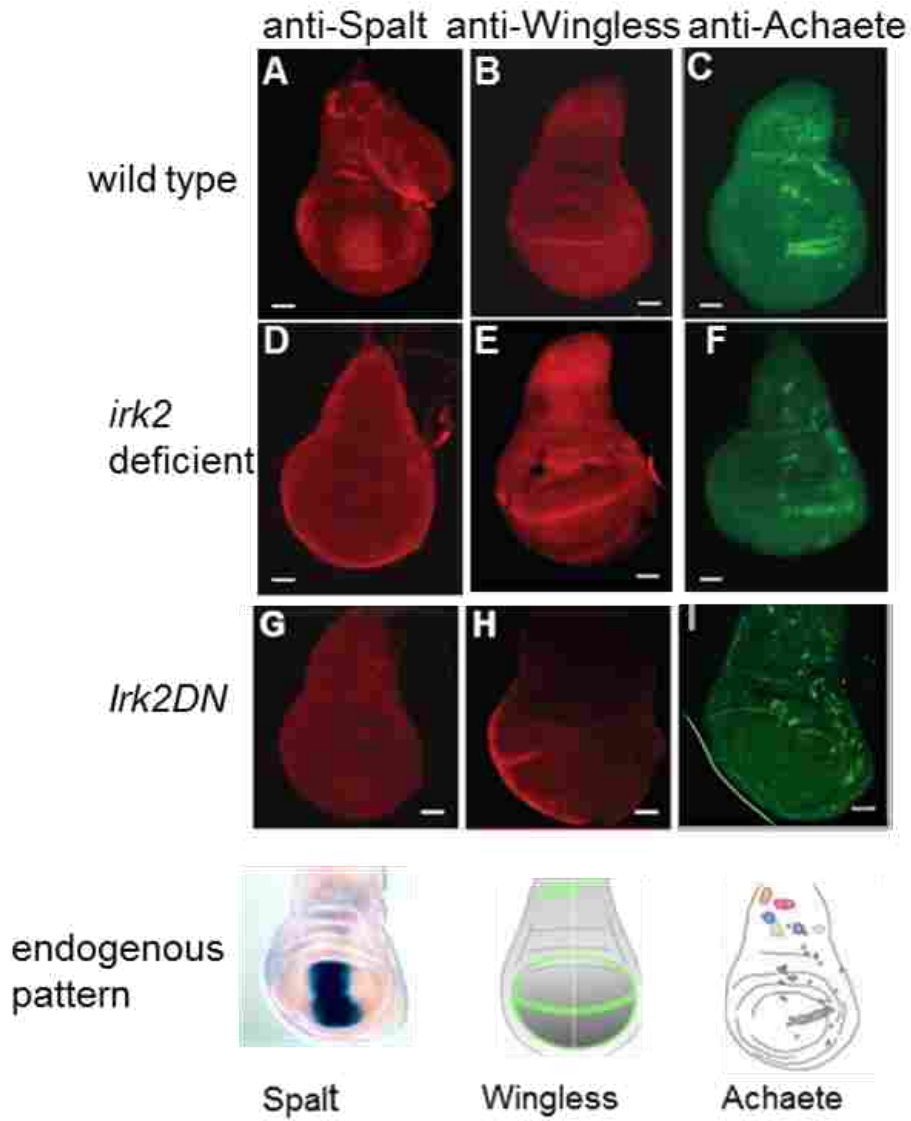


**Figure 2-11. Immunohistochemistry demonstrates that Dpp signaling is reduced in *Irk2DN* and *Irk2DfA/Irk2DfB*.** Wild-type wing discs (A-C), *irk2DfA/irk2DfB* (D,E) and *Irk2DN5.1* (G-I) stained with anti-Spalt (A,D,G), anti-Wingless (B,E,H) and anti-Achaete (C,F,I). (Bottom row) endogenous expression pattern of Spalt<sup>118</sup>, Wingless<sup>119</sup> and Achaete<sup>120</sup>. Scale bars: 50µm.

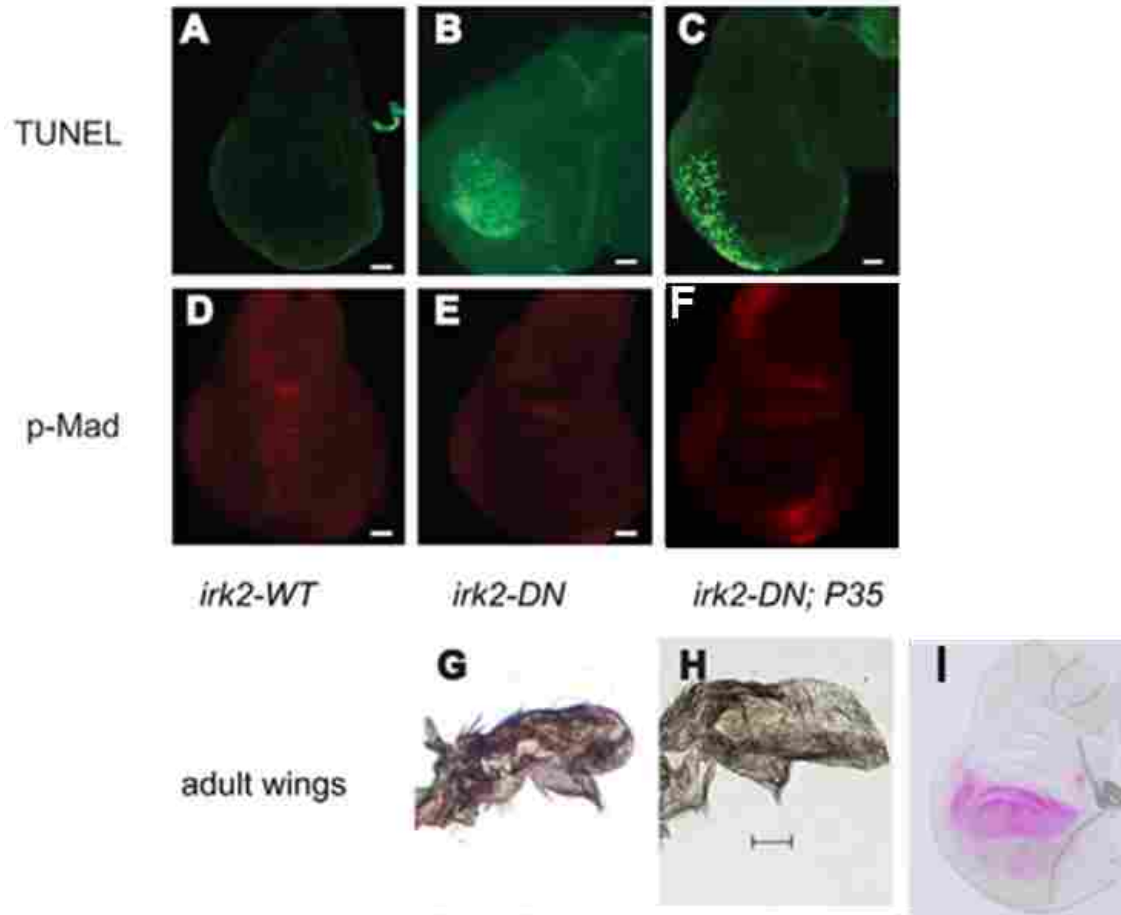


**Figure 2-12. *Irk2DN* expression causes apoptosis and eliminates p-Mad staining in the third instar larval imaginal wing disc.** (A-C) TUNEL stained wing disc. (D-F) Anti-p-Mad stained wing disc. (A, D) MS1096-GAL4-*Irk2*WT. (B, E) MS1096-GAL4;*UAS-Irk2DN*. (C, F) MS1096-GAL4-*UAS-Irk2DN*; *P35*. n>10 discs. (G) MS1096-GAL4-*UAS-Irk2DN*; *P35* male wing. (H) Control MS1096-GAL4-*UAS-Irk2DN* male wing. (I) MS1096-Gal4; *UAS-GFP* showing the wing pouch specific expression of MS1096 Gal4 promoter. Scale bars: 50  $\mu$ m.

Expression of *Irk2DN* causes the most severe wing phenotypes and is predicted to block the Irk channel completely. We found that when MS1096-Gal4 drives expression of *Irk2DN*, phosphorylation of Mad is completely blocked in the anterior/posterior boundary of wing pouch (Figure 2-12 E). P-Mad staining was intact when flies expressed the *irk2*WT transgene. *Irk2DN* expressed by other wing- directed Gal4 drivers<sup>121</sup>, *en-Gal4*; *Irk2DN5.1*, *A9-Gal4*; *Irk2-DN13* and *A9-Gal4*; *Irk2-DN5.1*, also profoundly decreases p-Mad staining and can decrease the size of

the wing disc (Figure 2-13). Less than 5% of *en-Gal4; Irk2-DN5.1* and *A9 Gal4-DN5.1* flies survive past early larval stage.

*MS1096-Gal4; UASIrk2DN5.1* wing discs are fragile and thinned in the wing pouch region that becomes the wing blade and hinge. TUNEL staining shows that apoptosis occurs in the wing pouch of *MS1096-Gal4; UASIrk2DN* wing discs. Very little apoptosis is detected in the wing discs of flies expressing *irk2WT* (Figure 2-12). In *Irk2DN*-expressing wing discs, *wingless* and *achaete* patterns are normal surrounding the region that dies via apoptosis (Figure 2-11).

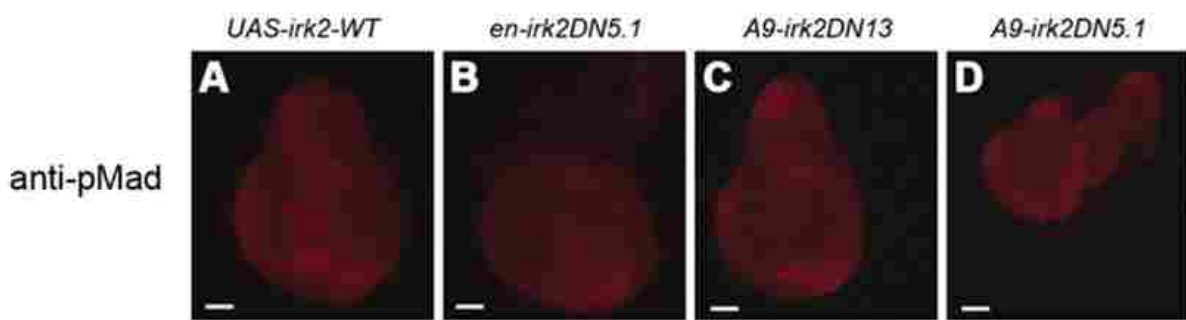


**Figure 2-13. Expression of *Irk2DN* using wing-directed Gal4 drivers decreases anti-p-Mad staining.** Wing discs of third instar larva stained with Anti-phospho-Smad 1/5 antibody (A) *en-Gal4; UAS-irk2WT*. (B) *A9-Gal4; UAS-irk2DN13*. (C) *A9-Gal4; UAS-irk2DN13* (D) *A9-Gal4; UAS-irk2DN5.1*

Disruption of the  $K^+$  current with *Irk2DN* causes complete loss of the two stripes of p-Mad that form the proximal-distal axis of the wing disc and also causes apoptosis of many of the cells that are under the influence of the Dpp signal. At least two possibilities explain these phenotypes. First, as Dpp protects against apoptosis in the wing<sup>103-104, 122-125</sup>, blocking the  $K^+$  current could interfere with Dpp signaling, leading to apoptosis and wing defects. Alternatively, blocking *Irk* could directly cause apoptosis, leading to reduced Dpp signaling. To test which of these possibilities explains *Irk2DN* wing defects, we blocked apoptosis in cells of the wing discs

that express *Irk2DN* and asked whether Dpp signaling occurs and whether the wing defects are rescued. P35 is a baculovirus protein that acts as pan-caspase inhibitor that suppresses the apoptosis<sup>126-127</sup>. Exogenous expression of P35 blocks caspase activity, preventing apoptosis<sup>126</sup>. TUNEL staining confirmed that apoptosis does not occur in the wing pouch cells that express both *Irk2DN* and *P35* (Figure 2-12). Wing pouch cells give rise to the wing blade. The severe wing phenotypes of *MS1096-GAL4-Irk2DN; P35* are indistinguishable from those of wings that express only *Irk2DN* (Figure 2-12). As blocking apoptosis in the wing pouch does not rescue the wing phenotype, we conclude that apoptosis is fully responsible for wing blade defects. Apoptosis occurs in periphery of the wing disc, but not in the center where both P35 and *Irk2DN* are expressed. Therefore, *Irk2DN* does not cause apoptosis cell- autonomously, but could cause apoptosis of peripheral cells by compromising a Dpp gradient<sup>122</sup>. Together, these data suggest that Dpp signaling is disrupted by *Irk2DN*, which leads to apoptosis and *Irk2DN* wing defects.

## DISCUSSION

The morphological defects associated with ATS suggest that Kir2.1 function is necessary for human development. We and others have shown that these defects are recapitulated in a mouse knockout of Kir2.1<sup>48</sup>. Here, we show that reducing function of the *Irk2* ion channel causes developmental defects in reducing function in *Drosophila*, probably by disrupting Dpp signaling. Four points support this conclusion. First, mouse and fly Kir2.1/*Irk2* phenotypes are similar to TGF $\beta$ /BMP mutant phenotypes. Second, reduced Dpp signaling enhances *Irk2DN* phenotypes. Third, phosphorylations of Mad and Spalt expression are decreased in mutant *Irk2* wing discs. Last, *Irk2DN* induces apoptosis of cells within the region of Dpp influence, but outside the region of *Irk2DN; P35* expression.

Our data show that the *Drosophila* Irk channel is heteromeric. Loss of any Irk subunit alone causes minor defects compared with severe defects caused by an *Irk2DN* subunit predicted to block the channel. This suggests that, in the absence of one Irk subunit, the others partially compensate.

*Irk2* phenotypes are more severe and penetrant when flies develop at colder temperatures, regardless of the mechanism by which Irk2 function is reduced: transgenic *Irk2DN* expression, *irk2* deletion, p-element insertion or *irk2 siRNA* expression. We observed this temperature effect for three independent *Irk2DN* transgenic lines under the control of many different GAL4 drivers. Although the GAL4 system generally increases transgene expression at higher temperatures, *Irk2DN* phenotypes are most severe at 18°C, less severe at 25°C and least severe at 29°C. This suggests that the process by which Irk channels contribute to signaling is dependent on temperature.

*Irk2* phenotypes are reminiscent of mutant *dpp*, *tkv* and *punt* wing phenotypes<sup>103, 128-130</sup>. The L2-3 and L4-5 collapse and loss of the majority of the wing blade are similar to mutant *dpp* or its target, optomotor-blind (*omb*)<sup>113, 116, 131</sup>. *irk2*-deficient flies, mutant *irk2* and *irk2 siRNA* flies have similar hinge phenotypes to those caused by mutant *dpp* alleles<sup>102, 114-115</sup>. Furthermore, *Irk2DN* phenotypes are enhanced by reducing function of Dpp or its receptor. Together, these data suggest that *irk2* wing phenotypes can be explained by disruption of Dpp signaling.

Reducing function of *irk2* by deletion, siRNA or *Irk2DN* reduces p-Mad in the wing disc. We confirmed that loss of *irk2* reduces Dpp signaling by measuring decreased levels of Spalt, a p-Mad transcriptional target. Activation of the Wg pathway negatively regulates Dpp signaling by reducing perdurance of p-Mad, presenting the possibility Wg is affected by Irk2<sup>132-134</sup>.



Expression of both *wingless* and *achaete* are normal in *irk2*-deficient wing discs and outside the region where cells have died via apoptosis in *Irk2DN*-expressing wing discs. However, we have not ruled out the possibility that Wingless or other developmental pathways are also affected by Irk channel function.

We find that blocking apoptosis in the cells that express *Irk2DN* does not rescue the associated wing phenotypes. A wing can develop with normal size and patterning after x-irradiation-induced apoptosis of half of the wing disc cells during development<sup>126, 135-138</sup>. Dpp signaling is responsible for compensation for the lost apoptotic cells and preservation of patterning in damaged wing discs<sup>137</sup>. The failure of *Irk2DN; P35*-expressing discs to compensate for apoptotic cells supports the hypothesis that Dpp signaling is disrupted in tissues that express *Irk2DN*.

How could Irk2 affect Dpp signaling? It could be that maintenance of membrane potential is important for the production, distribution or propagation of the Dpp signal. Alternatively, there may be communication between Irk channels and the Dpp signaling cascade upstream of Mad activation. Distribution and propagation of Dpp and other BMP/TGF $\beta$  signals are aided by the heparan sulfate proteoglycans (HSPGs)<sup>139-142</sup>. Changes in sodium concentrations inhibit sulfation of heparan sulfate and reduce the sensitivity of cells to FGF. It is interesting to speculate that a change in local K<sup>+</sup> concentrations could interfere with HSPGs, receptor localization, stabilization of the receptor complex, phosphorylation events or production or distribution of the Dpp ligand (Figure 2-14). It is also possible that Mad requires K<sup>+</sup> for recruitment to the membrane as actin requires Ca<sup>++</sup> for that purpose<sup>143</sup>. We have not directly established whether Irk2 is required cell-autonomously, but we favor the model that Irk2 function is required for Dpp signaling events outside the cell rather than for intracellular

phosphorylation for two reasons. First, *en-GAL4* expresses *UAS-irk2<sup>WT</sup>* in the posterior compartment of the wing disc, but rescues *irk2* deficient phenotypes in the whole wing. Second, when *Irk2<sup>DN</sup>* and *P35* are expressed together, apoptosis occurs well outside of the region of MS1096 expression, consistent with morphogen causation.

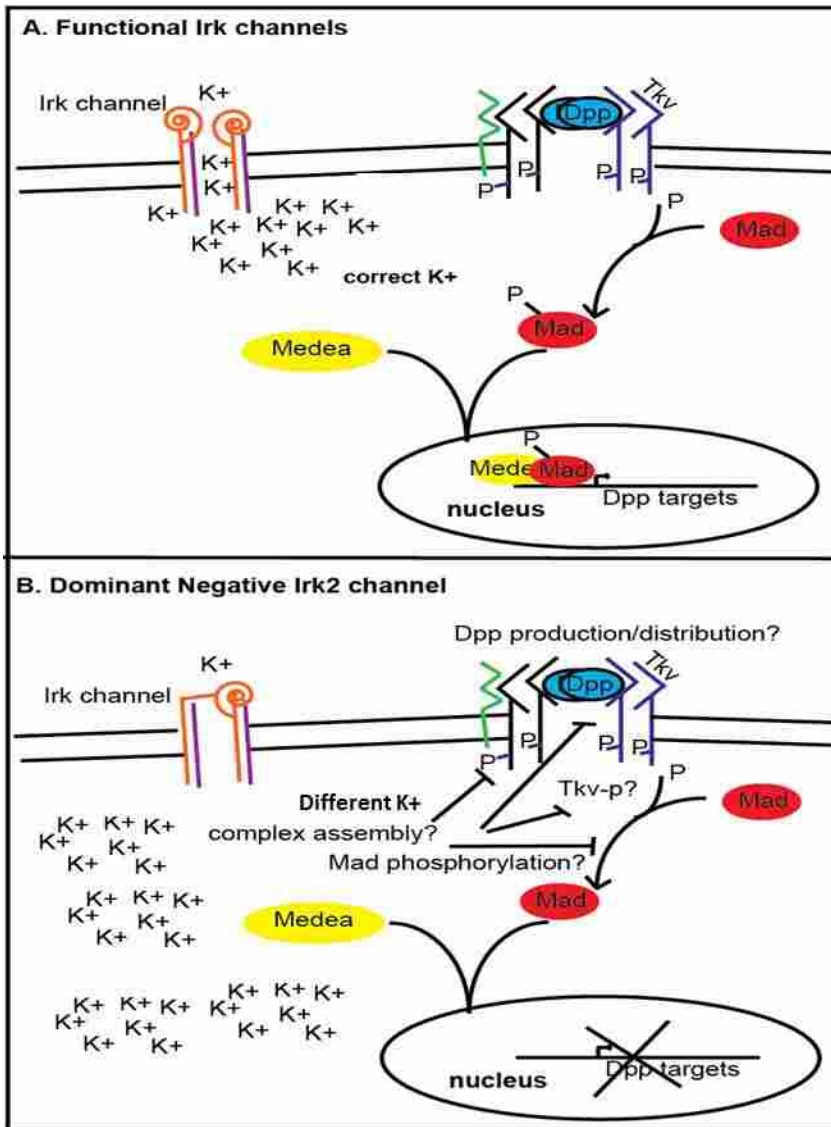


**Figure 2-14. Model for Irk channels in Dpp signaling.** (A) With functional Irk channels, Dpp binds type 1 (Thickveins) and type 2 (Punt) kinase receptors that are stabilized by proteoglycans (Dally, not shown). Upon Dpp binding, activated type 1 receptors phosphorylate Mad. P-Mad binds Medea and enters the nucleus to affect transcription. (B) Blocking Irk channels hinders Mad phosphorylation. Irk channels could be necessary for Dpp production/distribution, receptor complex stabilization or Tkv/Mad phosphorylation.

If inwardly rectifying K<sup>+</sup> channels are necessary for Dpp signaling to designate wing patterning, how could Irk subunits have been missed in Dpp modifier screens? The partial redundancies of the Irk subunits make severe phenotypes unlikely unless all of the subunits are compromised. Phenotypes are not severe at 25°C, the temperature at which development occurs for most screens. Third, the necessity of Irk2 seems to be tissue specific. Dpp is required for patterning of multiple structures, but in screening multiple GAL4 drivers, expression of *Irk2DN* causes defects in only a few of these.

Many BMP/TGFβ-dependent processes go awry when Kir2.1 is not functional in humans and in mice. The phenotypes of Kir2.1 knockout mice are reminiscent of the morphological defects of ATS: cleft palate, incomplete dentition and digit abnormalities. All of these phenotypes have also been associated with defects in TGFβ superfamily signaling. For example, TGFβ2 and TGFβ3 knockout animals have cleft palate<sup>108-109</sup>. Loss of BMP4 impedes proper tooth development<sup>93-94, 144-145</sup>. Deletion of Pax9, which activates BMP4 transcription, causes cleft palate, incomplete dentition, and extra digits in mice<sup>111</sup>. A conditional knockout of BMP2 and BMP4 in the forepaw causes extra digits like the *Kir2.1* knockout<sup>82</sup>. BMP signaling is responsible for inhibiting growth of extra digits and initiating apoptosis to separate digits in mice<sup>146-148</sup>. Although the developmental defects associated with *Kir2.1* knockout are incompletely characterized in the mouse, these BMP-like phenotypes support the hypothesis that disruption of *Kir2.1* interferes with TGFβ/BMP signaling in mammals.

The finding that inwardly rectifying K<sup>+</sup> channels are necessary for BMP signaling in the *Drosophila* wing alters the landscape of current research by demonstrating that K<sup>+</sup> channels contribute significantly to development. How broadly can these findings be applied to other K<sup>+</sup> channels? A gain-of-function GYG to SYG change in the selectivity filter of the G protein-

coupled Irk2 (GIRK2) channel allows it to pass Na<sup>+</sup> and Ca<sup>++</sup>, which alters cerebellar development in the weaver mouse<sup>149-154</sup>. However, deletion of GIRK2 allows mice to develop normally<sup>155</sup>. Therefore, developmental defects of weaver mice are presumed to be due to changes in Na<sup>+</sup> and Ca<sup>++</sup>, rather than changes in K<sup>+</sup>, levels. By contrast, the mutations that are associated with ATS cause loss of *Kir2.1* function<sup>44, 156</sup> and the *Kir2.1* knockout mouse has severe developmental defects. Our data presents a rationale for inquiry into the putative contribution of other K<sup>+</sup> channels to developmental signaling.

Altering Irk channels interferes with BMP signaling to contribute to morphological abnormalities in *Drosophila*. It is likely that the developmental defects associated with ATS and the *Kir2.1* knockout mouse are similarly due to defective TGFβ/BMP signaling. If *Kir2.1* channel function is necessary for TGFβ/BMP signaling in mammals, the Kir channels could represent new potential therapeutic targets for slowing tumor growth and metastasis.

## MATERIALS AND METHODS

### ***Maintenance of Drosophila stocks***

Stocks were maintained on cornmeal food at 25°C or 18°C in a Percival incubator model 122 vL (Percival Scientific).

### ***Generation of the UAS-Irk2DN and UAS-Irk2WT fly strains***

*irk2A* from Berlin<sup>w1118</sup> fly cDNA was cloned into the *EcoRI* and *XhoI* sites of the pUAST vector. PCR was performed with cDNA template and primers (GGAATTCATGCGTTTCAATTTCTCC and CCGCTCGAGCGGCTA-GGAGGCCTGGTCAGA) to add *EcoRI* and *XhoI* sites. Sequencing ensured fidelity of the construct. *UAS-Irk2 DN* was constructed by cutting *irk2A* out of *UAS-irk2 WT* with *EcoRI* and *XhoI*, and ligating into pET. The GYG of pET-Irk2A template plasmid was mutated to

AAA using a QuikChange Site-Directed Mutagenesis Kit (Stratagene, La Jolla, CA) with the following primers: ACGCAGCACACTATTGCCGCTGCCGTCC- GAACCACCTCG and CGAGGTGGTTCGGACGGCAGCGGCAATA- GTGTGCTGCGT. Irk2-DN was removed from the pET vector with EcoRI and XhoI restriction enzymes and ligated into pUAST. All constructs were sequenced to verify the GYG to AAA mutations. We injected UAS-Irk2 WT or UAS-Irk2 DN plasmid with transposase DNA into 1-hour-old Berlin<sup>w1118</sup> embryos. Matured injected flies were crossed to Berlin<sup>w1118</sup> and progeny with the transgene were selected by eye color. Irk1-AAA and irk3-AAA were generated with the same strategy using primer pairs: ACCCAGACGAC- GATAGCCGCTGCCAATC/CGTCACATAGCGATTGGCAGCGGCTAT- C (Irk1-AAA) and ATCGAGTCCAAGATACGAGTCTACATCATC/GAT- GATGTAGACTCGTATCTTGGACTCGATGGA (Irk3-AAA).

### ***Drosophila strains***

The Vienna *Drosophila* RNAi Center (VDRC) provided stocks that express short RNA hairpins complementary to *irk* channel genes under control of an inducible upstream activating sequence (UAS) promoter<sup>157-158</sup>. The GAL4 activator controls expression of genes behind UAS. Ubiquitous expression of GAL4 (and thus the *irk siRNA* or *irkX-AAA* subunits) was achieved with the *daughterless* or *actin* promoter. Wing-directed expression was achieved with MS1096-GAL4 or *engrailed-GAL4*. To accomplish *irk siRNA*, VDRC stocks *irk2* 108140, *irk1* 28430 and *irk3* 101174 were mated to the flies with appropriate GAL4 driver.

### ***Generation of Irk2Df strains***

An *irk2*-deficient stock was from the Exelixis custom deficiency generation system<sup>159</sup>. For clarity, we refer to this strain as *irk2DfA*. The *irk2DfA* deficiency covers 280 kb and removes 25 genes, including *irk2* and is homozygous lethal. We used the same scheme<sup>159</sup> to generate a

second *irk2* deficiency. FLP recombinase expression was induced in *Drosophila* larva carrying  $P^{(ry+t7.2:hsFLP)12}$ ,  $P^{(WH)f002619}$  and  $P^{Bac(RB)e01487}$  at 37°C in daily 1 hour increments. FLP expression induced recombination between *PiggyBac*  $P^{(WH)f002619}$  and  $P^{Bac(RB)e01487}$  generating flies that lack the genomic region between the two insertion sites, including *irk2* (designated *Irk2DfB*). *Irk2DfA/irk2DfB* flies are viable and lack *irk2* entirely without removing more than five surrounding genes. The deletion was verified by PCR.

### ***Irk2 in situ***

Standard *irk2* in situ was performed<sup>160</sup>. The *irk2* probe sequence was:

AGGCCTGGTCAGAATGATTGTGGGACAGTTGAC-  
GCATGGTAAAGGTGGTTTCTGGTGTGCGGAATCCCTCCTG-  
GATCTTGTAGATCTCGTTCAATCCCGAGCACTGCACAACG-  
GAGTGTCCACCTGAGTGGTTTCGTTAAAGCGAGCGTAGTC-  
GATTCATAGGCCTGCAGATCCTTGTTGTACAACACCACTG-  
GATCGAAACGATGTCCCAAAGGATCTCA.

### ***Quantitative RT-PCR***

Total RNA was isolated from third instar larvae (SV Total RNA Isolation System, Promega). Total cDNA was reverse transcribed in vitro using Super Script III reverse transcriptase (Invitrogen, Grand Island, NY). Real-time PCR was accomplished with 100 ng of template cDNA, the Syber Green Assay kit (Applied Biosystems) and 200 nM primers in a Step One plus Real-Time PCR thermal cycling block (Applied Biosystems, Carlsbad, CA). Primer sequences are as follows: *RP49*, AAGAAGCG- CACCAAGCACTTCATC and TCTGTTGTCGATACCCTTGGGCTT; *irk1*, GCCATCGTTTCGTGAATGTGGTGT and

AGTGTCCACGTCG- TAGGTGTTGTT; *irk2*, ATGGCCGGAATAGTGTTTGCCAA and GGCAAATTACGGCGTGTTTGGAGA; *irk3*, TTATTCTCTGGCCC- GATGTGGTGT and GGCAGCATTGAAGAGTTTCGCTGT. The data were obtained using Step one software V2.1 (Applied Biosystems, Carlsbad, CA). Fold difference was calculated with  $\Delta\Delta CT$ <sup>161</sup>.

### ***Immunohistochemistry and TUNEL staining***

Wing discs were isolated from third instar larvae. Discs were stained with anti-phospho-Smad1/5 Ser463/465 (Cell Signaling)<sup>162</sup> and 1:250 goat anti-rabbit IgG CY3 (Millipore). Anti-Spalt staining was accomplished with 1:250 anti-Spalt<sup>163</sup> from Adi Salzberg (Technion-Israel Institute of Technology, Haifa, Israel) and 1:200 goat-anti-rabbit IgG CY3. Achaete was stained with 1:5 mouse-anti-achaete [Developmental Studies Hybridoma Bank (DSHB), Iowa<sup>164</sup>], a 1:200 dilution of the secondary antibody, Alexa Fluor 488 anti-mouse IgG (Invitrogen). Wingless was stained with 1:20 mouse-anti-wingless [DSHB, Iowa<sup>165</sup>]. The secondary antibody was 1:200 goat-anti-mouse IgG CY5 (Millipore). Apoptosis was detected using DeadEnd Fluorometric TUNEL (Terminal deoxynucleotidyl transferase dUTP nick end labeling) system (Promega, Madison, WI). Wing discs were mounted with Vectashield mounting medium (Vector Laboratory, Burlingame, CA).

### ***Imaging***

Wing discs were imaged at 20 magnifications with a Zeiss AxioScope A1 (Carl Zeiss Microscopy LLC, NY) in bright field with a Texas-red filter for anti-pMAD, anti-Spalt, CY5 for anti-Wingless staining, and a GFP filter for anti-Achaete TUNEL and Achaete staining. An AxioCam HRc digital camera with the AxioScope A1 computer program photographed images. For the intensity analysis of anti-pMad staining, control and experimental samples were processed and imaged in parallel with identical settings for exposure (33.2 ms). The fluorescent

microscopy images were analyzed with Slidebook (Intelligent Imaging Innovations). Peak intensity was determined by subtracting the minimum fluorescence from the maximum fluorescence intensity in an anterior-to-posterior cross-section of the wing disc. Five independent cross-sections were used for each disc.

### ***Kir2.1 mouse***

Generation of the Kir2.1-knockout mouse has been described previously<sup>48</sup>. Bone and cartilage were dissected from newborn pups and placed into 95% ethanol. Ethanol was replaced with 0.03% Alcian Blue, 80% ethanol and 20% acetic acid. Tissue was washed with 95% ethanol before incubation in 2% KOH. Tissue was incubated in 0.03% Alizarin Red. Skeletons were cleared in 20% glycerol. All mouse protocols were approved by the UCSF IACUC.

### ***Statistical analysis***

Error bars represent the standard error of the mean (s.e.m.). Raw P values were determined using a two-tailed Student's t-test. Each experiment consisted of at least three repeated trials. The number of flies tested is given for each figure in the legend.

## ACKNOWLEDGEMENTS

We thank Dr Allen Buskirk, Dr Anthea Letsou, and Drs Peter and Alex Bates for editing. We thank the Bloomington Drosophila Stock Center, the Vienna Drosophila Stock Center, Dr. Anthea Letsou and Dr Sally Kornbluth for fly stocks. We also thank Adi Salzberg for anti-Spalt. We thank Ree Lu, Phoebe Lin, Devon Kinghorn, Alex Johnson, Elise Wilson and Abigail Gehrett for wing disc dissections.



## CHAPTER3: THE MECHANISM OF THE KIR2.1/IRK2 CONTRIBUTION TO DPP SIGNALING

### INTRODUCTION

*Drosophila* wing development can be used to study cellular signaling for organogenesis. Like other appendages in *Drosophila*, the wings are developed from larval structures called wing imaginal discs. These discs start with a mere 50 cells in the first instar larval stage. After 4 days of development, 50,000 cells make up the disc in the third instar larval stage. At pupation, cells arrest at the G2 phase and divide 2 more cycles to exit the dividing cycle at the G1 stage<sup>166</sup>. Finally, after metamorphosis, the adult fly emerges with intact wings<sup>166-167</sup>. Initially, all the wing disc cells are identical. As time passes, these discs become patterned into compartments with restricted fates. Cells from each compartment behave as an independent unit and form a boundary so that cells from other compartments do not mix. These compartments are also called growth units<sup>168</sup>. The compartments are defined by the morphogens secreted by the organizer cells within the compartments. The wing is formed by juxtaposed sheets of epithelium on dorsal and ventral sides. These cells release cuticular exoskeleton<sup>101</sup>. The wing contains stereotypical structures of veins that strengthen the structural integrity of the wing and provide vessels for trachea, nerves, hemolymph, and blood cells<sup>101</sup>.

Inducer cells produce and release proteins called morphogens to control cell proliferation and patterning across a long range of cells within a developing tissue. Some examples of morphogens include Dpp, Wg, and Hh<sup>128, 169-170</sup>. Dpp is a morphogen that is secreted by cells that are located immediately anterior to the anterior posterior (A/P) boundary of the wing disc. The Dpp ligand is secreted from those cells to form a gradient across the wing disc, with higher concentrations of Dpp in the middle and lower concentrations at the edges. The anterior and posterior compartment identity is determined by expression of *engrailed*<sup>171</sup>. The region where

*engrailed* expresses becomes the posterior compartment whereas the region where it does not express becomes the anterior compartment. Engrailed induces secreted protein Hh at the posterior compartment and suppresses Dpp at the posterior<sup>172</sup>. Hh in turn induces *dpp* at the anterior cells<sup>171, 173</sup>. Dpp controls the expression of its receptor Thickveins (Tkv); if cells receive a higher level of Dpp, then *tkv* expression becomes low and vice versa. When Dpp binds a complex of its receptors, Tkv and Punt or saxophone (Sax) and punt, Tkv or Sax phosphorylates Mad, an R-SMAD. Phosphorylated Mad can complex with Medea, a Co-SMAD. This p-Mad/Medea complex enters into the nucleus to induce expression of Dpp target genes such as *spalt*, *optomotor-blind* and *vestigial*. At the edges of a wing disc, a Dpp antagonist called *brinker* is expressed to sharpen the slope of Dpp activity. There is no consensus on how the Dpp ligand spreads. Three mechanisms have been suggested: diffusion through the extracellular matrix, diffusion through cellular extensions called cytonemes, and through endocytosis<sup>174-176</sup>

Precise levels of Dpp are essential for the proper development of the *Drosophila* wing. Decreased Dpp signaling reduces wing size severely<sup>114</sup>. Higher levels of Dpp cause increased disc growth<sup>118</sup> and can duplicate the wing pattern<sup>128</sup>. Some research suggests that decreased *dpp* expression in the A/P boundary causes apoptosis<sup>122, 177</sup>. Others argue that cell clones that lack Dpp signaling do not die but are removed from the epithelium<sup>178-179</sup>.

Another important pathway necessary for the wing patterning is *wingless*. A ligand called Wg is expressed by dorso-ventral (D/V) boundary cells and diffuses into the sides making a concentration gradient to express target genes *achaete*, *distal-less*, and *vestigial* depending on the concentration gradient of Wg<sup>170, 180-181</sup>. In the third instar larvae wing disc, *wg* is expressed in the D/V boundary, hinge, and notum regions of the disc, and regulates the patterning of the notum, hinge, blade, and wing margin<sup>181</sup>.

We established that *Irk2* is essential for Dpp signaling to pattern the *Drosophila* wing. Here, we attempt to define role of *Irk2* in the Dpp signaling cascade. We found that the *Irk* channels are necessary downstream of Dpp ligand translation and upstream of activation/phosphorylation of Mad. Preliminary evidence suggests that *Irk2* is necessary for the release of Dpp from the inductive cells or the spread of Dpp from the source cells to the responding cells.

## RESULTS

### ***Irk2 is not required for Hedgehog signaling***

In chapter 2, we showed that Dpp signaling requires the *Irk2* channel for the proper development of the wing. In contrast, we showed that *wg* expression and expression of its target gene *achaete* are not affected by the loss of *Irk* channels. This means that the developmental requirement for *Irk2* is specific to Dpp signaling and is not general to all signaling pathways.

Another essential signaling pathway for correct development of the wing is Hedgehog (Hh). Hh signaling induces expression of Dpp. Therefore, if *Irk2* were necessary for Hh signaling, we would also see a loss of Dpp signaling, consistent with our previous results.

To determine if Hh is expressed normally when *Irk2* is compromised, we used an enhancer trap system where the *hh* expression is monitored by a beta galactosidase reporter (LacZ) fused to the promoter of Hh. We expressed *irk2DN* in the whole wing pouch using MS1096-Gal4. We then used an antibody against LacZ to ask whether blocking *Irk2* would affect the Hh expression pattern. The result showed that blocking *Irk2* did not change Hh-LacZ expression in the disc (Figure 3-1 A, C). Therefore, *hh* expression does not depend on *Irk2*.

While Hh is expressed normally, it could also be that Hh signaling is compromised by the loss of Irk2. To address this hypothesis, we assayed the expression of *patched*, a gene whose expression depends on Hh signaling in the wing disc. The Hh target gene, *patched*, forms a sharp stripe in the A/P boundary. We checked *patched* expression when Irk2 was compromised by expression of *irk2DN* in wing discs and by deletion of Irk2 (*irk2Df*). In the wild type wing discs, Patched forms a stripe at the A/P boundary. In *Irk2DN* expressing discs, *patched* expression is lost, where cells also die via apoptosis, but is otherwise intact (Figure 3-1 B, D). Loss of *patched* expression is expected because *Irk2DN* expression induces apoptosis of those cells. We checked the *patched* expression in *irk2df* wing discs because discs with this genotype do not have increased apoptosis. *patched* expression is not lost or decreased in the *irk2df* discs indicating that Hh signaling is not compromised by the loss of Irk2 (Figure 3-1 B, E).

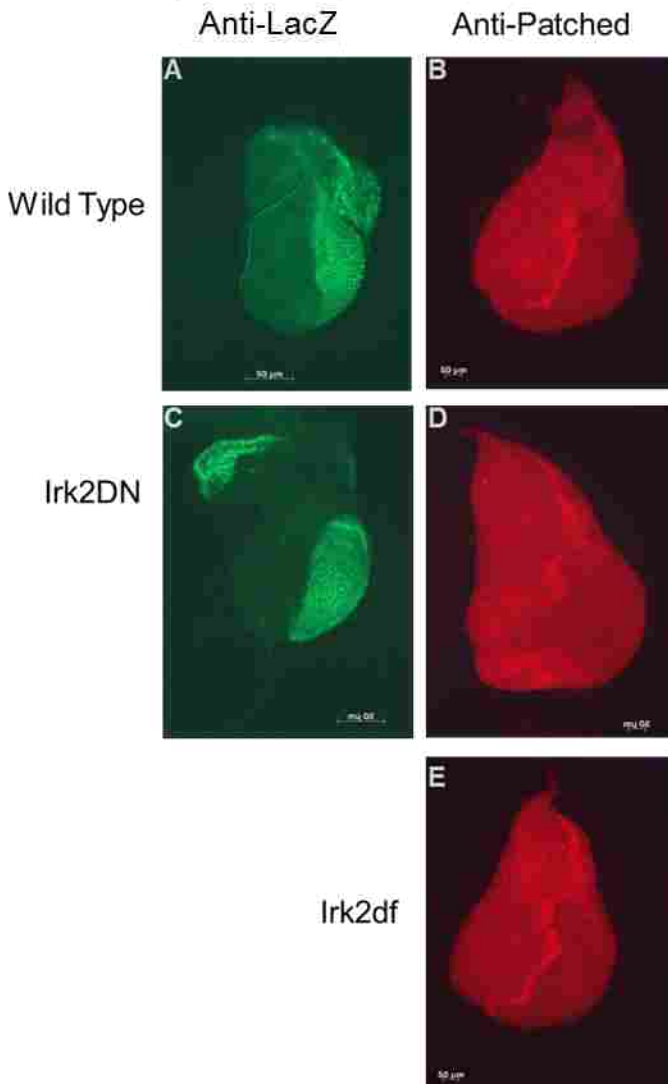


**Figure 3-1: Hedgehog signaling is not involved in Irk2 mediated wing patterning.**

Early third instar larvae wing discs were stained with anti-LacZ antibody to Hh-LacZ enhancer trap lines alone (A) and Hh-LacZ enhancer trap lines with MS1096 Gal4; *UAS-Irk2DN* (C). Late third instar larvae were stained with anti-patched antibody for wild type (B), MS1096 Gal4; *UAS-Irk2DN* (D), and *irk2df* (E) (Anterior is left and posterior right)

***Expression of Dpp, Tkv and Dally remains normal in the Irk2DN expressing wing disc***

Are all of the essential components of the Dpp signaling pathway expressed when Irk2 is blocked? To determine if the essential components of the pathway are expressed, we used

antibodies against Beta galactosidase (LacZ) in enhancer trap flies, where LacZ is fused to the promoter of different components of the Dpp pathway.

First we asked whether *dpp* expression is altered when Irk2 channels are blocked by expressing *Irk2DN* in the wing pouch. The ligand, Dpp, is expressed in the bordering anterior cells of A/P boundary cells by Hh signal at the posterior compartment<sup>182</sup>. We expressed *Irk2DN* in the whole wing pouch using MS1096-Gal4 in Dpp-LacZ enhancer trap lines to determine whether Irk2 was required for transcription of Dpp. We found that Irk2DN did not affect Dpp transcription (Figure 3-2 A, B). This shows that Irk2 is required downstream of Dpp transcription in the Dpp pathway.

We assessed whether the expression pattern of Tkv, a Dpp receptor, is altered when Irk channels are blocked. Two type I receptors Tkv and Saxophone (Sax), can bind to Dpp. However the interaction between Dpp and Tkv is stronger than the interaction between Dpp and Sax<sup>183</sup>. Sax binds to another ligand, Gbb, with a higher affinity<sup>184</sup>. In the wing disc, Tkv expresses in a well-restricted area. In contrast, Sax is expressed ubiquitously<sup>185</sup>. We checked Tkv expression because it is the primary receptor through which Dpp signals in the context of wing disc development. Tkv expression is low in the medial cells where Dpp is expressed, giving Dpp more room for dispersal because there are fewer Tkv receptors to bind<sup>186</sup>. Tkv expression is strongly suppressed in cells immediately in the center of the A/P boundary. Since Dpp signals through Tkv, the Dpp signaling is not transmitted in the very center of the A/P boundary. Thus Mad (Tkv's phosphorylation target) remains unphosphorylated in this region. Immediately adjacent to the center cells, Mad is phosphorylated in response to Dpp signaling through Tkv. This pattern of Dpp activity is measured with an antibody against the phosphorylated form of Mad (p-Mad)<sup>139</sup>. We blocked Irk channels using expression of dominant negative Irk2 (*Irk2DN*)

in the wing pouch. We then monitored Tkv expression by immunostaining (Figure 3-2 C, D). *Irk2DN* expression did not change the Tkv expression pattern meaning that Tkv transcription does not depend on Irk2 function.

Division abnormally delayed (*Dally*) is a glycoprotein that is necessary for Dpp to spread from inducer cells to target cells. *Dally* covalently attaches to a heparin sulfate chain in the extracellular matrix<sup>187</sup>. *Dally* helps to transport Dpp dimers that are released from medial inducer cells to the lateral responder cells by association-dissociation interactions<sup>78, 188</sup>. We expressed *Irk2DN* in the wing discs of the *Dally-LacZ* enhancer trap line and monitored the *LacZ* expression by immunohistochemistry. We found that blocking Irk channels using *Irk2* does not change the transcription of *Dally* (Figure 3-2 E, F).

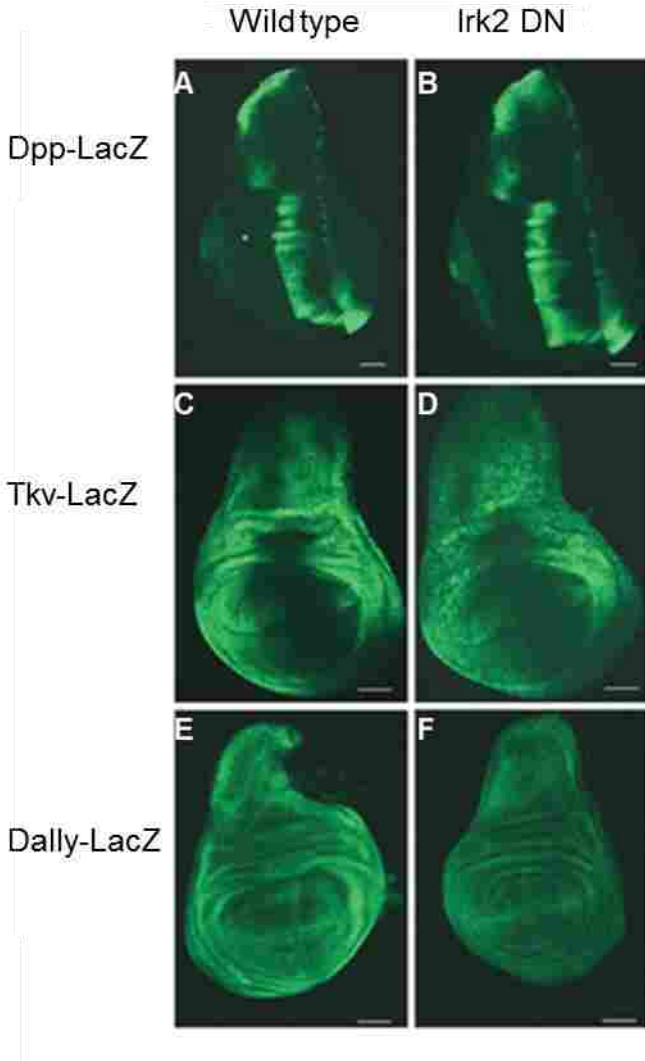


**Figure 3-2: Irk channel function is not required for transcription of Dpp, Tkv or Dally.** Late third instar larvae wing discs were stained with anti-LacZ antibody to Dpp-LacZ enhancer trap lines alone (A) Dpp-LacZ enhancer trap lines with MS1096 Gal4; *UAS-Irk2DN* (B); Tkv-LacZ enhancer trap line alone (C) or Tkv-LacZ enhancer trap line with MS1096 Gal4; *UAS-Irk2DN* (D) Dally-LacZ enhancer trap line alone (E) or Dally-LacZ enhancer trap line with MS1096 Gal4; *UAS-Irk2DN* (F). Scale bar-50 $\mu$ M.



### ***Irk2* is not directly required for phosphorylation of *Mad***

Our previous work showed that loss of *Irk2* in the wing disc caused reduced expression of the Dpp target gene *spalt*. Similarly, blocking or reducing the function of *Irk2* reduced phosphorylation of *Mad* (*p-Mad*)<sup>189</sup>. We also found that expression of Dpp signaling components *dpp*, *tkv* and *dally* remain normal in discs that express dominant negative *Irk2* channels. Now we asked, does phosphorylation of *Mad* directly require the *Irk2* channel? To determine if *Mad* could be phosphorylated without the function of *Irk2*, we expressed constitutively activated *Tkv* in cells to by-pass all upstream requirements in the signaling cascade. Activated *Tkv* (*tkv<sup>QD</sup>*) substitutes Q 253 to D transduce a downstream signal without Dpp binding<sup>190</sup>. We expressed *tkv<sup>QD</sup>* in the wing pouch alone or along with *Irk2DN* and asked whether *Irk2DN* expression allowed phosphorylation of *Mad* within those cells. P-*Mad* signal is retained in the disc where *Irk2DN* is expressed with activated *tkv<sup>QD</sup>* suggesting that phosphorylation of *Mad* does not directly require *Irk2* (Figure 3-3). In other words, *Irk2* is required in a different step of Dpp signal transmission.

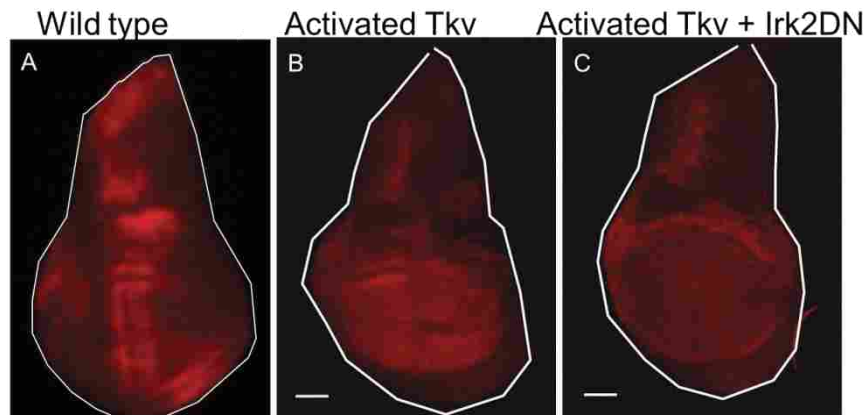


**Figure 3-3: *Irk2* does not directly target *Mad*.** Wing discs of wild type (A), MS1096 Gal4; *UAS-tkv<sup>Q253D</sup>* (B) and MS1096 Gal4; *UAS-Irk2DN*; *tkv<sup>Q253D</sup>* (C) were stained with anti-P-*Mad* antibody. Scale bar-50  $\mu$ M

### ***Diffusion of the Dpp ligand is affected by Irk2***

Proper spreading of a morphogen is important to pattern the structure of an organ because the level of morphogen activity at a target cell determines its cellular fate. Dpp is expressed in the cells of the A/P boundary. After translation, Dpp pro-protein gets cleaved into different isoforms. The longer isoform forms dimers, is released from producing cells, and binds receptors of target cells to affect wing patterning<sup>186</sup>. In the wing disc, Dpp localization peaks in the middle of the A/P boundary and decreases gradually towards the anterior half, but declines sharply at the posterior half. A Dpp receptor, Tkv, is highest at the edges of the disc and lowest at the middle. Hence, the absolute amount of the ligand concentration and its relation to neighboring cells in medial or lateral regions of the disc is important to properly pattern the disc. Uniform distribution of Dpp in the medial cells causes a change in disc size<sup>191</sup>. To understand how the ligand distribution was affected when Irk2 is inhibited, we expressed *Irk2DN* along with Dpp in the inducer cells. To this end, we designed transgenic flies that express both *irk2DN* and a *DPP-GFP* fusion gene under the control of the upstream activator sequence (UAS) and the *dpp-Gal4* driver. We found that discs of *dpp-Gal4 UAS::Irk2DN; UAS::DPP-GFP* were larger in size compared to *DPP-GFP* flies. Ectopic expression of Dpp alone can increase the disc size so we made a quantitative comparison of discs from both genotypes. To accomplish this, we crossed the flies and let them lay eggs for 4 hours and let larva grow for 130-134 hrs. We checked the Dpp expression using anti-GFP antibody to determine the compartment size. Discs with *DPP-GFP* expression alone (n=12) have an average posterior compartment size of 132.3 +/- 4.7  $\mu\text{m}$  and an anterior compartment size of 189 +/- 7  $\mu\text{m}$  whereas discs with *Irk2DN* expression along with *DPP-GFP* (n=16) have an average posterior compartment size of 162.6 +/-7.3 $\mu\text{m}$  and an anterior compartment size of 257.6 +/- 15.5  $\mu\text{m}$ . Blocking Irk2 in Dpp producing cells changes the ratio of size of the posterior to anterior compartments from 0.702 +/- 0.02 in *DPP-GFP*

expressing discs to  $0.64 \pm 0.02$  in *Irk2DN* and *DPP-GFP* expressing discs (Figure 3-4 A-C). The cells expressing Dpp-GFP mark the A/P border. We measured the distance from the A/P boundary to the anterior edge and to the posterior edge when those A/P border cells express *Irk2DN* and Dpp-GFP compared to discs that only express Dpp-GFP in those A/P border cells.

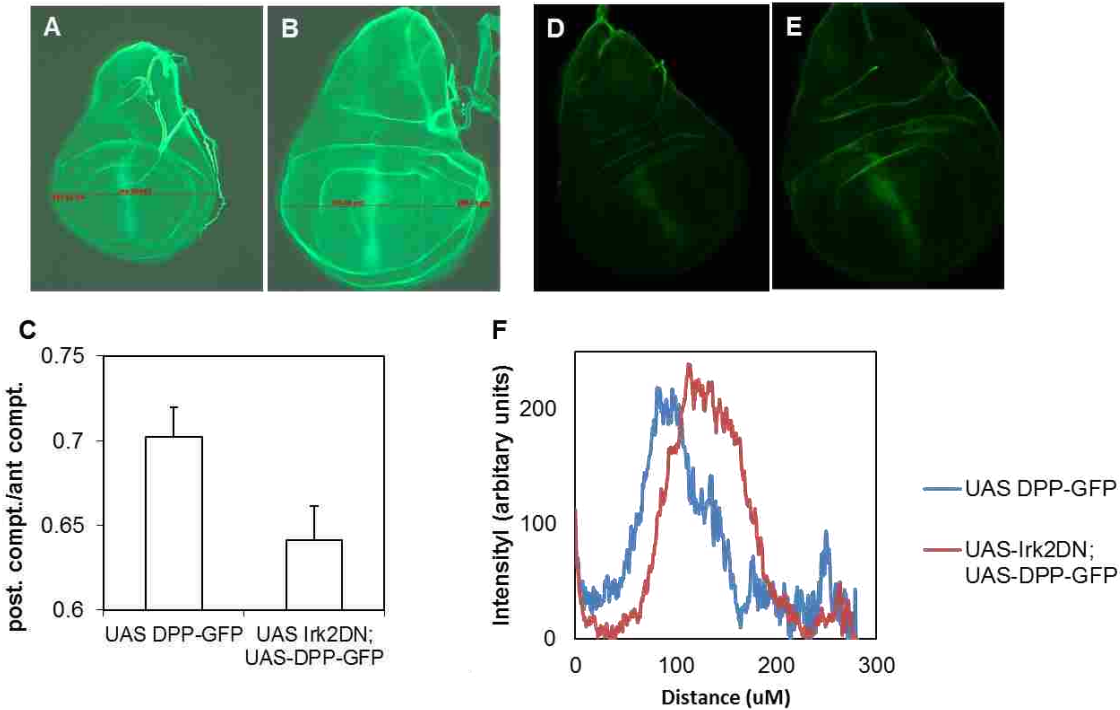


**Figure 3-4: The spread of Dpp is impacted by Irk channels loss.** (A-C) Wing discs from third instar larvae (130-134 hr. after egg lay (A.E.L.)). Discs were stained with anti-GFP antibody and imaged using a fluorescence microscope to measure compartment size (A) *dpp-Gal4; UAS-DPP-GFP* (n=12) (B) *Dpp-Gal4; UAS-Irk2DN; UAS-DPP-GFP* (n=16) (C) The size of anterior and posterior compartments are measured. The ratio of posterior over anterior compartments in *Irk2DN* expressing wing discs is significantly different from wild type ( $P= 0.029$ ). (D-F) Wing Discs from third instar larvae (130-134 hr A.E.L.) were stained with anti-GFP antibody and pictured using confocal microscope. Intensity profile of each discs were obtained using Fiji/Image J from anterior to posterior within wing disc pouch. (D) *Dpp-Gal4; UAS-DPP-GFP* (n=25) (E) *Dpp-Gal4; UAS-Irk2DN; UAS-DPP-GFP* (n=33) (F) The profiles of average intensity for each group is plotted. Notice the breadth of *UAS-Irk2DN; UAS-DPP-GFP* is wider than in wild type.

We found that Dpp-GFP spreads farther from its source when Irk2DN is expressed in Dpp producing cells (Figure 3-4 D-F). This spread explains the larger disc size because lateral cells receive a large amount the Dpp compared to wild type.

### ***The requirement for Irk2 is non-cell autonomous***

We showed that Irk2 is required for Dpp signal transmission. If Irk2 is blocked in one group of cells, does it only affect Dpp transmission in those cells or does it affect Dpp transmission in other cells? We showed that expression of *irk2DN* in the wing pouch causes apoptosis in the pouch<sup>189</sup>. We blocked apoptosis using the caspase inhibiting protein P35 and blocked Irk2 in the same cells. P35 blocked Irk2DN-induced apoptosis in the wing pouch where both Irk2 and P35 were expressed. However, apoptosis occurred at the edge of the pouch, outside the region where Irk2DN was expressed<sup>189</sup>. Therefore, Irk2DN causes cell death in cells where it is not expressed. This is consistent with the hypothesis that apoptosis occurs because Irk2DN changed an extracellular signal (such as Dpp). The result also suggests that the requirement for Irk2 is not cell-autonomous.

To directly test whether Irk2 is required for cells to receive the Dpp signal, we expressed *Irk2DN* in a set of clones within a wing pouch surrounded by wild type cells and measured phosphorylation of Mad (the intracellular transmission of the Dpp signal). The clones expressing Irk2DN are marked with GFP to distinguish them from their wild type neighbors. We monitored P-Mad intensity across the disc inside and outside of the clone and found that the level of Mad phosphorylation does not change in clones that express Irk2DN compared to those that do not (Figure 3-5). This shows that Irk2 is not required for the transmission of the Dpp signal within a Dpp receiving cell.

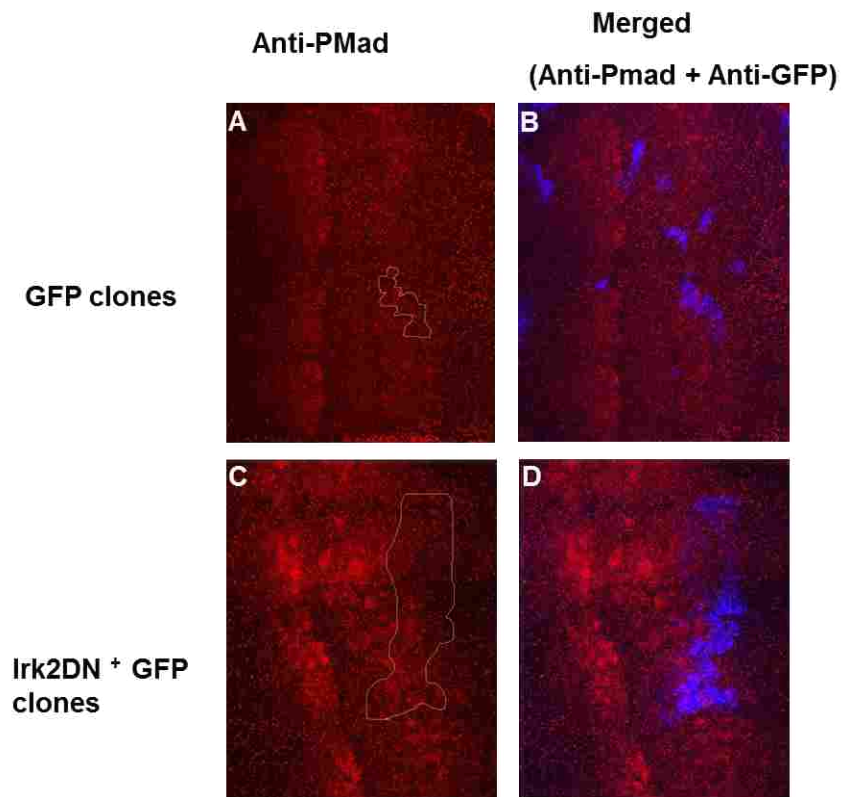


**Figure 3-5: Irk2 channel is not required for reception of the Dpp signal.** Clones of cells expressing GFP alone (**A, B**) or GFP+Irk2DN (**C, D**) were generated in third instar wing discs with wild type background and stained with anti-Pmad antibody and imaged in confocal microscope at 60x magnification. Left column (**A, C**) shows red channel alone and right column (**B, D**) shows merged image of red and blue channel on the same picture. Notice the red staining in (**A, C**) does not change within the trace line for clone and outside of it. The picture shows the center of wing pouch.

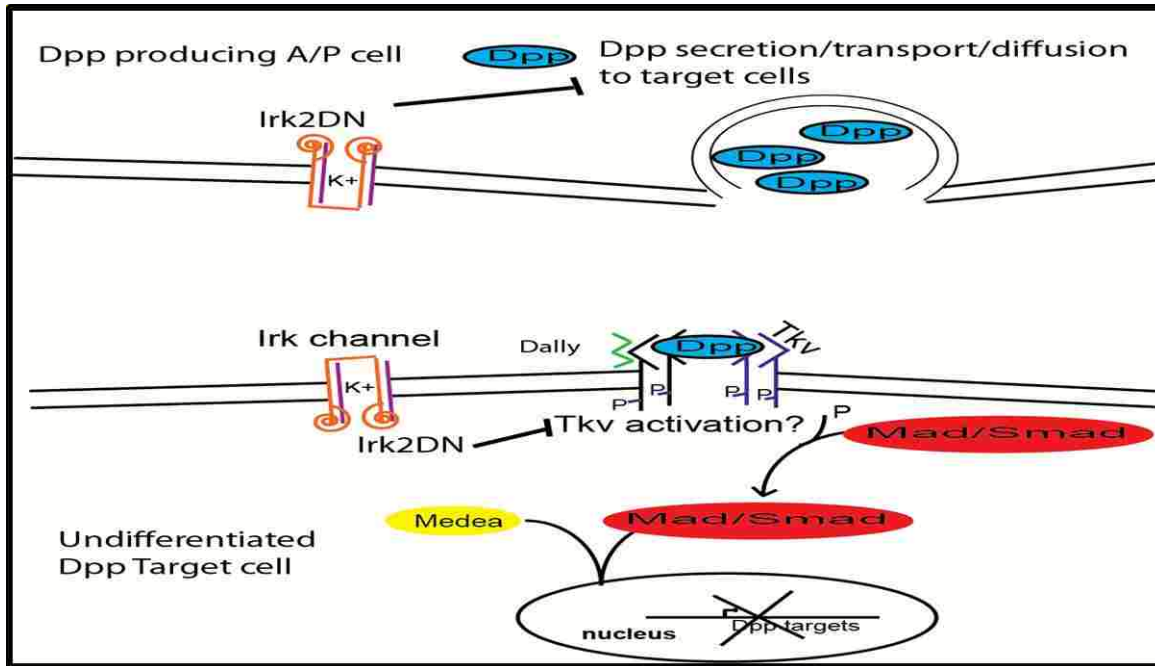


**Figure 3-6. Model for Irk channels in Dpp signaling.** Complete loss of Irk channel function causes disruption of Dpp secretion, transport, or diffusion. Irk channels are required upstream of Mad phosphorylation and downstream of Dpp translation.

## DISCUSSION

We showed that reducing Irk2 channel function throughout the wing disc reduces Dpp signaling, leading to *dpp*-like wing phenotypes, reduced expression of Dpp transcriptional targets, and apoptosis<sup>189</sup>. However, when Irk2 is blocked only in the Dpp producing cells, Dpp seems to spread further from its source cells and, as a result, the disc size increases (Figure 3-4). These seemingly paradoxical results may show a role of Irk2 in the dispersal of Dpp by altering transcytosis (Figure 3-6). Transcytosis is the process in which a ligand is captured in a vesicle by endocytosis and transported across long distances where it is released by exocytosis<sup>192</sup>.

A homolog of Irk2, Kir6.2, has been shown to be important for depolarization-induced exocytosis<sup>193</sup>. We can speculate that Irk2 may play similar role to affect Dpp release and transport in the wing disc.

Further support for a mechanism by which Irk2 affects Dpp distribution can be taken from other genes that similarly affect Dpp signaling. Mutations that disrupt *coronin*, a component of the cytoskeleton, reduce Dpp signaling<sup>191</sup>. *coronin* mutations reduce expression of Dpp transcriptional targets (*spalt* and *optomotor-blind*) and cause wing and eye phenotypes similar to those when Irk2 is disrupted<sup>189, 191</sup> (Figure 4-3). However, if Dpp is over-expressed in the same *coronin* mutant background, Dpp is increased in the lateral cells resulting in disc overgrowth similar to *Irk2DN*<sup>191</sup>. Coronin interacts with syntaxin, a component of the soluble N-ethylmaleimide-sensitive fusion protein-attachment protein receptor (SNARE) complex that plays a role in vesicle fusion<sup>191, 194</sup>. Thus, it is thought that the role of Coronin in endocytosis affects the release of Dpp from producing cells or transport of Dpp to receiving cells<sup>191</sup>. Additionally, a mammalian homolog of Irk2 also interacts with syntaxin<sup>195</sup>. Therefore, it could be that Irk2 is necessary for vesicle fusion for the release or transport of Dpp. Ours is the first suggestion that an ion channel is necessary for developmental signal transmission. More broadly, this presents the provocative idea that developmental signaling may require specific membrane potentials. In other words, developmental signaling may require an evoked response similar to that of neurotransmitter release in neural communication.

We ruled out the possibility that Irk2 affects transcription of components of the Dpp signaling pathway. We checked *dpp*, *tkv*, and *dally* expression in the discs expressing *Irk2DN* and found expression to remain normal compared to wild type (Figure 3-2). We demonstrated that phosphorylation of Mad does not directly require Irk2. We co-expressed activated Tkv

(*tkv<sup>QD</sup>*) along with Irk2DN to determine whether channel blockage disrupts the signal from the activated Tkv and found that it does not (Figure 3-3). This result suggests that Irk2 is required upstream of the Mad phosphorylation event.

Hh, Wg and Dpp are the major signaling pathways that pattern the wings. We ruled out the possibility that Irk2 is required for Wg signaling by showing that both expression of Wg and its transcriptional target *Achaete* are normal when Irk2 is compromised in the wing disc. Similarly, when Irk2 is compromised in the wing disc, the expression patterns of Hh and its transcriptional targets *patched* and *dpp* are similar to wild type (Figure 3-1). Thus, Irk2 is required for Dpp signal transduction for wing development, but is not necessary for Wg or Hh signaling.

We do not rule out the possibility that phosphorylation of receptor Tkv might require Irk2. Further studies are necessary to rule out the possibility that Irk2 affects Tkv phosphorylation. To this end, we will reduce the function of Irk2 and directly measure activation of Tkv with a fusion protein reporter called UbiTIPF. In this genetic tool, yellow fluorescence protein (YFP) fused to Tkv is quenched while the receptor is not active. Upon Dpp binding, Tkv is phosphorylated by the type II receptor. When Tkv is phosphorylated, the quench is released from YFP and fluorescence can be measured<sup>196</sup>. UbiTIPF expresses TIPF ubiquitously which allows direct measurement of Tkv activation throughout the wing disc<sup>196</sup>.

Finally, our study of Irk2 in *Drosophila* development opened a new frontier in ion channel function in development. Since ion channels are readily targeted pharmacologically, further knowledge about the role of ion channels in development will enhance the probability of



finding cures for different developmental disorders and may have applications in regenerative medicine.

## MATERIALS AND METHODS

### *Drosophila strains used*

$ry^{506}P\{PZ\}hh^{P30}$ ,  $cn^1P\{PZ\}dpp^{10638}/CyO$ ;  $ry^{506}$ ,  $tkv(y^1w^{67c23}; P\{lacW\}tkv^{k16713}/CyO)$ ,  $(P\{PZ\}dally^{06464}P\{PZ\}l(3)87Df^{06464}ry^{506}/TM3, ry^{RK}Sb^1Ser^1$  and  $w^*$ ;  $wg^{Sp-1}/CyO$ ;  $P\{GAL4-dpp.blk1\}40C.6/TM6B$ ,  $Tb^1$  were purchased from Bloomington Drosophila Stock Center, IN.  $w^*P\{UAS-tkv.Q253D.Nb\}3/TM3, Sb^1Ser^1$  is a kind gift from Dr. Robert E. Ward (University of Kansas, KS).  $hs\ flp; Actin>Y^+> Gal4: UAS-DPP-GFP/CyO$  is from Dr. Lily Jan and Dr. Yuh Nung Jan, (University of California San Francisco, CA).  $UAS-DPP-GFP/TM3, Sb$  is a kind gift from Dr. Edwin Ferguson (University of Chicago, IL).

### *Clone generation*

$hsflp; Actin>Y^+>Gal4, UAS-GFP/CyO$  virgin females flies were crossed with  $UAS-Irk2DN/CyO-GFP$  males. Clones were generated by heating the larvae for 1hr in a 37°C water bath every day after egg laying.

### *Immunohistochemistry*

Discs were isolated from larvae in ice cold PBS. Isolated discs were fixed in 4% paraformaldehyde in PBS solution to fix for 30 minute, washed with PBS, permeabilized using 0.3% triton and washed with 0.1% saponin. The samples were blocked in a blocking buffer (3%BSA, 5% goat serum, 0.1% saponin in 1X PBS) for 1 hr. at room temp. Afterwards, primary antibody diluted in blocking buffer was added to the sample and incubated at 4°C overnight. They were washed with 0.1% saponin in PBS and put in secondary antibody for 2 hr. at room temp, washed again with 0.1% saponin. Finally samples were put in slide and mounted in

Vectashield mounting medium (Vector Lab). Antibody used: primary antibodies (mouse anti-LacZ: 1:50 (developmental hybridoma bank); rabbit anti-P-mad1:20 (Cell signaling). Secondary antibody used: Alexa flour 488 Goat anti-mouse IgG (1:700) (Invitrogen), and Goat anti-rabbit IgG CY3 (1:700) (Invitrogen).

For staining extracellular DPP-GFP, wing discs were isolated on Schneider 2 culture medium (Life technologies) incubated on mouse monoclonal anti-GFP (1:50) for 1 hr. at ice. Briefly washed with PBS and fixed in 4% Paraformaldehyde. The rest of procedure is same as the other staining procedure for anti-LacZ. Secondary antibody used Alexa flour 488 Goat anti-mouse IgG (1:700) (Invitrogen).

Wing discs were stained with mouse anti-patched (1:50) (developmental hybridoma bank) and secondary antibody Goat anti-mouse IgG Cy5 (1:200) (Millipore) using protocol described in chapter-2.

### ***Imaging***

Fluorescence imaging is described in chapter 2. Confocal imaging is done using Confocal Laser Biological Microscopes FV1000 FLUOVIEW (Olympus). Control and experimental samples were imaged in the same setting. Intensity analysis is done using Fiji/ImageJ software (<http://fiji.sc/Fiji>).

### ***Wing disc measurement***

Anterior and posterior sizes were measured using an Axioscope A1 program and a Zeiss Axioscope A1 (Carl Zeiss Microscopy LLC, NY) microscope. A straight line is drawn just above the D/V boundary to measure the anterior and posterior compartment. The compartment boundary is defined by the Dpp expression.

## CHAPTER 4: IRK2 PLAYS A GLOBAL ROLE IN DROSOPHILA DEVELOPMENT

### INTRODUCTION

#### ***Drosophila Eye Development***

The *Drosophila* compound eye is composed of 750-800 eye units called ommatidia that are arranged in a beautiful hexagonal array<sup>197</sup>. The two eyes form an anterior-posterior reflection of each other<sup>198</sup>. Each light sensing ommatidium consists of 8 photoreceptors, 4 cone cells, 6 pigment cells and a mechanosensory bristle<sup>199</sup>. The photoreceptors express rhodopsin and are classified into three types according to the absorption pattern. R1-R6 absorb green light, R7 ultraviolet light and R8 absorbs light in the blue range<sup>200</sup>. Information is transmitted from the eye to the brain via axons that extend into optic lobes of the brain in two separate ganglion structures, the lamina and the medulla<sup>200</sup>.

Like all other *Drosophila* appendages, the compound eye is developed from a larval structure called the eye imaginal disc. A simple bilayer of undifferentiated cells turns into a precise, complex, stereotypical adult eye. The patterning of the eye starts in the third instar larvae with the origin of a transient vertical groove called the morphogenetic furrow (MF) at the posterior end of the eye disc<sup>197</sup>. The apical-basal region of the disc tightens and the apical region shrinks to form the morphogenetic furrow<sup>201</sup>. The morphogenetic furrow progressively moves from the posterior to the anterior of the disc causing differentiation of cells along the way. The cells anterior to morphogenetic furrow are undifferentiated and arrested in G1 phase. As the morphogenetic furrow moves, it causes cells to enter the second mitotic wave<sup>202</sup>. The second mitotic wave expands the number of cells which become the source of the majority of the cell types<sup>203</sup> <sup>199</sup>. It takes two days for the morphogenetic furrow to sweep across the disc causing a

precise sequence of events to differentiate cells into approximately 30 columns of regularly clustered photoreceptor cells<sup>199, 201, 204</sup>. The patterning event in the eye disc is different than in the wing disc. Wing disc patterning is controlled by factors that are expressed in a static space and these factors direct the differentiation of cells within their field of influence. In the eye disc, the factors are not static; they change their position constantly to carry out the differentiation in a smaller, specific field of cells<sup>201</sup>. It is interesting to note that eye development depends on positional information, but not on cell lineage<sup>197, 205</sup>.

### ***Morphogenetic Furrow and cellular signaling for cell fate decisions***

Initiation of the morphogenetic furrow (MF) is controlled by the Epidermal Growth Factor Receptor (EGFR), a member of the receptor tyrosine kinase (RTK) pathway and the Notch signaling pathway<sup>206</sup>. These two pathways act upstream of Hh and Dpp but downstream of Wg<sup>206</sup>. Progression of the morphogenetic furrow depends on Hh and Dpp signaling<sup>207</sup>. *hh* is expressed at the posterior end and remains there while the morphogenetic furrow initiates and progresses<sup>208-209</sup>. Loss of Hh prevents the morphogenetic furrow from progressing<sup>208, 210-211</sup>. Expression of *hh* causes differentiation of anterior cells and these differentiated cells start to secrete Hh, inducing the differentiation cycle<sup>212</sup>. *hh* induces the expression of Dpp which helps the movement of the morphogenetic furrow from the posterior to the anterior side of the eye disc<sup>213</sup>. *wg* is expressed in the lateral margins of the disc and suppresses initiation of the morphogenetic furrow and its progression. Thus, Wg helps to maintain the eye in its correct position<sup>13</sup>. Wingless and Dpp suppress each other<sup>214-215</sup> in such a way that loss of Dpp can cause increased activity of Wg. Wg overexpression disrupts ommatidia development and causes disorganized bristle growth, loss of the cornea nipple array (smoothened/glazed), planar cell

polarity defects. In severe cases, Wg overexpression causes tissues that should become eye to become head tissue instead<sup>216-221</sup>.

*dpp* expresses at the posterior end of the disc at an earlier stage of disc growth and moves along with the MF. Dpp induces transcription of *eyeless*, *eye absent*, *sine oculis* and *dachshund*, which are the transcription factors that specify cell fate within the homogenous epithelium of the eye disc<sup>207</sup>. Ectopic expression of *dpp* at the anterior edge causes duplication of the eye<sup>222</sup>. If a clone of cells loses the ability to respond to Dpp in the eye disc, pigment is lost, ommatidia develop aberrantly and eye size is reduced<sup>210</sup>. Dpp is responsible for the hexagonal shape of the ommatidia because it acts as a functional component of the cadherin adhesion system along with Hibris-Roughest and De-cadherin<sup>223</sup>.

### ***Drosophila trachea development***

The trachea is a respiratory organ of *Drosophila*. It is composed of interconnected tubes with stereotypical branching for gas exchange. The trachea system is analogous to lungs in higher animals<sup>224</sup>. Trachea starts out with 80 precursor cells during the embryonic stage and develops into approximately 10,000 interconnected tubes<sup>224-225</sup>. Transcription factors *trachealess* (*trh*) and *ventral veins lacking* (*vvl*) are essential for tracheal tube specification<sup>226-227</sup>. In wild type animals, embryonic dorsal branch cells will join the Dorsal Trunk (DT)<sup>228-229</sup>. Dpp signaling induces *trh* and *vvl* which then set the antero-posterior field and control the cell fate decision<sup>230</sup>. Because *Irk2* was required for Dpp signaling to pattern the *Drosophila* wing, we hypothesized that *Irk2* would also be required for the development of other tissues that require Dpp: the fly eye and the trachea.

We report that eye development requires Irk2 function. Loss of Irk channel function in the eye causes the loss of planar cell polarity, abnormal bristle arrangement, loss of integrity of hexagonal shape of ommatidia, and loss of cornea nipple array. These phenotypes are typical of Wg overexpression. Since Dpp antagonizes Wg in eye development, these phenotypes are consistent with the hypothesis that Irk2 is necessary for Dpp signaling in *Drosophila* eye development. Expression of *irk2DN* in trachea causes its incomplete development and eventual death of fly larva prematurely. Our findings in eye and trachea suggest that Irk channels are essential to Dpp signaling universally in fly development rather than constrained to one tissue or organ.

## RESULTS

### ***Irk2 is expressed in the eye disc***

To determine the signaling pathway involved in the Irk channels mediated adult eye phenotype, we relied on the eye imaginal disc as a model. The eye imaginal disc has been extensively used for the genetics of eye development. We wanted to find out whether Irk2 is expressed in the eye disc to ensure that phenotypes observed in the adult eye are due to reduction of complete loss of endogenous Irk2. We used anti-Irk2 antibody to stain the disc at early and late stages of the third instar larvae eye disc. We found that Irk2 is expressed throughout the eye disc (Figure 4-1).

### ***Loss of Irk channels causes visible eye phenotypes***

We found that Irk2 is necessary for the Dpp signaling pathway to pattern the *Drosophila* wing. Because Dpp plays an important role in patterning of different organs we hypothesized that Irk2 may also play such a role in the development of these structures.

## Anti-Irk2

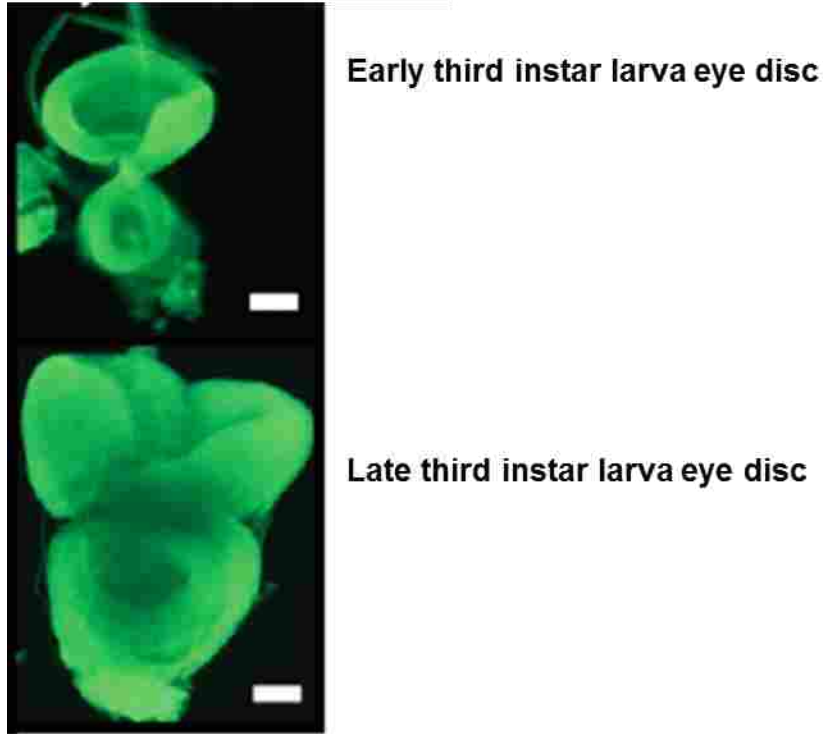


**Figure 4-1: Irk2 expresses in the eye disc.** Wild type eye discs were isolated from early and late third instar larva and stained with anti-Irk2 antibody.

To test this hypothesis, we examined development of the *Drosophila* eye in the absence of Irk2 function. The *Drosophila* eye has been studied by generations of scientists as a model for organ development. Thus a detailed map of eye development has been described. We expressed the dominant negative Irk2 in the eye using an eye specific promoter and examined the eye with a light microscope. We found that blocking Irk channels causes white patches due to the loss of red eye pigment (Figure 4-2). In some eyes, we found complete loss of pigment and a dark black spot in the center of the eye. We scored the penetrance of the defects. We found that *Irk2 DN5.1* caused eye defects in 47% of the flies when they were raised at 25 °C (n=119). We found that raising flies at 18 °C did not change the penetrance of the eye phenotype. Expression of *irk2DN* in

a different transgenic line increased penetrance and severity of the defects: *Irk2DN5.2* (n=117) caused eye defects in 90% of the flies at 25 °C and 81% eye defects at 18 °C. No defects were visible in the *irk2WT* (n=195) expressing eyes (Figure 4-2).

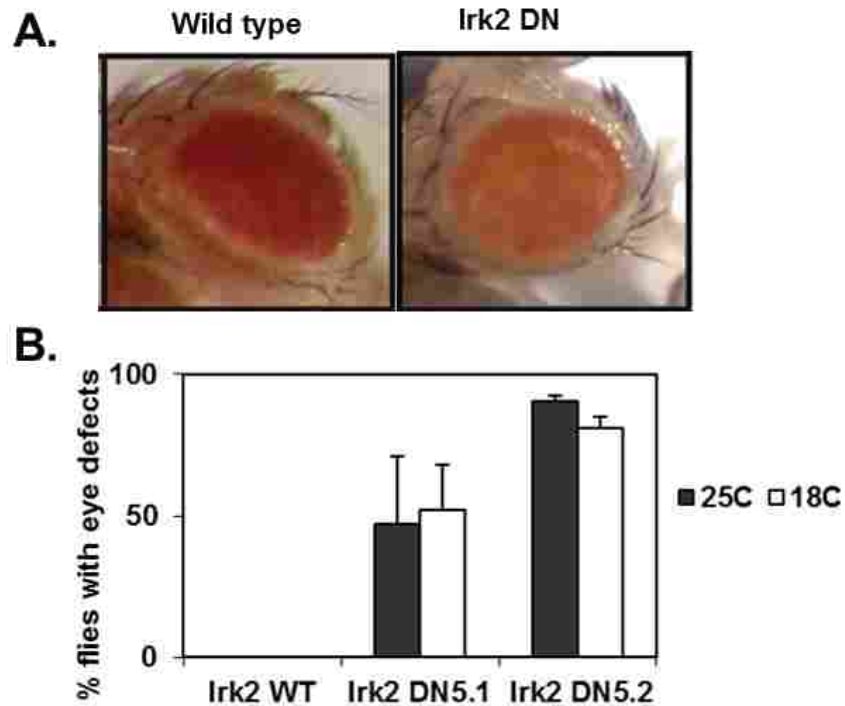


**Figure 4-2: Irk2DN expression causes eye defects.** A. *UAS:irk2WT* and *UAS:Irk2DN5.1* and *UAS:Irk2DN5.2* were expressed in the eye disc using *ninaE.GMR Gal4* promoter at 18 °C and 25 °C and eye phenotypes were counted using light microscope. (A) Normal eye in the wild type and loss of eye pigment in Irk2DN expressing eye (B) *ninaE.GMR Gal4; UAS:irk2WT* and *UAS:Irk2DN5.1* and *UAS:Irk2DN5.2* flies with eye defects were quantified using light microscopy.



### ***Eye phenotypes due to loss of Irk2 are similar to Wg overexpression phenotypes***

To determine the role of Irk2 in eye development, we examined eyes of Irk2 deficient (Irk2Df) and Irk2DN expressing fly eyes using a scanning electron microscope. We found that Irk2 deficiency and blockade of channels by Irk2DN causes disruption of the surface of the compound eye, loss of corneal nipple array, loss of integrity of the hexagonal shape of ommatidia and aberrant positioning of mechanosensory bristles (Figure 4-3). These phenotypes are similar to those caused by up regulation of Wg signaling and down regulation of Dpp signaling<sup>210, 216-221, 223</sup>.

For example, ectopic expression of *wg* suppresses bristle formation. Bristle formation can be rescued in these eyes by expressing dominant negative TCF, a downstream target of Wg<sup>231</sup>. Dpp and Wg are antagonists in the eye. Dpp is required to make the hexagonal shape of ommatidia. Thus it is possible that loss of Irk2 reduces Dpp activity leading to loss of ommatidia integrity<sup>223</sup>(Figure 4-3).

### ***Irk2DN does not cause apoptosis in the eye disc***

We showed that expression of *Irk2DN* in the wing disc causes apoptosis<sup>189</sup>. To determine if Irk2DN causes apoptosis in the eye and leads to structural defects, we expressed *irk2DN* in the eye disc using *ninaE.GMR-Gal4: UAS-Irk2DN5.1* and stained for apoptosis using TUNEL. We found that expression of *irk2DN* does not cause apoptosis (Figure 4-4). The few apoptotic cells that are seen in the Irk2DN expressing eye discs are the same number as occur in the wild type eye disc.

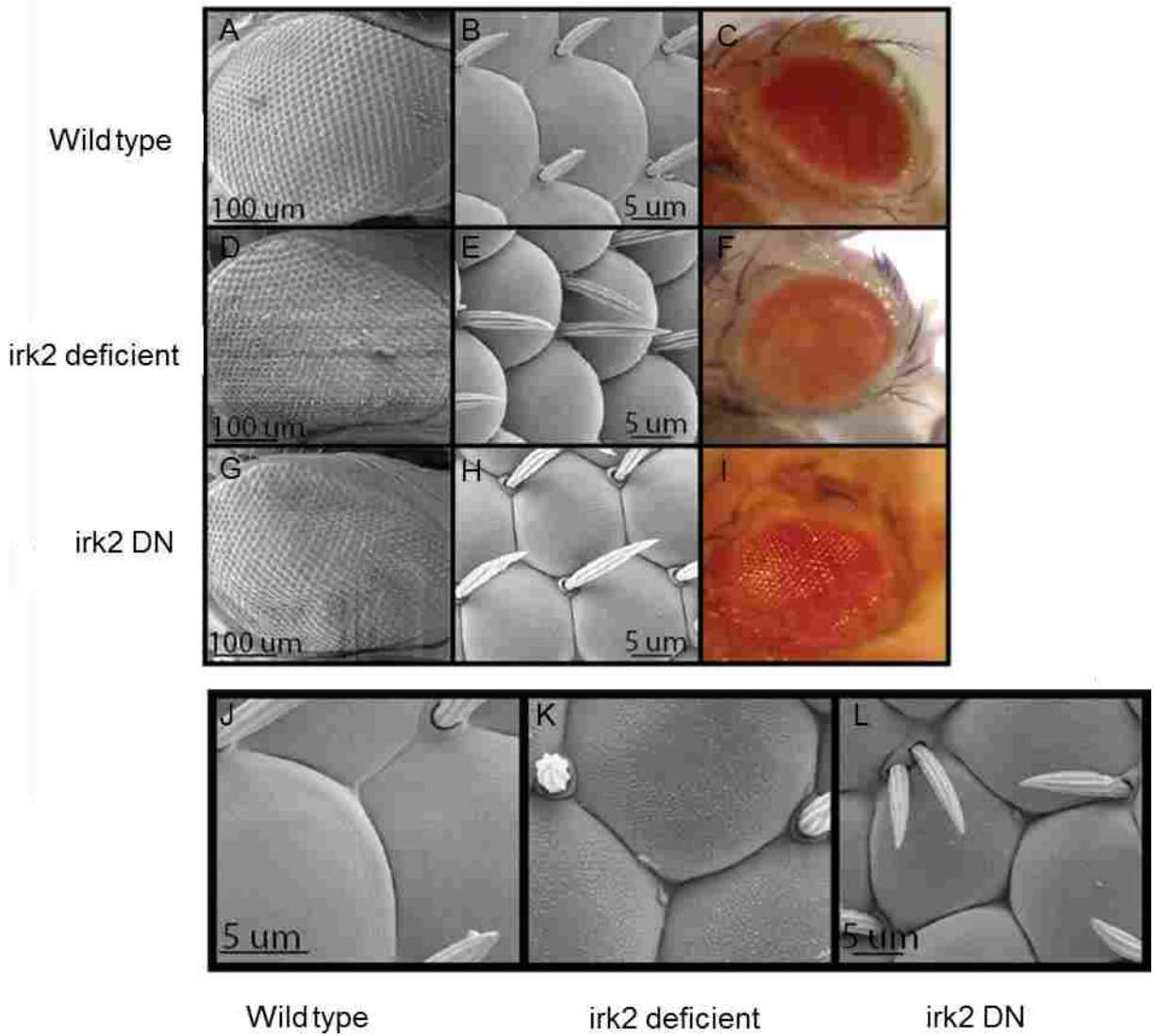


**Figure 4-3: Loss of Irk2 causes various eye phenotypes.** (A-C) Wild type eye. (A) Light microscope image of WT (B, C, J) SEM image of WT eye. (D-F, K) *irk2Df* eye. (F) Light microscope image. Notice loss of pigment. (D, E, K) SEM image. Notice rough eye (D) and disorganized bristle, loss of hexagonal shape of ommatidia (E, K). (G-I, L) *ninae.GMR. Gal4; UAS-Irk2DN* eye. (I) light microscope image. Notice the loss of red pigment. (G-H) SEM images. Abnormal eye shape (G) and bristle polarity changes (H, L)

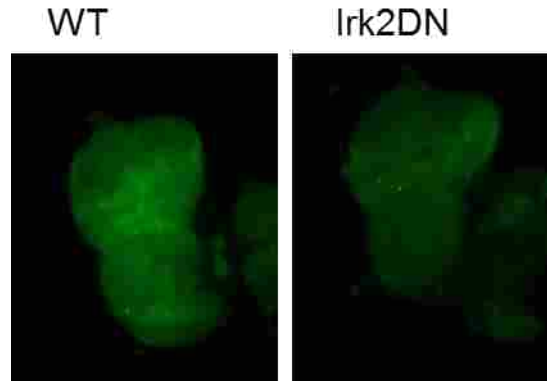


**Figure 4-4: Irk2DN does not cause apoptosis in the eye disc.** Wild type and *ninaE.GMR.Gal4; UAS Irk2DN* eye discs were isolated from third instar larva and stained for apoptosis using TUNEL.

***Irk2 is expressed in the trachea***

*Irk2* is expressed in the embryonic and larval trachea systems<sup>189</sup>. The expression is visible in the embryonic stage and persists in the larval stage (Figure 4-5). Since Dpp signaling patterns the development of the trachea and *Irk2* is necessary for Dpp signaling in the wing, we hypothesized that *Irk2* would also be important for Dpp signaling to correctly pattern the trachea<sup>232-235</sup>.

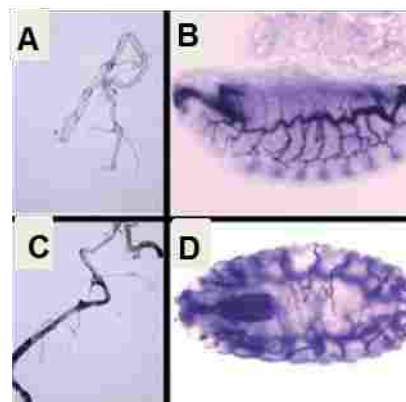


**Figure 4-5. *irk2* is expressed in trachea.** In situ with *irk2* sense (A) and *irk2* antisense (B, C, D) probes showing expression of isolated larval trachea (A, C) and embryonic trachea (B, D)

### ***Irk2 is required for trachea development***

To test our hypothesis, we used a trachea specific *breathless-Gal4* driver to express dominant negative Irk2 during trachea development. We found that expression of *irk2DN* causes thinning of branches, loss of branching, and complete loss of some sections of the main trachea trunks (Figure 4-6). The larvae were docile and 83% died before the third instar larval stage. The result confirms that Irk channels are important for proper patterning of the trachea.

Loss of proper trachea development could be one of the causes of earlier death in animals expressing Irk2DN ubiquitously (Figure 2-7 B).

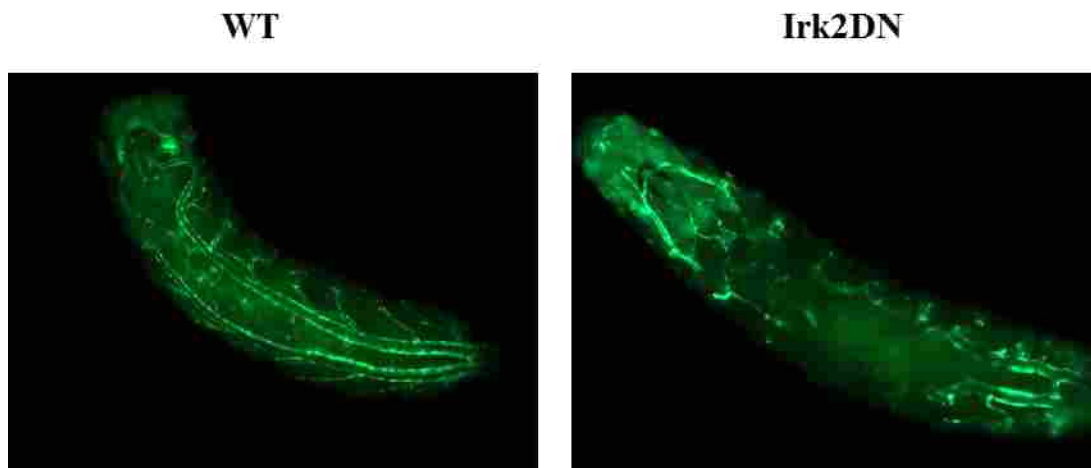


**Figure 4-6: Irk2DN expression causes defects in trachea development.** Trachea specific GFP was expressed using *btl-Gal4; UAS-GFP*. (**Left panel**) wild type larvae with normal tracheal pattern. (**Right panel**) *btl-Gal4; UAS-Irk2DN* larvae. Notice the two dorsal tubes are lost in the middle and anterior side, thinning of the tubes and loss of branching. Larva head is up

## DISCUSSION

Irk2 is essential for the development of the *Drosophila* wing, trachea, and eye. All of these structures require Dpp signaling. We also showed that Irk2 is necessary for the Dpp signaling pathway to pattern the wing<sup>189</sup>. Components of the Dpp signaling cascade and Irk2 are

expressed in the developing wing, trachea, and eye. These data led us to hypothesize that Irk2 plays a universal role in Dpp signaling for the development of multiple structures. We expressed *irk2DN* in the eye and trachea because Dpp patterns both structures. Both eye and trachea showed defects reminiscent of defects that occur with reduced Dpp signaling, consistent with our hypothesis.

Loss of Irk2 function causes eye phenotypes that include compromised hexagonal shape of ommatidia, aberrant bristle patterning, loss of the cornea nipple array, and loss of the planar cell polarity of the eye tissue. These phenotypes are similar to those that occur when Dpp signaling is reduced<sup>223</sup> or Wg activity is enhanced<sup>221, 231</sup>. Since Wg and Dpp suppress each other in eye development, less efficient Dpp signaling would lead to more Wg activity<sup>214-215</sup>. Therefore, our data are consistent with the hypothesis that that reduction of Irk2 channel function compromises Dpp signaling to cause Wg overexpression. If Wg expression completely suppresses Dpp signaling the cells in the eye disc doesn't commit to the eye structure fate. If Dpp is completely absent or more significantly compromised, cells along the border take on head or antenna fate instead of eye fate<sup>236-237</sup>. This could mean either that the requirement for Irk2 is after eye fate has been determined or that the *nina-E Gal4* driver expresses Irk2DN after eye fate has been determined. Further analysis is needed to confirm that downstream eye specific transcriptional targets of Dpp are compromised by the loss of Irk2 before we can make a definitive conclusion that the Dpp signaling pathway requires Irk2 in the eye. Unlike the wing disc, *irk2DN* expression in the eye disc does not cause apoptosis (Figure 4-4). Dpp plays different role in the wing and in the eye. Similarly, though loss of Dpp in the wing disc causes apoptosis, loss Dpp has not been shown to cause apoptosis in the eye disc. Loss of Hh and EGFR causes apoptosis in the eye disc<sup>238-239</sup>. We conclude that Irk2 is likely not required for Hh

and EGFR signaling because blocking Irk2 does not cause apoptosis. The lack of apoptosis in Irk2DN expressing eye discs is consistent with the hypothesis that Irk2 inhibits Dpp signaling rather than one of the other pathways to cause Dpp-like phenotypes.

In the trachea, loss of Irk channel function causes defects similar to loss of Dpp signaling (Figure 4-6). Loss of Dpp signaling causes disruption of dorsal branch fusion, disruption of tracheal cell migration, loss of dorsal branches, defective ganglion, and defective lateral branches in the embryo<sup>228-229, 233</sup>. More data are needed to fully appreciate the phenotypes observed when Irk channels are blocked compared to those observed with the loss of Dpp. However, the severe tracheal defects observed when Irk2 is blocked in tracheal cells is consistent with our hypothesis that Irk2 is necessary for Dpp signaling in tracheal development as it is in the wing. Since the trachea is a vital organ, blocking Irk channels in this tissue causes premature death of the fly before adulthood.

Altering Irk channels interferes with BMP signaling to contribute to morphological abnormalities in *Drosophila*. It is likely that the developmental defects associated with ATS and the *Kir2.1* knockout mouse are similarly due to defective TGF $\beta$ /BMP signaling. If Kir2.1 channel function is necessary for TGF $\beta$ /BMP signaling in mammals, the Kir channels could represent new potential therapeutic targets for slowing tumor growth and metastasis.

## MATERIALS AND METHODS

### ***Drosophila strains used***

ninaE.GMR-Gal4 is from BDSC. Btl-Gal4; UAS-GFP is a kind gift from Dr Mark Metzstein (University of Utah). Other flies were described in earlier chapters.

### ***Scoring eye phenotype***

Equal numbers of *irk2WT* and *Irk2DN* transgenic flies were crossed with *ninaE.GMR-Gal4*. Parents were discarded and adult progeny flies (F1) were scored for defects.

### ***Drosophila eye light microscopy imaging***

Adult flies were anesthetized using CO<sub>2</sub> and imaged in LEICA microscope.

### ***Drosophila eye preparation for Scanning Electron Microscopy***

Adult live flies were cut and put into 2% Gluteraldehyde in 0.06M Cacodylate buffer to fix overnight. The samples were washed with 0.06M Cacodylate buffer for 5 times 10 minutes each and fixed again in 1% Osmium tetra oxide (OsO<sub>4</sub>) for 2hr. The samples were washed with water 5 times for 10 minutes each and dehydrated in a series of acetone 10%, 30%, 50%, 70%, 90% and 100%. The samples were further dried in critical point dry (CPD) (Tousimis 931.66) and coated with AuPd to make them conductive for SEM observation and took pictures using SEM microscope FEI XL-30 ESEM FEG.

### ***Immunohistochemistry***

Eye discs were immunostained with primary antibody guinea pig anti-Irk2 (1:20) (kind gift from Dr Hong-Sheng, University of Massachusetts Medical School) and secondary antibody goat anti-guinea pig IgG alexa flour 488, using the protocol mentioned in chapter 3 and images were taken using fluorescence microscope.

### ***TUNEL staining***

TUNEL staining is done as described in chapter-2.

## ACKNOWLEDGEMENTS

I would like to thank Mr. Michael Standing (Microscopy Technician, BYU Microscopy Lab) for his help in SEM imaging of *Drosophila* eyes. I am thankful to my lab members Nick Spendlove and Ian Soane for their effort in the *Drosophila* trachea experiments.



## REFERENCES

1. Perrimon, N.; Pitsouli, C.; Shilo, B. Z., Signaling mechanisms controlling cell fate and embryonic patterning. *Cold Spring Harbor perspectives in biology* **2012**, *4* (8), a005975.
2. Moustakas, A.; Heldin, C. H., The regulation of TGFbeta signal transduction. *Development* **2009**, *136* (22), 3699-714.
3. Derynck, R.; Miyazono, K., 2 TGF- $\beta$  and the TGF- $\beta$  Family. *Cold Spring Harbor Monograph Archive* **2008**, *50*, 29-43.
4. Attisano, L.; Wrana, J. L., Signal transduction by the TGF-beta superfamily. *Science* **2002**, *296* (5573), 1646-7.
5. Massague, J., TGF-beta signal transduction. *Annual review of biochemistry* **1998**, *67*, 753-91.
6. Weis-Garcia, F.; Massague, J., Complementation between kinase-defective and activation-defective TGF-beta receptors reveals a novel form of receptor cooperativity essential for signaling. *The EMBO journal* **1996**, *15* (2), 276.
7. Ebner, R.; Chen, R.-H.; Shum, L.; Lawler, S.; Zioncheck, T. F.; Lee, A.; Lopez, A. R.; Derynck, R., Cloning of a type I TGF-beta receptor and its effect on TGF-beta binding to the type II receptor. *Science* **1993**, *260* (5112), 1344-1348.
8. Heldin, C. H.; Miyazono, K.; ten Dijke, P., TGF-beta signalling from cell membrane to nucleus through SMAD proteins. *Nature* **1997**, *390* (6659), 465-71.
9. Massague, J.; Blain, S. W.; Lo, R. S., TGFbeta signaling in growth control, cancer, and heritable disorders. *Cell* **2000**, *103* (2), 295-309.
10. Massague, J., TGFbeta in Cancer. *Cell* **2008**, *134* (2), 215-30.
11. Kiecker, C.; Niehrs, C., A morphogen gradient of Wnt/beta-catenin signalling regulates anteroposterior neural patterning in Xenopus. *Development* **2001**, *128* (21), 4189-201.
12. Geetha-Loganathan, P.; Nimmagadda, S.; Scaal, M., Wnt signaling in limb organogenesis. *Organogenesis* **2008**, *4* (2), 109-115.
13. Treisman, J. E.; Rubin, G. M., wingless inhibits morphogenetic furrow movement in the Drosophila eye disc. *Development* **1995**, *121* (11), 3519-3527.
14. Diaz-Benjumea, F. J.; Cohen, S. M., Serrate signals through Notch to establish a Wingless-dependent organizer at the dorsal/ventral compartment boundary of the Drosophila wing. *Development* **1995**, *121* (12), 4215-4225.
15. Bhanot, P.; Brinkl, M.; Samosl, C. H.; Hsieh, J.-C.; Wang, Y.; Macke, J. P.; Andrew, D.; Nathans, J., A new member of the frizzled family from Drosophila functions as a Wingless. *Nature* **1996**, *382*, 18.
16. Rattner, A.; Hsieh, J.-C.; Smallwood, P. M.; Gilbert, D. J.; Copeland, N. G.; Jenkins, N. A.; Nathans, J., A family of secreted proteins contains homology to the cysteine-rich ligand-binding domain of frizzled receptors. *Proceedings of the National Academy of Sciences* **1997**, *94* (7), 2859-2863.
17. Logan, C. Y.; Nusse, R., The Wnt signaling pathway in development and disease. *Annu. Rev. Cell Dev. Biol.* **2004**, *20*, 781-810.
18. Molenaar, M.; van de Wetering, M.; Oosterwegel, M.; Peterson-Maduro, J.; Godsave, S.; Korinek, V.; Roose, J.; Destree, O.; Clevers, H., XTcf-3 transcription factor mediates  $\beta$ -catenin-induced axis formation in Xenopus embryos. *Cell* **1996**, *86* (3), 391-399.

19. Wang, X.; Sutton, V. R.; Peraza-Llanes, J. O.; Yu, Z.; Rosetta, R.; Kou, Y.-C.; Eble, T. N.; Patel, A.; Thaller, C.; Fang, P., Mutations in X-linked PORCN, a putative regulator of Wnt signaling, cause focal dermal hypoplasia. *Nature genetics* **2007**, *39* (7), 836-838.
20. Mani, A.; Radhakrishnan, J.; Wang, H.; Mani, A.; Mani, M.-A.; Nelson-Williams, C.; Carew, K. S.; Mane, S.; Najmabadi, H.; Wu, D., LRP6 mutation in a family with early coronary disease and metabolic risk factors. *Science Signaling* **2007**, *315* (5816), 1278.
21. Christodoulides, C.; Scarda, A.; Granzotto, M.; Milan, G.; Dalla Nora, E.; Keogh, J.; De Pergola, G.; Stirling, H.; Pannacciulli, N.; Sethi, J., WNT10B mutations in human obesity. *Diabetologia* **2006**, *49* (4), 678-684.
22. Bass, A. J.; Lawrence, M. S.; Brace, L. E.; Ramos, A. H.; Drier, Y.; Cibulskis, K.; Sougnez, C.; Voet, D.; Saksena, G.; Sivachenko, A., Genomic sequencing of colorectal adenocarcinomas identifies a recurrent VTI1A-TCF7L2 fusion. *Nature genetics* **2011**, *43* (10), 964-968.
23. Grant, S. F.; Thorleifsson, G.; Reynisdottir, I.; Benediktsson, R.; Manolescu, A.; Sainz, J.; Helgason, A.; Stefansson, H.; Emilsson, V.; Helgadottir, A., Variant of transcription factor 7-like 2 (TCF7L2) gene confers risk of type 2 diabetes. *Nature genetics* **2006**, *38* (3), 320-323.
24. Morin, P. J.; Sparks, A. B.; Korinek, V.; Barker, N.; Clevers, H.; Vogelstein, B.; Kinzler, K. W., Activation of  $\beta$ -catenin-Tcf signaling in colon cancer by mutations in  $\beta$ -catenin or APC. *Science* **1997**, *275* (5307), 1787-1790.
25. Chan, E. F.; Gat, U.; McNiff, J. M.; Fuchs, E., A common human skin tumour is caused by activating mutations in beta-catenin. *Nature genetics* **1999**, *21* (4), 410-3.
26. Ingham, P. W.; McMahon, A. P., Hedgehog signaling in animal development: paradigms and principles. *Genes & development* **2001**, *15* (23), 3059-3087.
27. Tanimoto, H.; Itoh, S.; ten Dijke, P.; Tabata, T., Hedgehog Creates a Gradient of DPP Activity in *Drosophila* Wing Imaginal Discs. *Molecular cell* **2000**, *5* (1), 59-71.
28. Taipale, J.; Cooper, M.; Maiti, T.; Beachy, P., Patched acts catalytically to suppress the activity of Smoothed. *Nature* **2002**, *418* (6900), 892-896.
29. Lum, L.; Zhang, C.; Oh, S.; Mann, R. K.; von Kessler, D. P.; Taipale, J.; Weis-Garcia, F.; Gong, R.; Wang, B.; Beachy, P. A., Hedgehog signal transduction via Smoothed association with a cytoplasmic complex scaffolded by the atypical kinesin, Costal-2. *Molecular cell* **2003**, *12* (5), 1261-1274.
30. Kim, J.; Kato, M.; Beachy, P. A., Gli2 trafficking links Hedgehog-dependent activation of Smoothed in the primary cilium to transcriptional activation in the nucleus. *Proceedings of the National Academy of Sciences* **2009**, *106* (51), 21666-21671.
31. Hui, C.-c.; Angers, S., Gli proteins in development and disease. *Annual review of cell and developmental biology* **2011**, *27*, 513-537.
32. Bale, A. E., Hedgehog signaling and human disease. *Annual review of genomics and human genetics* **2002**, *3* (1), 47-65.
33. Adams, D. S.; Levin, M., Endogenous voltage gradients as mediators of cell-cell communication: strategies for investigating bioelectrical signals during pattern formation. *Cell and Tissue Research* **2012**, 1-28.
34. Beane, W. S.; Morokuma, J.; Lemire, J. M.; Levin, M., Bioelectric signaling regulates head and organ size during planarian regeneration. *Development* **2013**, *140* (2), 313-322.
35. Fromm, J.; Hajirezaei, M.; Wilke, I., The biochemical response of electrical signaling in the reproductive system of Hibiscus plants. *Plant physiology* **1995**, *109* (2), 375-384.

36. Pai, V. P.; Aw, S.; Shomrat, T.; Lemire, J. M.; Levin, M., Transmembrane voltage potential controls embryonic eye patterning in *Xenopus laevis*. *Development* **2012**, *139* (2), 313-323.
37. Adams, D. S.; Masi, A.; Levin, M., H<sup>+</sup> pump-dependent changes in membrane voltage are an early mechanism necessary and sufficient to induce *Xenopus* tail regeneration. *Science Signaling* **2007**, *134* (7), 1323.
38. Beane, W. S.; Morokuma, J.; Adams, D. S.; Levin, M., A chemical genetics approach reveals H, K-ATPase-mediated membrane voltage is required for planarian head regeneration. *Chemistry & biology* **2011**, *18* (1), 77-89.
39. Shi, R.; Borgens, R. B., Three-dimensional gradients of voltage during development of the nervous system as invisible coordinates for the establishment of embryonic pattern. *Developmental Dynamics* **1995**, *202* (2), 101-114.
40. Pu, J.; McCaig, C. D.; Cao, L.; Zhao, Z.; Segall, J. E.; Zhao, M., EGF receptor signalling is essential for electric-field-directed migration of breast cancer cells. *Science Signaling* **2007**, *120* (19), 3395.
41. McCaig, C. D.; Song, B.; Rajnicek, A. M., Electrical dimensions in cell science. *Journal of cell science* **2009**, *122* (23), 4267-4276.
42. Yao, L.; Shanley, L.; McCaig, C.; Zhao, M., Small applied electric fields guide migration of hippocampal neurons. *Journal of cellular physiology* **2008**, *216* (2), 527-535.
43. Reid, B.; Song, B.; McCaig, C. D.; Zhao, M., Wound healing in rat cornea: the role of electric currents. *The FASEB journal* **2005**, *19* (3), 379-386.
44. Hibino, H.; Inanobe, A.; Furutani, K.; Murakami, S.; Findlay, I.; Kurachi, Y., Inwardly rectifying potassium channels: their structure, function, and physiological roles. *Physiol Rev* **90** (1), 291-366.
45. Kuo, A.; Gulbis, J. M.; Antcliff, J. F.; Rahman, T.; Lowe, E. D.; Zimmer, J.; Cuthbertson, J.; Ashcroft, F. M.; Ezaki, T.; Doyle, D. A., Crystal structure of the potassium channel KirBac1. 1 in the closed state. *Science Signaling* **2003**, *300* (5627), 1922.
46. Nishida, M.; Cadene, M.; Chait, B. T.; MacKinnon, R., Crystal structure of a Kir3. 1-prokaryotic Kir channel chimera. *The EMBO journal* **2007**, *26* (17), 4005-4015.
47. Doring, F.; Wischmeyer, E.; Kuhnlein, R. P.; Jackle, H.; Karschin, A., Inwardly rectifying K<sup>+</sup> (Kir) channels in *Drosophila*. A crucial role of cellular milieu factors Kir channel function. *The Journal of biological chemistry* **2002**, *277* (28), 25554-61.
48. Zaritsky, J. J.; Eckman, D. M.; Wellman, G. C.; Nelson, M. T.; Schwarz, T. L., Targeted disruption of Kir2.1 and Kir2.2 genes reveals the essential role of the inwardly rectifying K<sup>(+)</sup> current in K<sup>(+)</sup>-mediated vasodilation. *Circ Res* **2000**, *87* (2), 160-6.
49. McLerie, M.; Lopatin, A. N., Dominant-negative suppression of I(K1) in the mouse heart leads to altered cardiac excitability. *Journal of molecular and cellular cardiology* **2003**, *35* (4), 367-78.
50. Kurachi, Y.; Nakajima, T.; Sugimoto, T., Short-term desensitization of muscarinic K<sup>+</sup> channel current in isolated atrial myocytes and possible role of GTP-binding proteins. *Pflugers Arch* **1987**, *410* (3), 227-33.
51. Genzel, Y.; Behrendt, I.; Konig, S.; Sann, H.; Reichl, U., Metabolism of MDCK cells during cell growth and influenza virus production in large-scale microcarrier culture. *Vaccine* **2004**, *22* (17-18), 2202-8.

52. Fischer-Lougheed, J.; Liu, J. H.; Espinos, E.; Mordasini, D.; Bader, C. R.; Belin, D.; Bernheim, L., Human myoblast fusion requires expression of functional inward rectifier Kir2.1 channels. *J Cell Biol* **2001**, *153* (4), 677-86.
53. Schimpf, R.; Wolpert, C.; Gaita, F.; Giustetto, C.; Borggrefe, M., Short QT syndrome. *Cardiovasc Res* **2005**, *67* (3), 357-66.
54. Romanenko, V. G.; Rothblat, G. H.; Levitan, I., Modulation of endothelial inward-rectifier K<sup>+</sup> current by optical isomers of cholesterol. *Biophys J* **2002**, *83* (6), 3211-22.
55. Donaldson, M. R.; Yoon, G.; Fu, Y. H.; Ptacek, L. J., Andersen-Tawil syndrome: a model of clinical variability, pleiotropy, and genetic heterogeneity. *Ann Med* **2004**, *36 Suppl 1*, 92-7.
56. Andersen, E. D.; Krasilnikoff, P. A.; Overvad, H., Intermittent muscular weakness, extrasystoles, and multiple developmental anomalies. A new syndrome? *Acta Paediatr Scand* **1971**, *60* (5), 559-64.
57. Tawil, R.; Ptacek, L. J.; Pavlakis, S. G.; DeVivo, D. C.; Penn, A. S.; Ozdemir, C.; Griggs, R. C., Andersen's syndrome: potassium-sensitive periodic paralysis, ventricular ectopy, and dysmorphic features. *Ann Neurol* **1994**, *35* (3), 326-30.
58. Plaster, N. M.; Tawil, R.; Tristani-Firouzi, M.; Canun, S.; Bendahhou, S.; Tsunoda, A.; Donaldson, M. R.; Iannaccone, S. T.; Brunt, E.; Barohn, R.; Clark, J.; Deymeer, F.; George, A. L., Jr.; Fish, F. A.; Hahn, A.; Nitu, A.; Ozdemir, C.; Serdaroglu, P.; Subramony, S. H.; Wolfe, G.; Fu, Y. H.; Ptacek, L. J., Mutations in Kir2.1 cause the developmental and episodic electrical phenotypes of Andersen's syndrome. *Cell* **2001**, *105* (4), 511-9.
59. Yoon, G.; Oberoi, S.; Tristani-Firouzi, M.; Etheridge, S. P.; Quitania, L.; Kramer, J. H.; Miller, B. L.; Fu, Y. H.; Ptacek, L. J., Andersen-Tawil syndrome: prospective cohort analysis and expansion of the phenotype. *Am J Med Genet A* **2006**, *140* (4), 312-21.
60. Andelfinger, G.; Tapper, A. R.; Welch, R. C.; Vanoye, C. G.; George, A. L., Jr.; Benson, D. W., KCNJ2 mutation results in Andersen syndrome with sex-specific cardiac and skeletal muscle phenotypes. *Am J Hum Genet* **2002**, *71* (3), 663-8.
61. Smith, A. H.; Fish, F. A.; Kannankeril, P. J., Andersen-Tawil syndrome. *Indian Pacing Electrophysiol J* **2006**, *6* (1), 32-43.
62. Davies, N.; Imbrici, P.; Fialho, D.; Herd, C.; Bilisland, L.; Weber, A.; Mueller, R.; Hilton-Jones, D.; Ealing, J.; Boothman, B., Andersen–Tawil syndrome New potassium channel mutations and possible phenotypic variation. *Neurology* **2005**, *65* (7), 1083-1089.
63. Haruna, Y.; Kobori, A.; Makiyama, T.; Yoshida, H.; Akao, M.; Tsuji, K.; Ono, S.; Nishio, Y.; Shimizu, W.; Inoue, T., Genotype-phenotype correlations of KCNJ2 mutations in Japanese patients with Andersen-Tawil syndrome. *Human mutation* **2007**, *28* (2), 208-208.
64. Kimura, H.; Zhou, J.; Kawamura, M.; Itoh, H.; Mizusawa, Y.; Ding, W.-G.; Wu, J.; Ohno, S.; Makiyama, T.; Miyamoto, A., Phenotype variability in patients carrying KCNJ2 mutations. *Circulation: Cardiovascular Genetics* **2012**, *5* (3), 344-353.
65. Tan, S. V.; Z'Graggen, W. J.; Boërio, D.; Rayan, D. L. R.; Howard, R.; Hanna, M. G.; Bostock, H., Membrane dysfunction in Andersen-Tawil syndrome assessed by velocity recovery cycles. *Muscle & nerve* **2012**, *46* (2), 193-203.
66. Tristani-Firouzi, M.; Etheridge, S. P., Kir 2.1 channelopathies: the Andersen–Tawil syndrome. *Pflügers Archiv-European Journal of Physiology* **2010**, *460* (2), 289-294.

67. Zhang, L.; Benson, D. W.; Tristani-Firouzi, M.; Ptacek, L. J.; Tawil, R.; Schwartz, P. J.; George, A. L.; Horie, M.; Andelfinger, G.; Snow, G. L.; Fu, Y. H.; Ackerman, M. J.; Vincent, G. M., Electrocardiographic features in Andersen-Tawil syndrome patients with KCNJ2 mutations: characteristic T-U-wave patterns predict the KCNJ2 genotype. *Circulation* **2005**, *111* (21), 2720-6.
68. Eckhardt, L. L.; Farley, A. L.; Rodriguez, E.; Ruwaldt, K.; Hammill, D.; Tester, D. J.; Ackerman, M. J.; Makielski, J. C., < i> KCNJ2</i> mutations in arrhythmia patients referred for LQT testing: A mutation T305A with novel effect on rectification properties. *Heart Rhythm* **2007**, *4* (3), 323-329.
69. Doi, T.; Makiyama, T.; Morimoto, T.; Haruna, Y.; Tsuji, K.; Ohno, S.; Akao, M.; Takahashi, Y.; Kimura, T.; Horie, M., A novel KCNJ2 nonsense mutation, S369X, impedes trafficking and causes a limited form of Andersen-Tawil syndrome. *Circulation: Cardiovascular Genetics* **2011**, *4* (3), 253-260.
70. Ma, D.; Tang, X. D.; Rogers, T. B.; Welling, P. A., An andersen-Tawil syndrome mutation in Kir2. 1 (V302M) alters the G-loop cytoplasmic K<sup>+</sup> conduction pathway. *Journal of Biological Chemistry* **2007**, *282* (8), 5781-5789.
71. Canun, S.; Perez, N.; Beirana, L. G., Andersen syndrome autosomal dominant in three generations. *American journal of medical genetics* **1999**, *85* (2), 147-56.
72. Yoon, G.; Quitania, L.; Kramer, J. H.; Fu, Y. H.; Miller, B. L.; Ptacek, L. J., Andersen-Tawil syndrome: definition of a neurocognitive phenotype. *Neurology* **2006**, *66* (11), 1703-10.
73. Liu, J. H.; Bijlenga, P.; Fischer-Lougheed, J.; Occhiodoro, T.; Kaelin, A.; Bader, C. R.; Bernheim, L., Role of an inward rectifier K<sup>+</sup> current and of hyperpolarization in human myoblast fusion. *J Physiol* **1998**, *510* ( Pt 2), 467-76.
74. Jongsma, H. J.; Wilders, R., Channelopathies: Kir2.1 mutations jeopardize many cell functions. *Curr Biol* **2001**, *11* (18), R747-50.
75. Tristani-Firouzi, M.; Etheridge, S. P., Kir 2.1 channelopathies: the Andersen-Tawil syndrome. *Pflugers Arch* **460** (2), 289-94.
76. Doi, T.; Makiyama, T.; Morimoto, T.; Haruna, Y.; Tsuji, K.; Ohno, S.; Akao, M.; Takahashi, Y.; Kimura, T.; Horie, M., A novel KCNJ2 nonsense mutation, S369X, impedes trafficking and causes a limited form of Andersen-Tawil syndrome. *Circ Cardiovasc Genet* **4** (3), 253-60.
77. Ai, T.; Fujiwara, Y.; Tsuji, K.; Otani, H.; Nakano, S.; Kubo, Y.; Horie, M., Novel KCNJ2 mutation in familial periodic paralysis with ventricular dysrhythmia. *Circulation* **2002**, *105* (22), 2592-2594.
78. Sansone, V.; Griggs, R.; Meola, G.; Ptacek, L.; Barohn, R.; Iannaccone, S.; Bryan, W.; Baker, N.; Janas, S.; Scott, W., Andersen's syndrome: a distinct periodic paralysis. *Annals of neurology* **1997**, *42* (3), 305-312.
79. Choe, S., Potassium channel structures. *Nature reviews. Neuroscience* **2002**, *3* (2), 115-21.
80. MacLean, S. J.; Andrews, B. C.; Verheyen, E. M., Characterization of Dir: a putative potassium inward rectifying channel in Drosophila. *Mechanisms of development* **2002**, *116* (1-2), 193-7.
81. Bichet, D.; Haass, F. A.; Jan, L. Y., Merging functional studies with structures of inward-rectifier K(+) channels. *Nature reviews. Neuroscience* **2003**, *4* (12), 957-67.

82. Bandyopadhyay, A.; Tsuji, K.; Cox, K.; Harfe, B. D.; Rosen, V.; Tabin, C. J., Genetic analysis of the roles of BMP2, BMP4, and BMP7 in limb patterning and skeletogenesis. *PLoS genetics* **2006**, *2* (12), e216.
83. Casey, L. M.; Lan, Y.; Cho, E. S.; Maltby, K. M.; Gridley, T.; Jiang, R., Jag2-Notch1 signaling regulates oral epithelial differentiation and palate development. *Developmental dynamics : an official publication of the American Association of Anatomists* **2006**, *235* (7), 1830-44.
84. Dudas, M.; Sridurongrit, S.; Nagy, A.; Okazaki, K.; Kaartinen, V., Craniofacial defects in mice lacking BMP type I receptor Alk2 in neural crest cells. *Mechanisms of development* **2004**, *121* (2), 173-82.
85. Ferretti, E.; Li, B.; Zewdu, R.; Wells, V.; Hebert, J. M.; Karner, C.; Anderson, M. J.; Williams, T.; Dixon, J.; Dixon, M. J.; Depew, M. J.; Selleri, L., A conserved Pbx-Wnt-p63-Irf6 regulatory module controls face morphogenesis by promoting epithelial apoptosis. *Developmental cell* **2011**, *21* (4), 627-41.
86. He, F.; Xiong, W.; Wang, Y.; Li, L.; Liu, C.; Yamagami, T.; Taketo, M. M.; Zhou, C.; Chen, Y., Epithelial Wnt/beta-catenin signaling regulates palatal shelf fusion through regulation of Tgfbeta3 expression. *Developmental biology* **2011**, *350* (2), 511-9.
87. Jiang, R.; Lan, Y.; Chapman, H. D.; Shawber, C.; Norton, C. R.; Serreze, D. V.; Weinmaster, G.; Gridley, T., Defects in limb, craniofacial, and thymic development in Jagged2 mutant mice. *Genes & development* **1998**, *12* (7), 1046-57.
88. Jin, Y. R.; Turcotte, T. J.; Crocker, A. L.; Han, X. H.; Yoon, J. K., The canonical Wnt signaling activator, R-spondin2, regulates craniofacial patterning and morphogenesis within the branchial arch through ectodermal-mesenchymal interaction. *Developmental biology* **2011**, *352* (1), 1-13.
89. Lin, C.; Fisher, A. V.; Yin, Y.; Maruyama, T.; Veith, G. M.; Dhandha, M.; Huang, G. J.; Hsu, W.; Ma, L., The inductive role of Wnt-beta-Catenin signaling in the formation of oral apparatus. *Developmental biology* **2011**, *356* (1), 40-50.
90. Liu, W.; Sun, X.; Braut, A.; Mishina, Y.; Behringer, R. R.; Mina, M.; Martin, J. F., Distinct functions for Bmp signaling in lip and palate fusion in mice. *Development* **2005**, *132* (6), 1453-61.
91. Menezes, R.; Letra, A.; Kim, A. H.; Kuchler, E. C.; Day, A.; Tannure, P. N.; Gomes da Motta, L.; Paiva, K. B.; Granjeiro, J. M.; Vieira, A. R., Studies with Wnt genes and nonsyndromic cleft lip and palate. *Birth defects research. Part A, Clinical and molecular teratology* **2010**, *88* (11), 995-1000.
92. Richardson, R. J.; Dixon, J.; Jiang, R.; Dixon, M. J., Integration of IRF6 and Jagged2 signalling is essential for controlling palatal adhesion and fusion competence. *Human molecular genetics* **2009**, *18* (14), 2632-42.
93. Tucker, A. S.; Al Khamis, A.; Sharpe, P. T., Interactions between Bmp-4 and Msx-1 act to restrict gene expression to odontogenic mesenchyme. *Developmental dynamics : an official publication of the American Association of Anatomists* **1998**, *212* (4), 533-9.
94. Tucker, A. S.; Matthews, K. L.; Sharpe, P. T., Transformation of tooth type induced by inhibition of BMP signaling. *Science* **1998**, *282* (5391), 1136-8.
95. Xu, J.; Krebs, L. T.; Gridley, T., Generation of mice with a conditional null allele of the Jagged2 gene. *Genesis* **2010**, *48* (6), 390-3.
96. Derynck, R.; Jarrett, J. A.; Chen, E. Y.; Eaton, D. H.; Bell, J. R.; Assoian, R. K.; Roberts, A. B.; Sporn, M. B.; Goeddel, D. V., Human transforming growth factor-beta

- complementary DNA sequence and expression in normal and transformed cells. *Nature* **1985**, *316* (6030), 701-5.
97. Mason, A. J.; Hayflick, J. S.; Ling, N.; Esch, F.; Ueno, N.; Ying, S. Y.; Guillemin, R.; Niall, H.; Seeburg, P. H., Complementary DNA sequences of ovarian follicular fluid inhibin show precursor structure and homology with transforming growth factor-beta. *Nature* **1985**, *318* (6047), 659-63.
  98. Ohta, M.; Greenberger, J. S.; Anklesaria, P.; Bassols, A.; Massague, J., Two forms of transforming growth factor-beta distinguished by multipotential haematopoietic progenitor cells. *Nature* **1987**, *329* (6139), 539-41.
  99. Padgett, R. W.; St Johnston, R. D.; Gelbart, W. M., A transcript from a Drosophila pattern gene predicts a protein homologous to the transforming growth factor-beta family. *Nature* **1987**, *325* (6099), 81-4.
  100. Sampath, T. K.; Rashka, K. E.; Doctor, J. S.; Tucker, R. F.; Hoffmann, F. M., Drosophila transforming growth factor beta superfamily proteins induce endochondral bone formation in mammals. *Proceedings of the National Academy of Sciences of the United States of America* **1993**, *90* (13), 6004-8.
  101. Blair, S. S., Wing vein patterning in Drosophila and the analysis of intercellular signaling. *Annual review of cell and developmental biology* **2007**, *23*, 293-319.
  102. Gelbart, W. M., Synapsis-dependent allelic complementation at the decapentaplegic gene complex in Drosophila melanogaster. *Proceedings of the National Academy of Sciences of the United States of America* **1982**, *79* (8), 2636-40.
  103. Letsou, A.; Arora, K.; Wrana, J. L.; Simin, K.; Twombly, V.; Jamal, J.; Staehling-Hampton, K.; Hoffmann, F. M.; Gelbart, W. M.; Massague, J.; et al., Drosophila Dpp signaling is mediated by the punt gene product: a dual ligand-binding type II receptor of the TGF beta receptor family. *Cell* **1995**, *80* (6), 899-908.
  104. O'Connor, M. B.; Umulis, D.; Othmer, H. G.; Blair, S. S., Shaping BMP morphogen gradients in the Drosophila embryo and pupal wing. *Development* **2006**, *133* (2), 183-93.
  105. Nellen, D.; Affolter, M.; Basler, K., Receptor serine/threonine kinases implicated in the control of Drosophila body pattern by decapentaplegic. *Cell* **1994**, *78* (2), 225-37.
  106. Ruberte, E.; Marty, T.; Nellen, D.; Affolter, M.; Basler, K., An absolute requirement for both the type II and type I receptors, punt and thick veins, for dpp signaling in vivo. *Cell* **1995**, *80* (6), 889-97.
  107. Kim, J.; Johnson, K.; Chen, H. J.; Carroll, S.; Laughon, A., Drosophila Mad binds to DNA and directly mediates activation of vestigial by Decapentaplegic. *Nature* **1997**, *388* (6639), 304-8.
  108. Sanford, L. P.; Ormsby, I.; Gittenberger-de Groot, A. C.; Sariola, H.; Friedman, R.; Boivin, G. P.; Cardell, E. L.; Doetschman, T., TGFbeta2 knockout mice have multiple developmental defects that are non-overlapping with other TGFbeta knockout phenotypes. *Development* **1997**, *124* (13), 2659-70.
  109. Taya, Y.; O'Kane, S.; Ferguson, M. W., Pathogenesis of cleft palate in TGF-beta3 knockout mice. *Development* **1999**, *126* (17), 3869-79.
  110. Bjork, B. C.; Turbe-Doan, A.; Prysak, M.; Herron, B. J.; Beier, D. R., Prdm16 is required for normal palatogenesis in mice. *Human molecular genetics* **2010**, *19* (5), 774-89.
  111. Peters, H.; Neubuser, A.; Balling, R., Pax genes and organogenesis: Pax9 meets tooth development. *European journal of oral sciences* **1998**, *106 Suppl 1*, 38-43.

112. Segal, D.; Gelbart, W. M., Shortvein, a new component of the decapentaplegic gene complex in *Drosophila melanogaster*. *Genetics* **1985**, *109* (1), 119-43.
113. Cook, O.; Biehs, B.; Bier, E., brinker and optomotor-blind act coordinately to initiate development of the L5 wing vein primordium in *Drosophila*. *Development* **2004**, *131* (9), 2113-24.
114. Spencer, F. A.; Hoffmann, F. M.; Gelbart, W. M., Decapentaplegic: a gene complex affecting morphogenesis in *Drosophila melanogaster*. *Cell* **1982**, *28* (3), 451-61.
115. Irish, V. F.; Gelbart, W. M., The decapentaplegic gene is required for dorsal-ventral patterning of the *Drosophila* embryo. *Genes & development* **1987**, *1* (8), 868-79.
116. del Alamo Rodriguez, D.; Terriente Felix, J.; Diaz-Benjumea, F. J., The role of the T-box gene optomotor-blind in patterning the *Drosophila* wing. *Developmental biology* **2004**, *268* (2), 481-92.
117. Teleman, A. A.; Cohen, S. M., Dpp gradient formation in the *Drosophila* wing imaginal disc. *Cell* **2000**, *103* (6), 971-80.
118. Nellen, D.; Burke, R.; Struhl, G.; Basler, K., Direct and long-range action of a DPP morphogen gradient. *Cell* **1996**, *85* (3), 357-368.
119. Widmann, T. J.; Dahmann, C., Wingless signaling and the control of cell shape in *Drosophila* wing imaginal discs. *Developmental biology* **2009**, *334* (1), 161-173.
120. Calleja, M.; Renaud, O.; Usui, K.; Pistillo, D.; Morata, G.; Simpson, P., How to pattern an epithelium: lessons from *achaete-scute* regulation on the notum of *Drosophila*. *Gene* **2002**, *292* (1), 1-12.
121. Marquez, R. M.; Singer, M. A.; Takaesu, N. T.; Waldrip, W. R.; Kravtsov, Y.; Newfeld, S. J., Transgenic analysis of the Smad family of TGF-beta signal transducers in *Drosophila melanogaster* suggests new roles and new interactions between family members. *Genetics* **2001**, *157* (4), 1639-48.
122. Adachi-Yamada, T.; Fujimura-Kamada, K.; Nishida, Y.; Matsumoto, K., Distortion of proximodistal information causes JNK-dependent apoptosis in *Drosophila* wing. *Nature* **1999**, *400* (6740), 166-169.
123. Adachi-Yamada, T.; O'Connor, M. B., Morphogenetic apoptosis: a mechanism for correcting discontinuities in morphogen gradients. *Developmental biology* **2002**, *251* (1), 74-90.
124. Moreno, E.; Basler, K.; Morata, G., Cells compete for decapentaplegic survival factor to prevent apoptosis in *Drosophila* wing development. *Nature* **2002**, *416* (6882), 755-9.
125. Ziv, O.; Suissa, Y.; Neuman, H.; Dinur, T.; Geuking, P.; Rhiner, C.; Portela, M.; Lolo, F.; Moreno, E.; Gerlitz, O., The co-regulator dNAB interacts with Brinker to eliminate cells with reduced Dpp signaling. *Development* **2009**, *136* (7), 1137-45.
126. Hay, B. A.; Wolff, T.; Rubin, G. M., Expression of baculovirus P35 prevents cell death in *Drosophila*. *Development* **1994**, *120* (8), 2121-9.
127. Bump, N. J.; Hackett, M.; Hugunin, M.; Seshagiri, S.; Brady, K.; Chen, P.; Ferenz, C.; Franklin, S.; Ghayur, T.; Li, P., Inhibition of ICE family proteases by baculovirus antiapoptotic protein p35. *Science* **1995**, *269* (5232), 1885-1888.
128. Zecca, M.; Basler, K.; Struhl, G., Sequential organizing activities of engrailed, hedgehog and decapentaplegic in the *Drosophila* wing. *Development* **1995**, *121* (8), 2265-78.
129. de Celis, J. F., Expression and function of decapentaplegic and thick veins during the differentiation of the veins in the *Drosophila* wing. *Development* **1997**, *124* (5), 1007-18.



130. Adachi-Yamada, T.; Fujimura-Kamada, K.; Nishida, Y.; Matsumoto, K., Distortion of proximodistal information causes JNK-dependent apoptosis in *Drosophila* wing. *Nature* **1999**, *400* (6740), 166-9.
131. Tabata, T.; Kornberg, T. B., Hedgehog is a signaling protein with a key role in patterning *Drosophila* imaginal discs. *Cell* **1994**, *76* (1), 89-102.
132. Eivers, E.; Demagny, H.; De Robertis, E. M., Integration of BMP and Wnt signaling via vertebrate Smad1/5/8 and *Drosophila* Mad. *Cytokine & growth factor reviews* **2009**, *20* (5-6), 357-65.
133. Eivers, E.; Fuentealba, L. C.; Sander, V.; Clemens, J. C.; Hartnett, L.; De Robertis, E. M., Mad is required for wingless signaling in wing development and segment patterning in *Drosophila*. *PLoS one* **2009**, *4* (8), e6543.
134. Eivers, E.; Demagny, H.; Choi, R. H.; De Robertis, E. M., Phosphorylation of Mad controls competition between wingless and BMP signaling. *Science signaling* **2011**, *4* (194), ra68.
135. Huh, J. R.; Guo, M.; Hay, B. A., Compensatory proliferation induced by cell death in the *Drosophila* wing disc requires activity of the apical cell death caspase Dronc in a nonapoptotic role. *Current biology : CB* **2004**, *14* (14), 1262-6.
136. Martin, F. A.; Perez-Garijo, A.; Moreno, E.; Morata, G., The brinker gradient controls wing growth in *Drosophila*. *Development* **2004**, *131* (20), 4921-30.
137. Perez-Garijo, A.; Martin, F. A.; Struhl, G.; Morata, G., Dpp signaling and the induction of neoplastic tumors by caspase-inhibited apoptotic cells in *Drosophila*. *Proceedings of the National Academy of Sciences of the United States of America* **2005**, *102* (49), 17664-9.
138. Ryoo, H. D.; Gorenc, T.; Steller, H., Apoptotic cells can induce compensatory cell proliferation through the JNK and the Wingless signaling pathways. *Developmental cell* **2004**, *7* (4), 491-501.
139. Fujise, M.; Takeo, S.; Kamimura, K.; Matsuo, T.; Aigaki, T.; Izumi, S.; Nakato, H., Dally regulates Dpp morphogen gradient formation in the *Drosophila* wing. *Development* **2003**, *130* (8), 1515-22.
140. Grisaru, S.; Cano-Gauci, D.; Tee, J.; Filmus, J.; Rosenblum, N. D., Glypican-3 modulates BMP- and FGF-mediated effects during renal branching morphogenesis. *Developmental biology* **2001**, *231* (1), 31-46.
141. Jackson, S. M.; Nakato, H.; Sugiura, M.; Jannuzi, A.; Oakes, R.; Kaluza, V.; Golden, C.; Selleck, S. B., dally, a *Drosophila* glypican, controls cellular responses to the TGF-beta-related morphogen, Dpp. *Development* **1997**, *124* (20), 4113-20.
142. Paine-Saunders, S.; Viviano, B. L.; Economides, A. N.; Saunders, S., Heparan sulfate proteoglycans retain Noggin at the cell surface: a potential mechanism for shaping bone morphogenetic protein gradients. *The Journal of biological chemistry* **2002**, *277* (3), 2089-96.
143. Lu, R.; Niesen, M. J.; Hu, W.; Vaidehi, N.; Shively, J. E., Interaction of actin with carcinoembryonic antigen-related cell adhesion molecule 1 (CEACAM1) receptor in liposomes is Ca<sup>2+</sup>- and phospholipid-dependent. *The Journal of biological chemistry* **2011**, *286* (31), 27528-36.
144. Jernvall, J.; Aberg, T.; Kettunen, P.; Keranen, S.; Thesleff, I., The life history of an embryonic signaling center: BMP-4 induces p21 and is associated with apoptosis in the mouse tooth enamel knot. *Development* **1998**, *125* (2), 161-9.

145. Neubuser, A.; Peters, H.; Balling, R.; Martin, G. R., Antagonistic interactions between FGF and BMP signaling pathways: a mechanism for positioning the sites of tooth formation. *Cell* **1997**, *90* (2), 247-55.
146. Schaller, S. A.; Li, S.; Ngo-Muller, V.; Han, M. J.; Omi, M.; Anderson, R.; Muneoka, K., Cell biology of limb patterning. *International review of cytology* **2001**, *203*, 483-517.
147. Schaller, S. A.; Muneoka, K., Inhibition of polarizing activity in the anterior limb bud is regulated by extracellular factors. *Developmental biology* **2001**, *240* (2), 443-56.
148. Zuzarte-Luis, V.; Hurler, J. M., Programmed cell death in the embryonic vertebrate limb. *Seminars in cell & developmental biology* **2005**, *16* (2), 261-9.
149. Hatten, M. E.; Liem, R. K.; Mason, C. A., Defects in specific associations between astroglia and neurons occur in microcultures of weaver mouse cerebellar cells. *The Journal of neuroscience : the official journal of the Society for Neuroscience* **1984**, *4* (4), 1163-72.
150. Hatten, M. E.; Liem, R. K.; Mason, C. A., Weaver mouse cerebellar granule neurons fail to migrate on wild-type astroglial processes in vitro. *The Journal of neuroscience : the official journal of the Society for Neuroscience* **1986**, *6* (9), 2676-83.
151. Patil, N.; Cox, D. R.; Bhat, D.; Faham, M.; Myers, R. M.; Peterson, A. S., A potassium channel mutation in weaver mice implicates membrane excitability in granule cell differentiation. *Nature genetics* **1995**, *11* (2), 126-9.
152. Rakic, P.; Sidman, R. L., Weaver mutant mouse cerebellum: defective neuronal migration secondary to abnormality of Bergmann glia. *Proceedings of the National Academy of Sciences of the United States of America* **1973**, *70* (1), 240-4.
153. Silverman, S. K.; Kofuji, P.; Dougherty, D. A.; Davidson, N.; Lester, H. A., A regenerative link in the ionic fluxes through the weaver potassium channel underlies the pathophysiology of the mutation. *Proceedings of the National Academy of Sciences of the United States of America* **1996**, *93* (26), 15429-34.
154. Tong, Y.; Wei, J.; Zhang, S.; Strong, J. A.; Dlouhy, S. R.; Hodes, M. E.; Ghetti, B.; Yu, L., The weaver mutation changes the ion selectivity of the affected inwardly rectifying potassium channel GIRK2. *FEBS letters* **1996**, *390* (1), 63-8.
155. Signorini, S.; Liao, Y. J.; Duncan, S. A.; Jan, L. Y.; Stoffel, M., Normal cerebellar development but susceptibility to seizures in mice lacking G protein-coupled, inwardly rectifying K<sup>+</sup> channel GIRK2. *Proceedings of the National Academy of Sciences of the United States of America* **1997**, *94* (3), 923-7.
156. Bendahhou, S.; Donaldson, M. R.; Plaster, N. M.; Tristani-Firouzi, M.; Fu, Y. H.; Ptacek, L. J., Defective potassium channel Kir2.1 trafficking underlies Andersen-Tawil syndrome. *The Journal of biological chemistry* **2003**, *278* (51), 51779-85.
157. Dietzl, G.; Chen, D.; Schnorrer, F.; Su, K. C.; Barinova, Y.; Fellner, M.; Gasser, B.; Kinsey, K.; Oettel, S.; Scheiblauer, S.; Couto, A.; Marra, V.; Keleman, K.; Dickson, B. J., A genome-wide transgenic RNAi library for conditional gene inactivation in *Drosophila*. *Nature* **2007**, *448* (7150), 151-6.
158. Yapici, N.; Kim, Y. J.; Ribeiro, C.; Dickson, B. J., A receptor that mediates the post-mating switch in *Drosophila* reproductive behaviour. *Nature* **2008**, *451* (7174), 33-7.
159. Parks, A. L.; Cook, K. R.; Belvin, M.; Dompe, N. A.; Fawcett, R.; Huppert, K.; Tan, L. R.; Winter, C. G.; Bogart, K. P.; Deal, J. E.; Deal-Herr, M. E.; Grant, D.; Marcinko, M.; Miyazaki, W. Y.; Robertson, S.; Shaw, K. J.; Tabios, M.; Vysotskaia, V.; Zhao, L.; Andrade, R. S.; Edgar, K. A.; Howie, E.; Killpack, K.; Milash, B.; Norton, A.; Thao, D.;

- Whittaker, K.; Winner, M. A.; Friedman, L.; Margolis, J.; Singer, M. A.; Kopczynski, C.; Curtis, D.; Kaufman, T. C.; Plowman, G. D.; Duyk, G.; Francis-Lang, H. L., Systematic generation of high-resolution deletion coverage of the *Drosophila melanogaster* genome. *Nature genetics* **2004**, *36* (3), 288-92.
160. Lecuyer, E.; Parthasarathy, N.; Krause, H. M., Fluorescent in situ hybridization protocols in *Drosophila* embryos and tissues. *Methods in molecular biology* **2008**, *420*, 289-302.
161. Livak, K. J.; Schmittgen, T. D., Analysis of relative gene expression data using real-time quantitative PCR and the 2(-Delta Delta C(T)) Method. *Methods* **2001**, *25* (4), 402-8.
162. Cao, J.; Pellock, B.; White, K.; Raftery, L., A commercial phospho-Smad antibody detects endogenous BMP signaling in *Drosophila* tissues. *Drosophila Information Services* **2006**, *89*, 131-135.
163. Halachmi, N.; Schulze, K. L.; Inbal, A.; Salzberg, A., Additional sex combs affects antennal development by means of spatially restricted repression of Antp and wg. *Developmental dynamics : an official publication of the American Association of Anatomists* **2007**, *236* (8), 2118-30.
164. Skeath, J. B.; Carroll, S. B., Regulation of achaete-scute gene expression and sensory organ pattern formation in the *Drosophila* wing. *Genes & development* **1991**, *5* (6), 984-95.
165. Brook, W. J.; Cohen, S. M., Antagonistic interactions between wingless and decapentaplegic responsible for dorsal-ventral pattern in the *Drosophila* Leg. *Science* **1996**, *273* (5280), 1373-7.
166. Neto-Silva, R. M.; Wells, B. S.; Johnston, L. A., Mechanisms of growth and homeostasis in the *Drosophila* wing. *Annual review of cell and developmental biology* **2009**, *25*, 197.
167. Weigmann, K.; Cohen, S. M.; Lehner, C. F., Cell cycle progression, growth and patterning in imaginal discs despite inhibition of cell division after inactivation of *Drosophila* Cdc2 kinase. *Development* **1997**, *124* (18), 3555-3563.
168. Blair, S. S., Compartments and appendage development in *Drosophila*. *BioEssays* **1995**, *17* (4), 299-309.
169. Posakony, L. G.; Raftery, L. A.; Gelbart, W. M., Wing formation in *Drosophila melanogaster* requires decapentaplegic gene function along the anterior-posterior compartment boundary. *Mechanisms of development* **1990**, *33* (1), 69-82.
170. Zecca, M.; Basler, K.; Struhl, G., Direct and long-range action of a wingless morphogen gradient. *Cell* **1996**, *87* (5), 833-844.
171. Zecca, M.; Basler, K.; Struhl, G., Sequential organizing activities of engrailed, hedgehog and decapentaplegic in the *Drosophila* wing. *Development* **1995**, *121* (8), 2265-2278.
172. Sanicola, M.; Sekelsky, J.; Elson, S.; Gelbart, W. M., Drawing a stripe in *Drosophila* imaginal disks: negative regulation of decapentaplegic and patched expression by engrailed. *Genetics* **1995**, *139* (2), 745.
173. Guillén, I.; Mullor, J. L.; Capdevila, J.; Sanchez-Herrero, E.; Morata, G.; Guerrero, I., The function of engrailed and the specification of *Drosophila* wing pattern. *Development* **1995**, *121* (10), 3447-3456.
174. Müller, P.; Rogers, K. W.; Shuizi, R. Y.; Brand, M.; Schier, A. F., Morphogen transport. *Development* **2013**, *140* (8), 1621-1638.
175. Rogers, K. W.; Schier, A. F., Morphogen gradients: from generation to interpretation. *Annual review of cell and developmental biology* **2011**, *27*, 377-407.

176. Ramírez-Weber, F.-A.; Kornberg, T. B., Cytonemes: cellular processes that project to the principal signaling center in *Drosophila* imaginal discs. *Cell* **1999**, *97* (5), 599-607.
177. Milan, M.; Campuzano, S.; García-Bellido, A., Developmental parameters of cell death in the wing disc of *Drosophila*. *Proceedings of the National Academy of Sciences* **1997**, *94* (11), 5691-5696.
178. Gibson, M. C.; Perrimon, N., Extrusion and death of DPP/BMP-compromised epithelial cells in the developing *Drosophila* wing. *Science Signaling* **2005**, *307* (5716), 1785.
179. Shen, J.; Dahmann, C., Extrusion of cells with inappropriate Dpp signaling from *Drosophila* wing disc epithelia. *Science Signaling* **2005**, *307* (5716), 1789.
180. Neumann, C. J.; Cohen, S. M., Long-range action of Wingless organizes the dorsal-ventral axis of the *Drosophila* wing. *Development* **1997**, *124* (4), 871-880.
181. Polakis, P., Wnt signaling in cancer. *Cold Spring Harbor perspectives in biology* **2012**, *4* (5).
182. Tabata, T., Genetics of morphogen gradients. *Nature Reviews Genetics* **2001**, *2* (8), 620-630.
183. Haerry, T. E., The interaction between two TGF- $\beta$  type I receptors plays important roles in ligand binding, SMAD activation, and gradient formation. *Mechanisms of development* **2010**, *127* (7), 358-370.
184. Bangi, E.; Wharton, K., Dpp and Gbb exhibit different effective ranges in the establishment of the BMP activity gradient critical for *Drosophila* wing patterning. *Developmental biology* **2006**, *295* (1), 178-193.
185. Brummel, T. J.; Twombly, V.; Marques, G.; Wrana, J. L.; Newfeld, S. J.; Attisano, L.; Massague, J.; O'Connor, M. B.; Gelbart, W. M., Characterization and relationship of Dpp receptors encoded by the saxophone and thick veins genes in *Drosophila*. *Cell* **1994**, *78* (2), 251.
186. Raftery, L. A.; Umulis, D. M., Regulation of BMP activity and range in *Drosophila* wing development. *Current Opinion in Cell Biology* **2012**, *24* (2), 158-165.
187. Nakato, H.; Futch, T. A.; Selleck, S. B., The division abnormally delayed (dally) gene: a putative integral membrane proteoglycan required for cell division patterning during postembryonic development of the nervous system in *Drosophila*. *Development* **1995**, *121* (11), 3687-3702.
188. Dejima, K.; Kanai, M. I.; Akiyama, T.; Levings, D. C.; Nakato, H.; Dejima, K.; Kanai, M. I.; Akiyama, T.; Levings, D. C.; Nakato, H., Novel contact-dependent bone morphogenetic protein (BMP) signaling mediated by heparan sulfate proteoglycans. *Journal of Biological Chemistry* **2011**, *286* (19), 17103-17111.
189. Dahal, G. R.; Rawson, J.; Gassaway, B.; Kwok, B.; Tong, Y.; Ptáček, L. J.; Bates, E., An inwardly rectifying K<sup>+</sup> channel is required for patterning. *Development* **2012**, *139* (19), 3653-3664.
190. Lecuit, T.; Brook, W. J.; Ng, M.; Calleja, M.; Sun, H.; Cohen, S. M., Two distinct mechanisms for long-range patterning by Decapentaplegic in the *Drosophila* wing. *Nature* **1996**, *381* (6581), 387-393.
191. Bharathi, V.; Pallavi, S.; Bajpai, R.; Emerald, B.; Shashidhara, L., Genetic characterization of the *Drosophila* homologue of coronin. *Journal of cell science* **2004**, *117* (10), 1911-1922.

192. Tuma, P. L.; Hubbard, A. L., Transcytosis: crossing cellular barriers. *Physiological Reviews* **2003**, *83* (3), 871-932.
193. Xia, F.; Gao, X.; Kwan, E.; Lam, P. P.; Chan, L.; Sy, K.; Sheu, L.; Wheeler, M. B.; Gaisano, H. Y.; Tsushima, R. G., Disruption of pancreatic  $\beta$ -cell lipid rafts modifies Kv2.1 channel gating and insulin exocytosis. *Journal of Biological Chemistry* **2004**, *279* (23), 24685-24691.
194. Munson, M.; Bryant, N., A role for the syntaxin N-terminus. *Biochem. J* **2009**, *418*, e1-e3.
195. Leung, Y. M.; Kwan, E. P.; Ng, B.; Kang, Y.; Gaisano, H. Y., SNAREing voltage-gated K<sup>+</sup> and ATP-sensitive K<sup>+</sup> channels: tuning  $\beta$ -cell excitability with syntaxin-1A and other exocytotic proteins. *Endocrine reviews* **2007**, *28* (6), 653-663.
196. Michel, M.; Raabe, I.; Kupinski, A. P.; Pérez-Palencia, R.; Bökel, C., Local BMP receptor activation at adherens junctions in the *Drosophila* germline stem cell niche. *Nature Communications* **2011**, *2*, 415.
197. Ready, D. F.; Hanson, T. E.; Benzer, S., Development of the *Drosophila* retina, a neurocrystalline lattice. *Developmental biology* **1976**, *53* (2), 217-240.
198. Reifegerste, R.; Moses, K., Genetics of epithelial polarity and pattern in the *Drosophila* retina. *Bioessays* **1999**, *21* (4), 275-285.
199. Wolff, T.; Ready, D., Pattern formation in the *Drosophila* retina. *The development of Drosophila melanogaster* **1993**, *2*, 1277-1325.
200. Clandinin, T. R.; Zipursky, S. L., Making connections in the fly visual system. *Neuron* **2002**, *35* (5), 827-841.
201. Roignant, J.-Y.; Treisman, J. E., Pattern formation in the *Drosophila* eye disc. *The International journal of developmental biology* **2009**, *53* (5-6), 795.
202. Thomas, B. J.; Gunning, D. A.; Cho, J.; Zipursky, S. L., Cell cycle progression in the developing *Drosophila* eye: *roughex* encodes a novel protein required for the establishment of G1. *Cell* **1994**, *77* (7), 1003-1014.
203. Firth, L. C.; Baker, N. E., Extracellular Signals Responsible for Spatially Regulated Proliferation in the Differentiating *Drosophila* Eye. *Developmental cell* **2005**, *8* (4), 541-551.
204. Tomlinson, A.; Ready, D. F., Cell fate in the *Drosophila* ommatidium. *Developmental biology* **1987**, *123* (1), 264-275.
205. Lawrence, P. A.; Green, S. M., Cell lineage in the developing retina of *Drosophila*. *Developmental biology* **1979**, *71* (1), 142-152.
206. Kumar, J. P.; Moses, K., The EGF receptor and notch signaling pathways control the initiation of the morphogenetic furrow during *Drosophila* eye development. *Development* **2001**, *128* (14), 2689-2697.
207. Curtiss, J.; Mlodzik, M., Morphogenetic furrow initiation and progression during eye development in *Drosophila*: the roles of decapentaplegic, hedgehog and eyes absent. *Development* **2000**, *127* (6), 1325-1336.
208. Ma, C.; Zhou, Y.; Beachy, P. A.; Moses, K., The segment polarity gene *hedgehog* is required for progression of the morphogenetic furrow in the developing *Drosophila* eye. *Cell* **1993**, *75* (5), 927-938.
209. Domínguez, M.; Hafen, E., Hedgehog directly controls initiation and propagation of retinal differentiation in the *Drosophila* eye. *Genes & development* **1997**, *11* (23), 3254-3264.

210. Heberlein, U.; Wolff, T.; Rubin, G. M., The TGF $\beta$  homolog *dpp* and the segment polarity gene *hedgehog* are required for propagation of a morphogenetic wave in the *Drosophila* retina. *Cell* **1993**, *75* (5), 913-926.
211. Heberlein, U.; Singh, C. M.; Luk, A. Y.; Donohoe, T. J., Growth and differentiation in the *Drosophila* eye coordinated by *hedgehog*. **1995**.
212. Heberlein, U.; Moses, K., Mechanisms of *Drosophila* retinal morphogenesis: the virtues of being progressive. *Cell* **1995**, *81* (7), 987-990.
213. Pappu, K. S.; Chen, R.; Middlebrooks, B. W.; Woo, C.; Heberlein, U.; Mardon, G., Mechanism of *hedgehog* signaling during *Drosophila* eye development. *Development* **2003**, *130* (13), 3053-3062.
214. Hazelett, D. J.; Bourouis, M.; Walldorf, U.; Treisman, J. E., Decapentaplegic and wingless are regulated by eyes absent and eyegone and interact to direct the pattern of retinal differentiation in the eye disc. *Development* **1998**, *125* (18), 3741-3751.
215. Ma, C.; Moses, K., Wingless and patched are negative regulators of the morphogenetic furrow and can affect tissue polarity in the developing *Drosophila* compound eye. *Development* **1995**, *121* (8), 2279-2289.
216. Baonza, A.; Freeman, M., Control of *Drosophila* eye specification by Wingless signalling. *Development* **2002**, *129* (23), 5313-5322.
217. Bejsovec, A., Flying at the head of the pack: Wnt biology in *Drosophila*. *Oncogene* **2006**, *25* (57), 7442-7449.
218. Brunner, E.; Brunner, D.; Fu, W.; Hafen, E.; Basler, K., The Dominant Mutation *Glazed* Is a Gain-of-Function Allele of *wingless* That, Similar to Loss of APC, Interferes with Normal Eye Development. *Developmental biology* **1999**, *206* (2), 178-188.
219. Wehrli, M.; Tomlinson, A., Independent regulation of anterior/posterior and equatorial/polar polarity in the *Drosophila* eye; evidence for the involvement of Wnt signaling in the equatorial/polar axis. *Development* **1998**, *125* (8), 1421-1432.
220. Kryuchkov, M.; Katanaev, V. L.; Enin, G. A.; Sergeev, A.; Timchenko, A. A.; Serdyuk, I. N., Analysis of Micro- and Nano-Structures of the Corneal Surface of *Drosophila* and Its Mutants by Atomic Force Microscopy and Optical Diffraction. *PloS one* **2011**, *6* (7), e22237.
221. Greaves, S.; Sanson, B.; White, P.; Vincent, J.-P., A screen for identifying genes interacting with *armadillo*, the *Drosophila* homolog of  $\beta$ -catenin. *Genetics* **1999**, *153* (4), 1753-1766.
222. Pignoni, F.; Zipursky, S. L., Induction of *Drosophila* eye development by decapentaplegic. *Development* **1997**, *124* (2), 271-278.
223. Cordero, J. B.; Larson, D. E.; Craig, C. R.; Hays, R.; Cagan, R., Dynamic decapentaplegic signaling regulates patterning and adhesion in the *Drosophila* pupal retina. *Development* **2007**, *134* (10), 1861-1871.
224. Ghabrial, A.; Luschnig, S.; Metzstein, M. M.; Krasnow, M. A., Branching morphogenesis of the *Drosophila* tracheal system. *Annual review of cell and developmental biology* **2003**, *19* (1), 623-647.
225. Manning, G.; Krasnow, M.; Bate, M.; Arias, A. M., The Development of *Drosophila melanogaster*. *Development of the Drosophila tracheal system* **1993**, 609-685.
226. Zelzer, E.; Shilo, B. Z., Cell fate choices in *Drosophila* tracheal morphogenesis. *Bioessays* **2000**, *22* (3), 219-226.

227. Sedaghat, Y.; Miranda, W. F.; Sonnenfeld, M. J., The jing Zn-finger transcription factor is a mediator of cellular differentiation in the Drosophila CNS midline and trachea. *Development* **2002**, *129* (11), 2591-2606.
228. Vincent, S.; Ruberte, E.; Grieder, N. C.; Chen, C.-K.; Haerry, T.; Schuh, R.; Affolter, M., DPP controls tracheal cell migration along the dorsoventral body axis of the Drosophila embryo. *Development* **1997**, *124* (14), 2741-2750.
229. Ribeiro, C.; Ebner, A.; Affolter, M., In vivo imaging reveals different cellular functions for FGF and Dpp signaling in tracheal branching morphogenesis. *Developmental cell* **2002**, *2* (5), 677-683.
230. de Celis, J. F.; Llimargas, M.; Casanova, J., Ventral veinless, the gene encoding the Cfla transcription factor, links positional information and cell differentiation during embryonic and imaginal development in Drosophila melanogaster. *Development* **1995**, *121* (10), 3405-3416.
231. Cadigan, K. M.; Jou, A. D.; Nusse, R., Wingless blocks bristle formation and morphogenetic furrow progression in the eye through repression of Daughterless. *Development* **2002**, *129* (14), 3393-3402.
232. Wappner, P.; Gabay, L.; Shilo, B.-Z., Interactions between the EGF receptor and DPP pathways establish distinct cell fates in the tracheal placodes. *Development* **1997**, *124* (22), 4707-4716.
233. Steneberg, P.; Hemphälä, J.; Samakovlis, C., Dpp and Notch specify the fusion cell fate in the dorsal branches of the Drosophila trachea. *Mechanisms of development* **1999**, *87* (1), 153-163.
234. Kato, K.; Chihara, T.; Hayashi, S., Hedgehog and Decapentaplegic instruct polarized growth of cell extensions in the Drosophila trachea. *Development* **2004**, *131* (21), 5253-5261.
235. Affolter, M.; Shilo, B.-Z., Genetic control of branching morphogenesis during Drosophila tracheal development. *Current opinion in cell biology* **2000**, *12* (6), 731-735.
236. Pichaud, F.; Casares, F., *homothorax* and *iroquois-C* genes are required for the establishment of territories within the developing eye disc. *Mechanisms of development* **2000**, *96* (1), 15-25.
237. Royet, J.; Finkelstein, R., hedgehog, wingless and orthodenticle specify adult head development in Drosophila. *Development* **1996**, *122* (6), 1849-1858.
238. Vrailas, A. D.; Marena, D. R.; Cook, S. E.; Powers, M. A.; Lorenzen, J. A.; Perkins, L. A.; Moses, K., smoothed and thickveins regulate Moleskin/Importin 7-mediated MAP kinase signaling in the developing Drosophila eye. *Development* **2006**, *133* (8), 1485-1494.
239. Yu, S.-Y.; Yoo, S. J.; Yang, L.; Zapata, C.; Srinivasan, A.; Hay, B. A.; Baker, N. E., A pathway of signals regulating effector and initiator caspases in the developing Drosophila eye. *Development* **2002**, *129* (13), 3269-3278.